

# **Snow avalanches (and related beasts) — theory and practice**

Fluid-mediated Particle Transport  
in Geophysical Flows @ KITP  
2013-10-07

Dieter Issler  
Norwegian Geotechnical Institute



# Acknowledgements

Margareta E. Eglit, Anders Elverhøi, Peter Gauer, Hansueli Gubler, Fridtjov Irgens, Tómas Jóhannesson, Thea Knudsen, Jean-Sébastien L'Heureux, Jim McElwaine, Arne Moe, Mohamed Naaim, Manuel Pastor, Mark Schaer

Fellowship fund of NGI

EU projects SATSIE, COSTA

Swiss National Science Foundation

Norwegian Research Council / Department of Oil and Energy

NILS Mobility Project



# Outline

- 0 Relevant scales
- 1 Brief introduction to the phenomenology
- 2 The practical needs...
- 3 A lesson to be learnt from statistical analysis
- 4 How to model flow-regime transitions in snow avalanches?
- 5 Erosion, entrainment and all that
- 6 Transformation of the flowing material



# 0. Relevant scales

Ambient fluid density	$1 \text{ kg/m}^3$ (air)	/	$1000 \text{ kg/m}^3$ (water)
Particle density	$300\text{--}1000 \text{ kg/m}^3$	/	$\sim 2500 \text{ kg/m}^3$
Particle concentration	$0.0001\text{--}0.6$		
Particle size	$10^{-4}\text{--}10^0 \text{ m}$		
Flow length	$10^0\text{--}10^6 \text{ m}$		
Flow depth	$10^{-2}\text{--}10^2 \text{ m}$		
Flow speed	$10^{-2}\text{--}10^2 \text{ m/s}$		
Flow duration	$10^1\text{--}10^5 \text{ s}$		



# 0. Relevant scales

Ambient fluid density	1 kg/m <sup>3</sup> (air)	/	1000 kg/m <sup>3</sup> (water)
Particle density	300–1000 kg/m <sup>3</sup>	/	~ 2500 kg/m <sup>3</sup>
Particle concentration	0.0001–0.6		
Particle size	10 <sup>-4</sup> –10 <sup>0</sup> m		
Flow length	10 <sup>0</sup> –10 <sup>6</sup> m		
Flow depth	10 <sup>-2</sup> –10 <sup>2</sup> m		
Flow speed	10 <sup>-2</sup> –10 <sup>2</sup> m/s		
Flow duration	10 <sup>1</sup> –10 <sup>5</sup> s		
Simulation duration	1–100 (occasionally 1000) s		
Number of grid cells	10 <sup>2</sup> –10 <sup>5</sup> (occasionally 10 <sup>6</sup> )		

# 1. Brief introduction to the phenomenology

- Snow avalanches  
(different release types, different flow types, erosion, «freak» behavior)
- Slush avalanches
- Subaerial and subaqueous debris flows  
(sorting, levée formation, flow transformation, excess pore pressure, hydroplaning)
- Quick-clay slides  
(remolding)

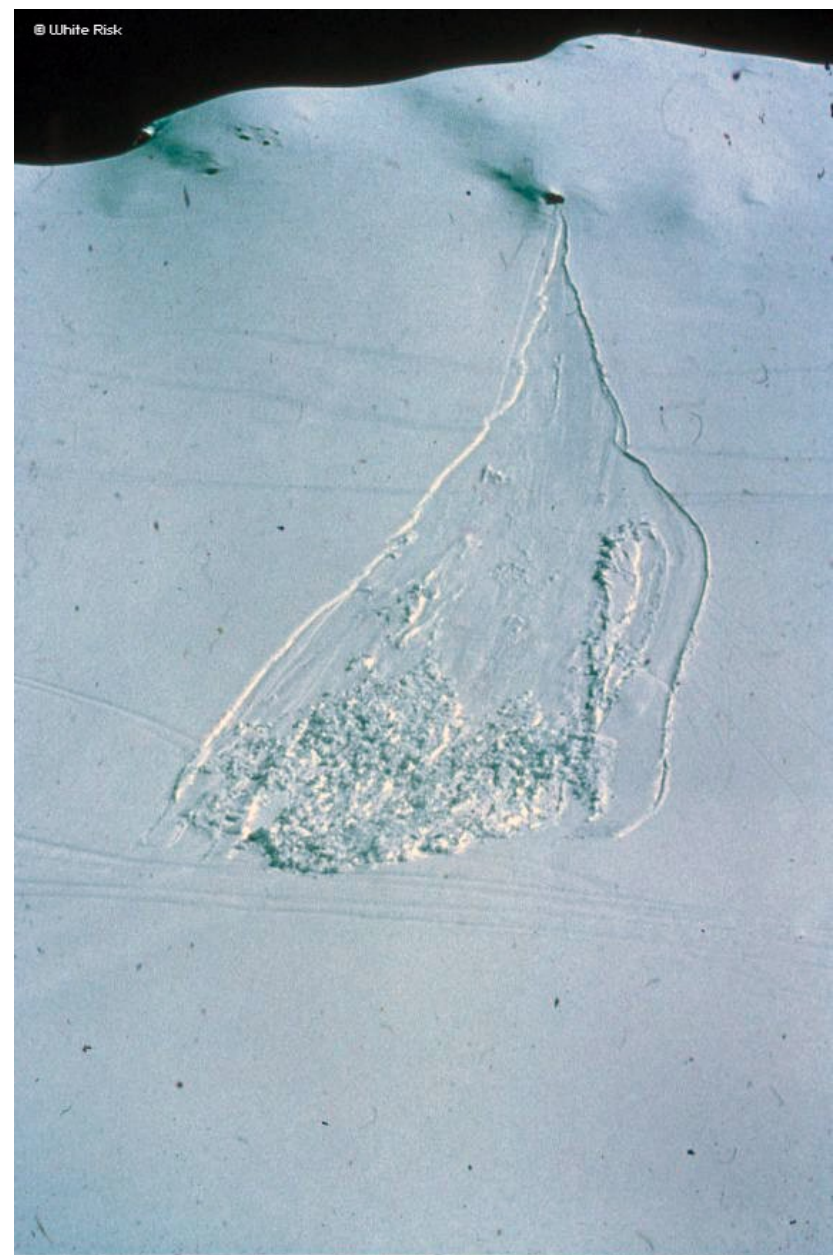
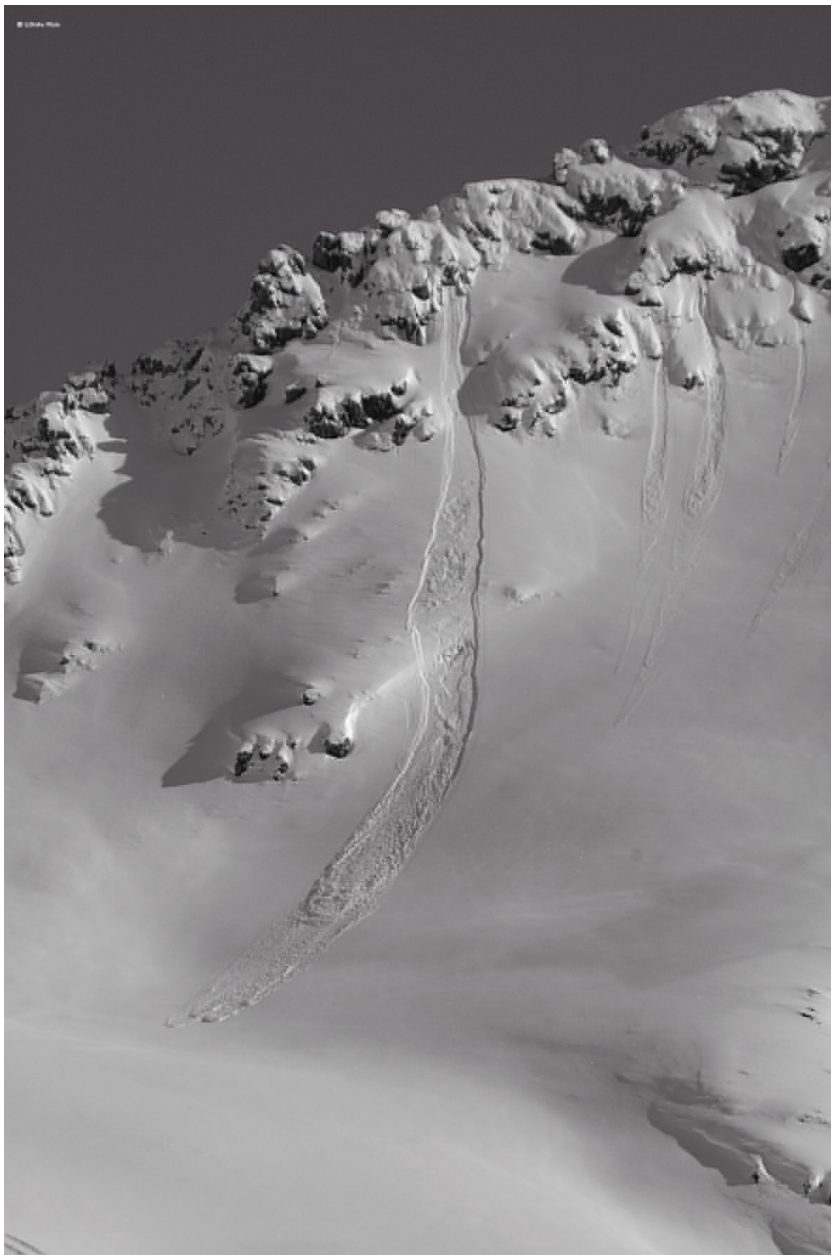


# Avalanche classification by release type

- *Point-release or loose-snow avalanches:*

Occur in early winter or spring, usually small and of restricted practical importance. Not very well studied.





Loose-snow avalanches (photos SLF)





Mini slides of loose snow inside an avalanche path. Photo D. Issler, 2005.

# Avalanche classification by release type

- *Point-release or loose-snow avalanches:*

Occur in early winter or spring, usually small and of restricted practical importance. Not very well studied.

- *Slab avalanches:*

Relatively hard layer on weak layer or interface, on 30–50° slopes. Shear fracture on sliding surface and sides, tensile fracture at crown.







Release area of a medium-size slab avalanche. Taferna path, Davos, Switzerland, February 2005. Photo J. Schweizer.





Photo C. Pielmeier, SLF

Primary release induced many secondary releases

NGI





Recent slab  
avalanches

Someone  
enjoying the  
snow conditions



About 2 s later

Heldiggris



NGI





Break-up of slab sets in very early.

Break-up energy is only a moderate fraction of the total potential energy.

# Avalanche classification by release type

- *Point-release or loose-snow avalanches:*

Occur in early winter or spring, usually small and of restricted practical importance. Not very well studied.

- *Slab avalanches:*

Relatively hard layer on weak layer or interface, on 30–50° slopes. Shear fracture on sliding surface and sides, tensile fracture at crown.

- *Slush avalanches:*

In water-saturated snowpack on gentle slopes (3–10°), mostly in (sub-)arctic areas or on glaciers. Share some features with slab avalanches. Needs more dedicated research and experiments.





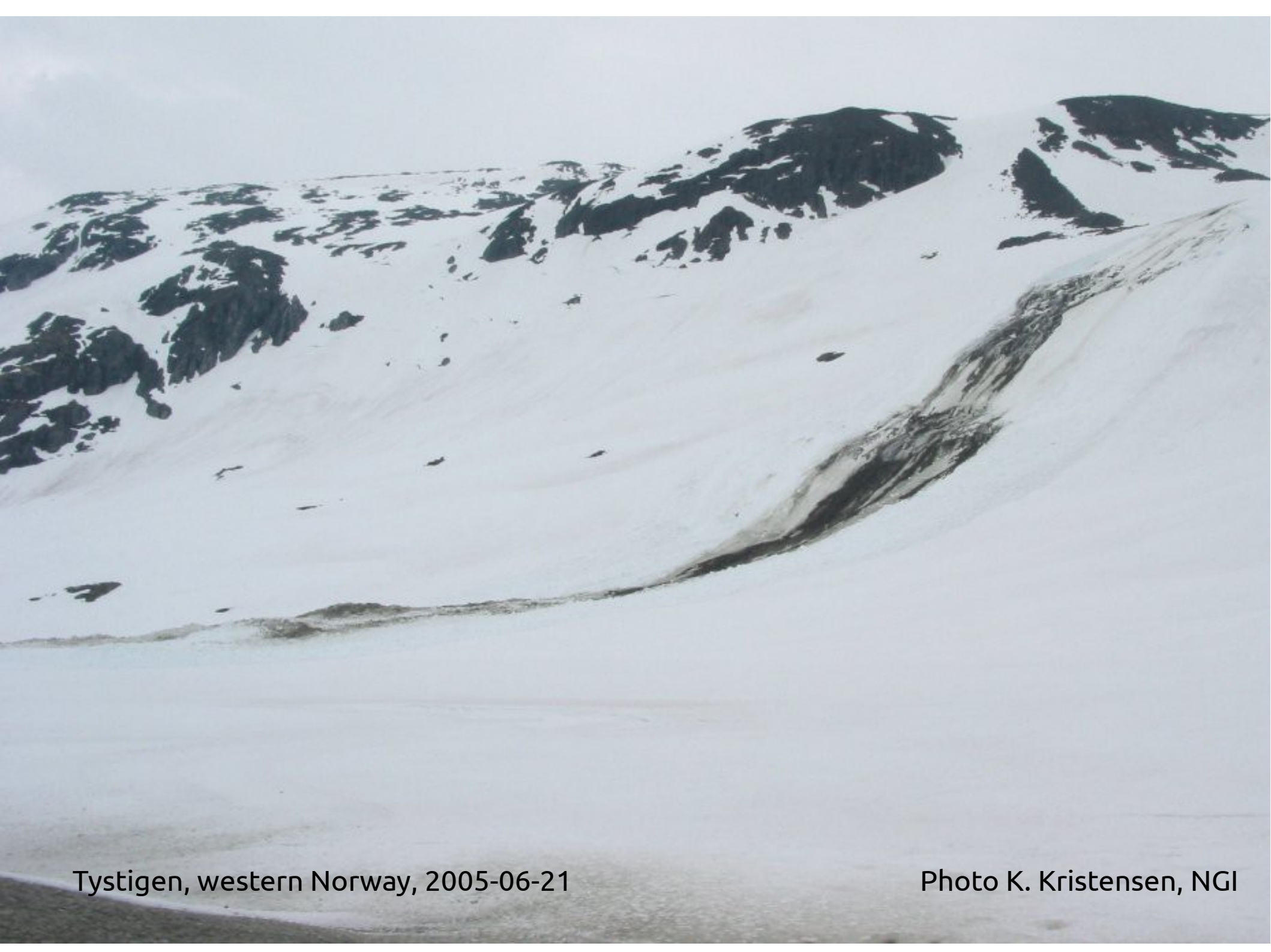


Telemark, south-eastern Norway. 28.04.1984. Photo Erik Hestnes, NGL.





Fivelstad, Stranda, western Norway. 05.02.1990. Photo Erik Hestnes, NGL.  
Extremely low runout angle and devastating effects.



Tystigen, western Norway, 2005-06-21

Photo K. Kristensen, NGI





Tystigen, western Norway, 2005-06-21

Photo K. Kristensen, NGI





Tystigen, western Norway, 2005-06-21

Photo K. Kristensen, NGI

# Flow regimes of snow avalanches

Behavior of snow avalanches in motion is varied because of

- differences in snow properties (dense/fluffy, wet/dry, clod size)
- differences in velocity (due to varying path steepness)

Avalanches in the same path may exhibit different flow regimes according to meteo-nivological conditions.

Flow regime may change in the course of an event.

Several flow regimes may be realized at the same time in different parts of an avalanche.

Flow regime has strong effect on runout, velocity and pressure of an avalanche.



- *Sliding wet-snow avalanches:*

Viscoplastic plug flow sliding on a plane (hard layer inside the snow cover, soil surface). Lubrification by a water film? Slow.





Indications of free  
water lubricating the  
flow.

10.06.2004

Längenboden near Davos, Switzerland. Photo Thomas Wiesinger, SLF





Photo D. Issler



Icy glide plane created by  
the avalanche through  
frictional melting and  
refreezing.

Photo D. Issler



- *Sliding wet-snow avalanches:*

*Viscoplastic plug flow sliding on a plane (hard layer inside the snow cover, soil surface). Lubrification by a water film? Slow.*

- *Granular wet-snow avalanches*

High *density*, coalescing particles. Flow is dominated by inter-particle friction. Slow.





Dorfberg, Davos, Switzerland, 2005-03-20. Photo H. Gubler





Dorfberg, Davos, Switzerland, 2005-03-20. Photo H. Gubler



Dorfberg, Davos, Switzerland. Photo SLF



- *Sliding wet-snow avalanches*

Viscoplastic plug flow sliding on the bed (hard layer in snow pack or soil), possibly lubricated by water film. Slow.

- *Granular wet-snow avalanches:*

High density, coalescing particles. Flow is dominated by inter-particle friction. Slow.

- *Dense dry-snow avalanche:*

High density. Particles fracture due to friction or collisions. Inverse grading may occur. Moderate velocities.







Flow direction

Dense granular deposit

What happened here???  
Massive erosion (0.5–1 m),  
no deposit.





Often very hard deposits with  
embedded snowballs and/or topsoil

- *Sliding wet-snow avalanche*

Viscoplastic plug flow sliding on the bed (hard layer in snow pack or soil), possibly lubricated by water film. Slow.

- *Granular wet-snow avalanche*

High density, coalescing particles. Flow is dominated by inter-particle friction. Slow.

- *Dense dry-snow avalanche:*

High density. Particles fracture due to friction or collisions. Inverse grading may occur. Moderate velocities.


- *Fluidized dry-snow avalanche:*

Medium density, wide particle size distribution. High speed.



*Example: 1995 Albristhorn avalanche, Switzerland*

 Deposit area of dense flow

 Deposit of fluidized layer

Powder-snow deposit extends ~ 500 m to left (uphill).

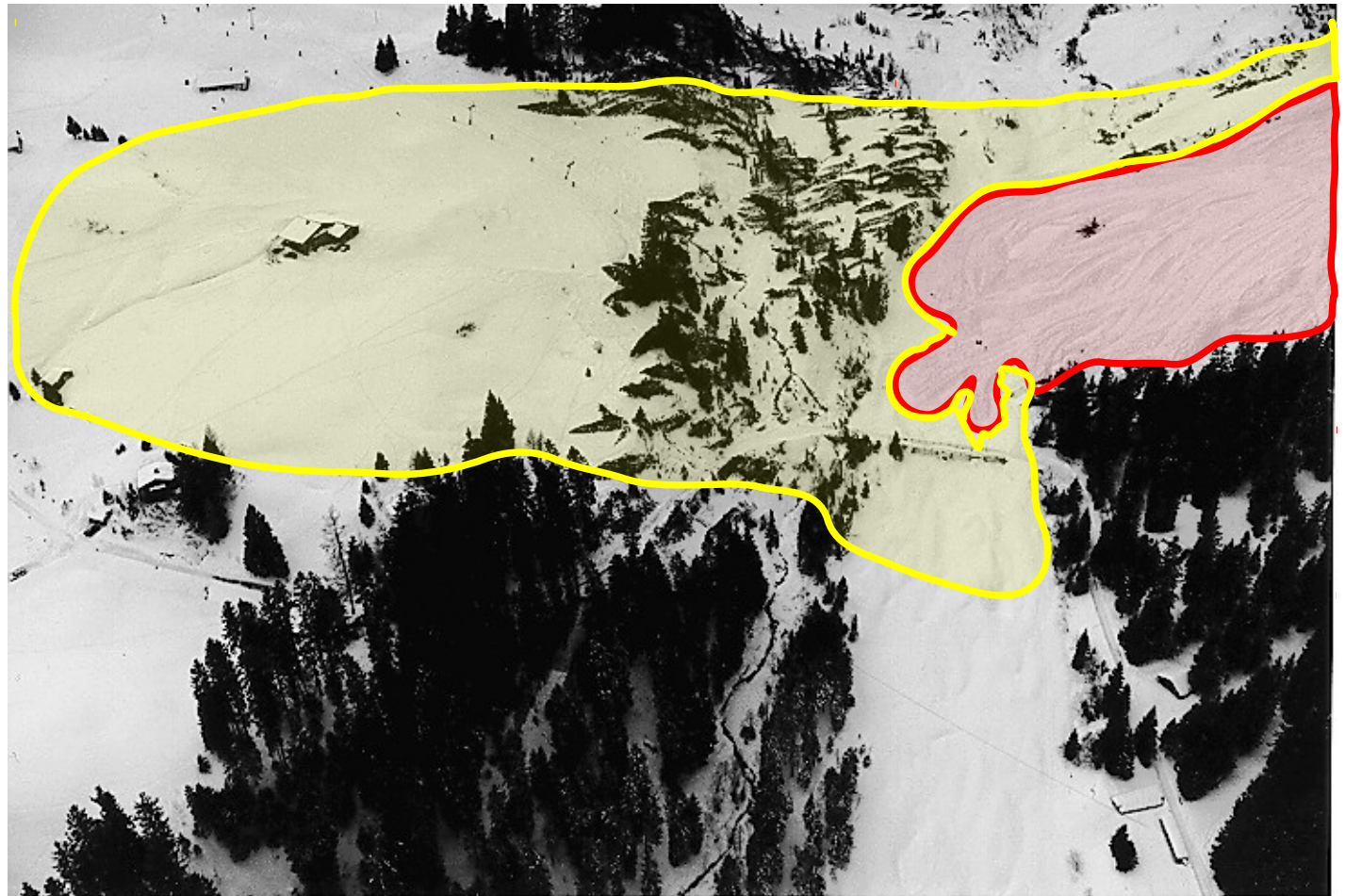
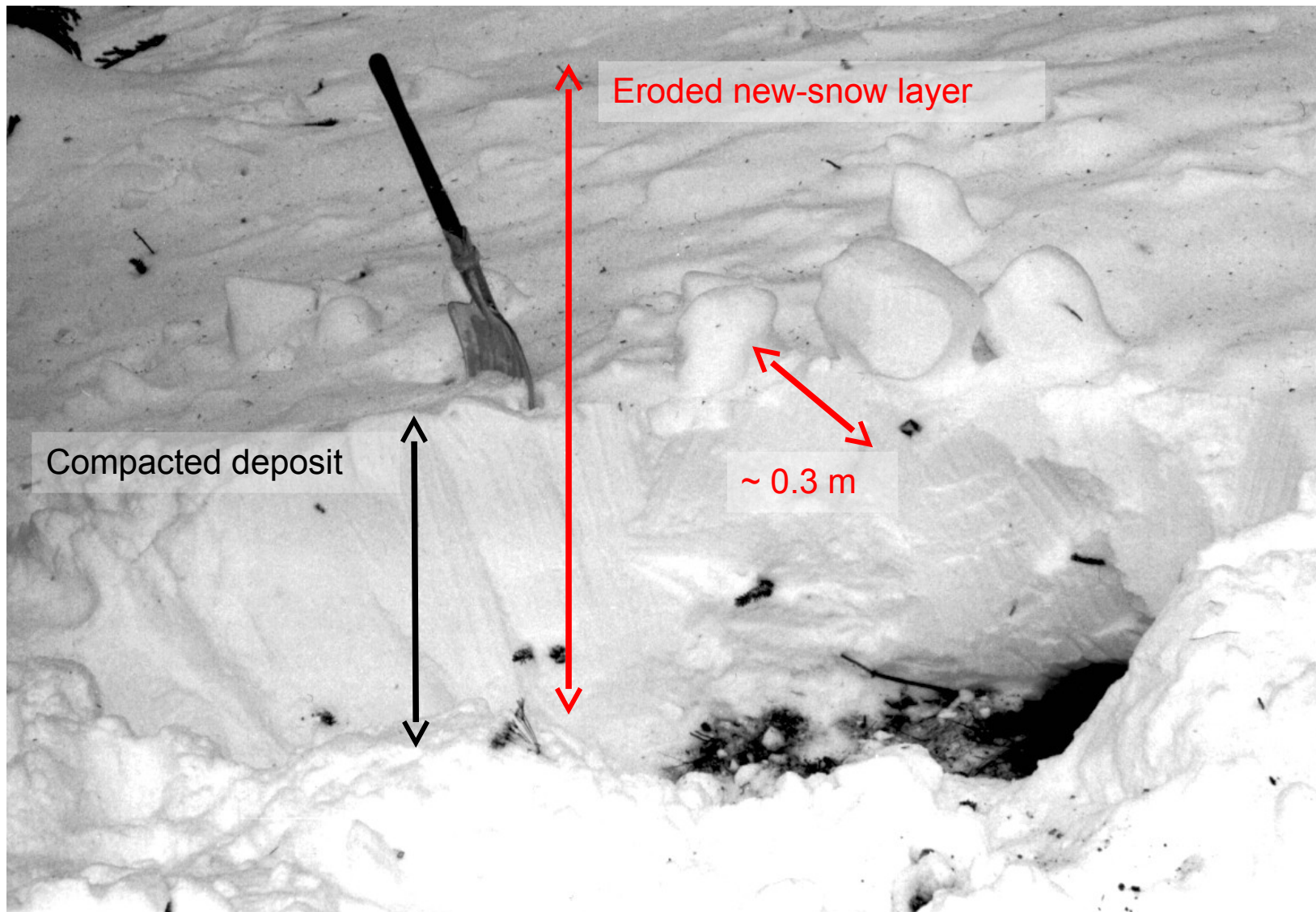


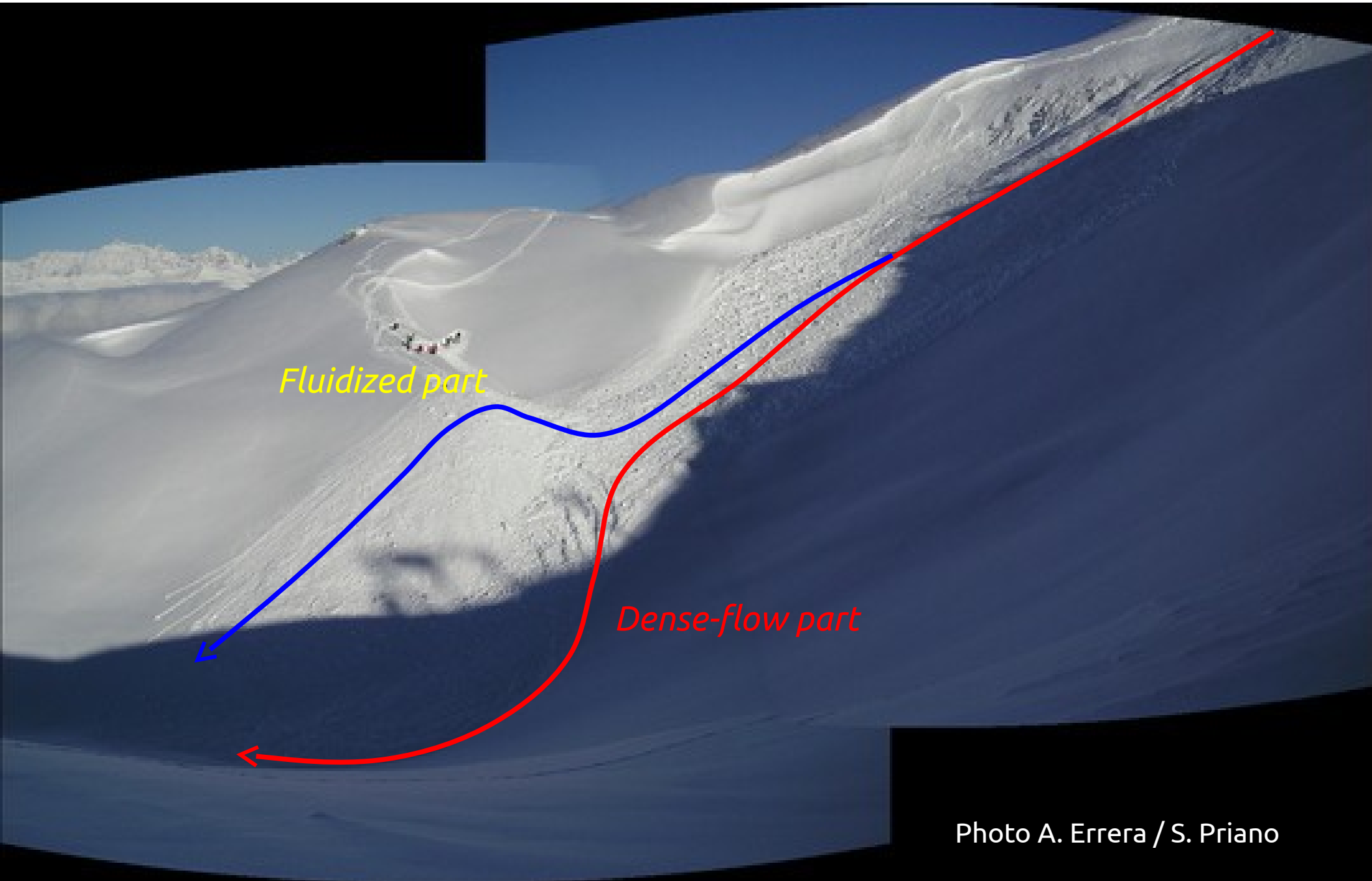
Photo S. Keller





Deposit of a small mixed avalanche, photo taken in a region not reached by dense flow (after sharp bend of gully). Photo M. Schaer, SLF.

Even small avalanches may develop a highly mobile fluidized part.





## Small avalanche in Davos:

- *Drop height* ~ 100 m
- Ratio of fluidized to total mass approx. 1%
- Fluidized front approx. twice as fast as dense part
- Fluidization does occur in small avalanches, but is more important in large ones.

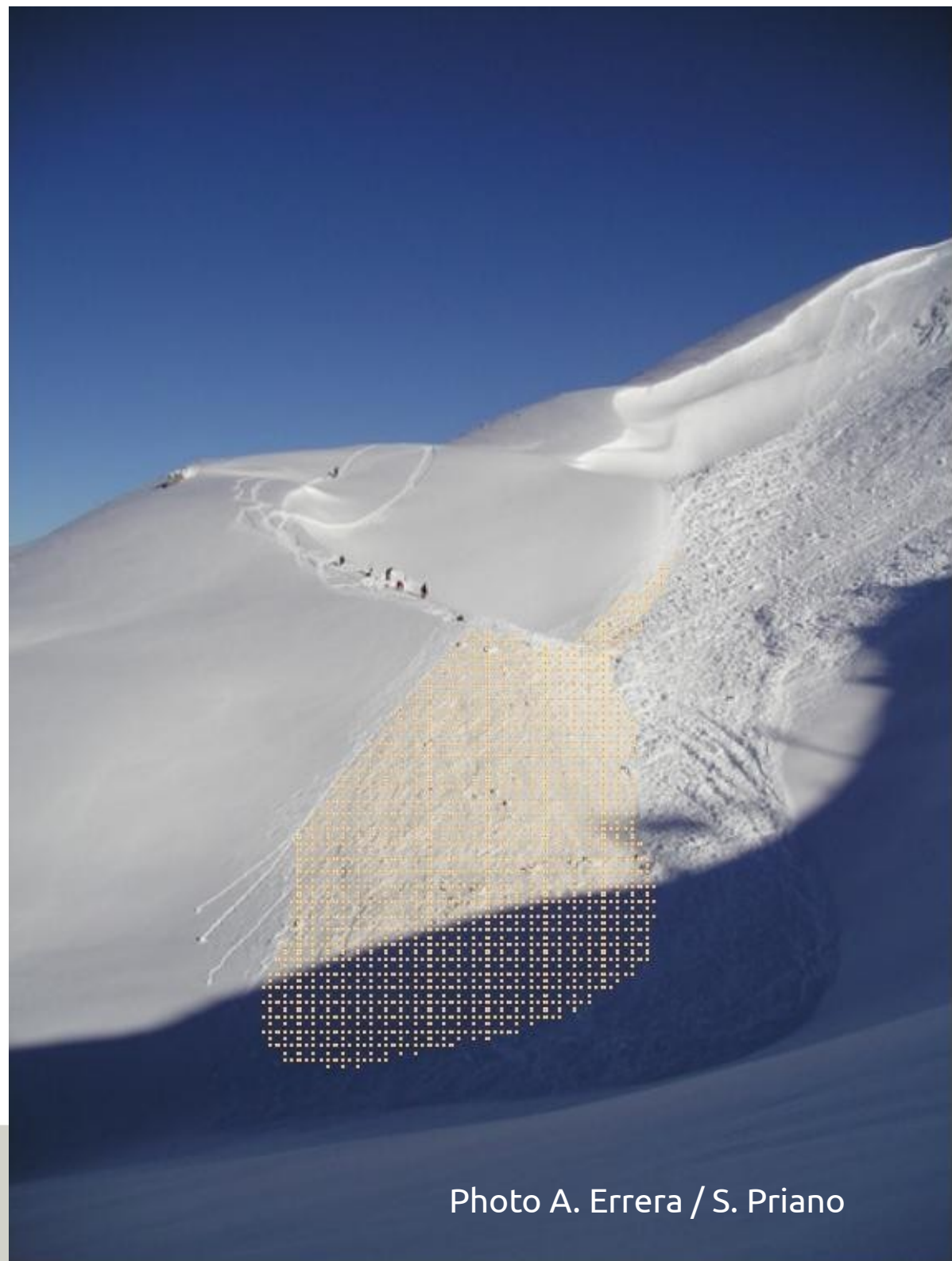


Photo A. Errera / S. Priano



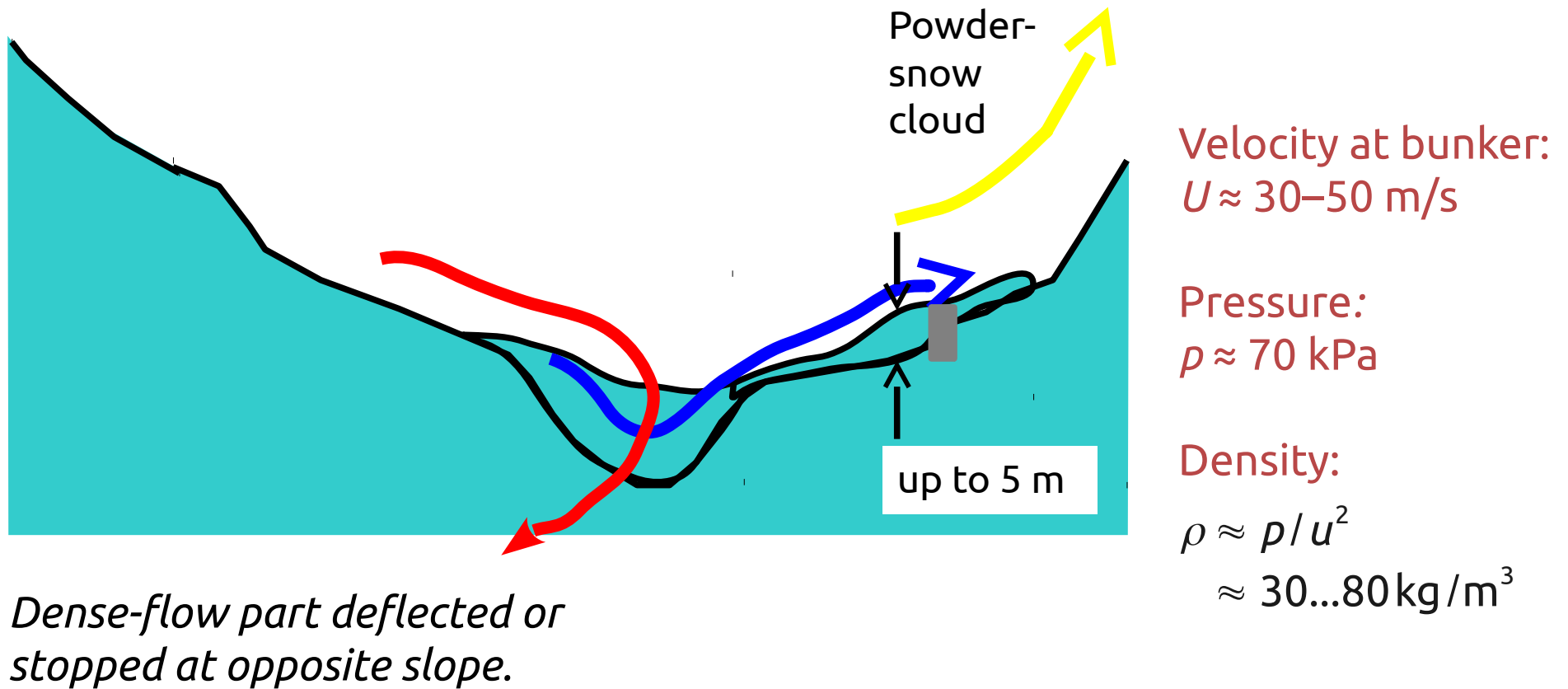
Photos: <http://www.geodar.net>, SLF



NGI

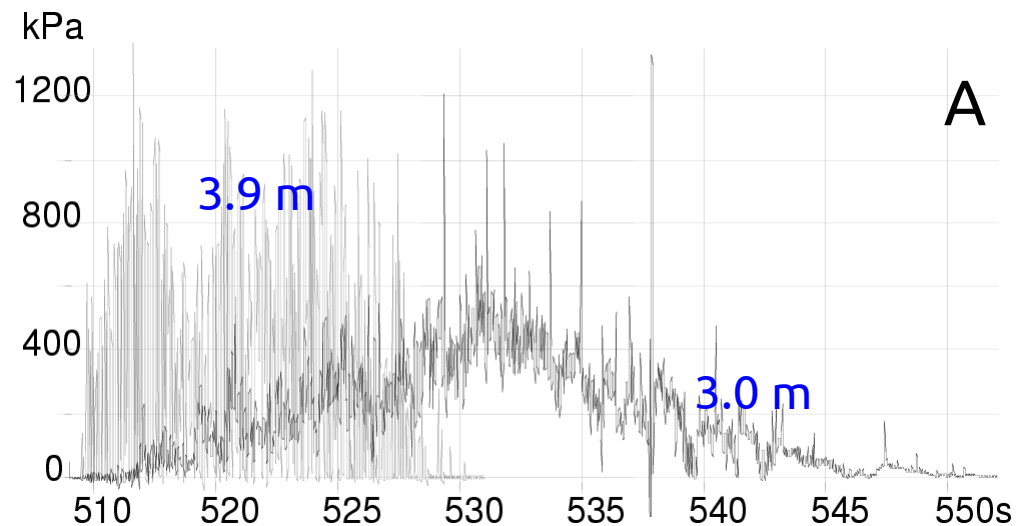


1999-02-25: *Why was the bunker at Vallée de la Sionne **not** destroyed?*

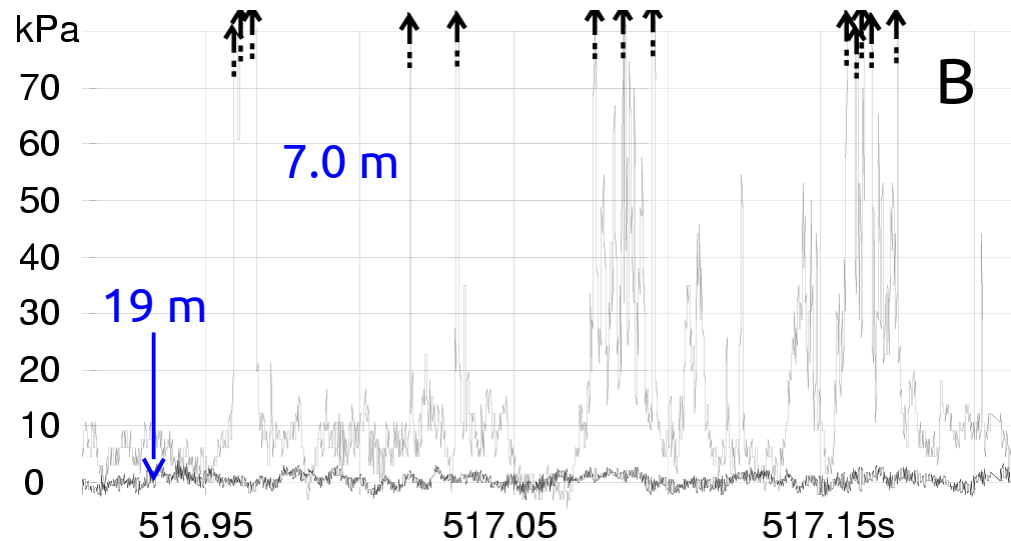


*Density of fluidized layer  $\ll$  Density of dense flow.*

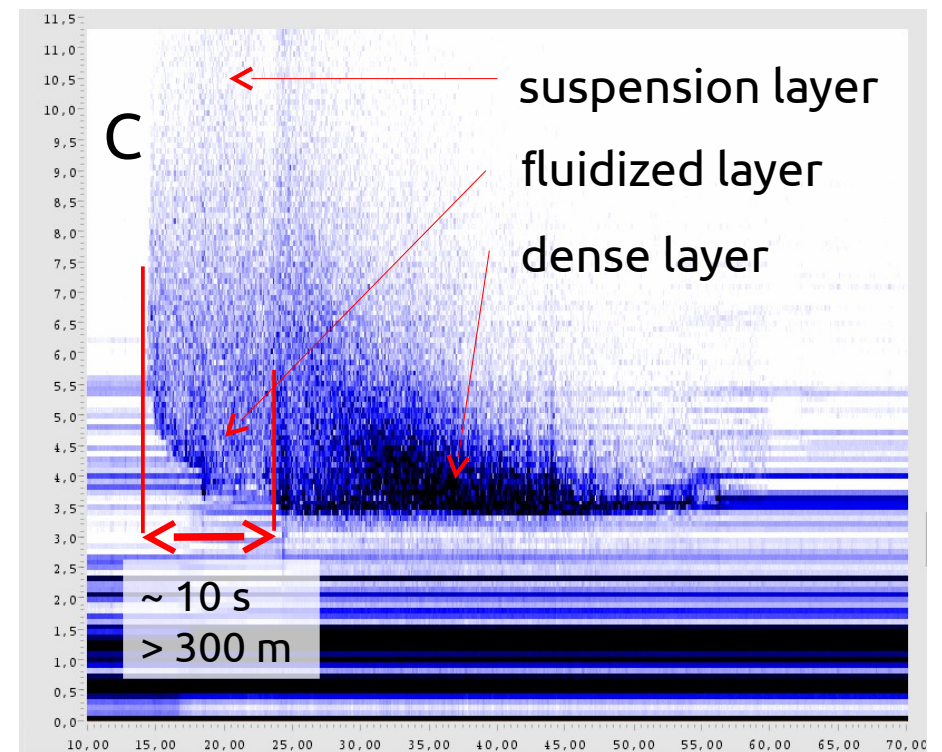
1999 measurements at Vallée de la Sionne  
(from Schaer and Issler (2001). *Annals Glaciol.* **32**)



Load cell measurements



FMCW radar profile





### *Explanation of the preceding slide (1):*

Plots A and B show the pressure time series during the passage of a large mixed dry-snow avalanche.

- At 3 m, very high mean pressures superposed by violent short-term fluctuations.  
→ Dense part arrives much later than the front.
- At 3.9 m, some pressure peaks exceed 1 MPa, but pressure drops to near zero between impacts.  
→ Fluidized layer, moderate density, impact of snowballs up to 30 cm at ~ 40–50 m/s.
- At 7 m, intermittent swarms of impacts up to ~100 kPa.  
→ Fluidized layer, smaller particles and lower density.
- At 19 m, turbulent eddies O(1kPa) from the suspension layer.  
→ Small snow grains, low density, moderate velocity.

### *Explanation of the preceding slide (2):*

Plot C is the time-series of the output of a profiling radar looking upward from a cavern in the ground. Abscissa – time; ordinate – distance from ground; darkness – strength of echo from the respective distance.

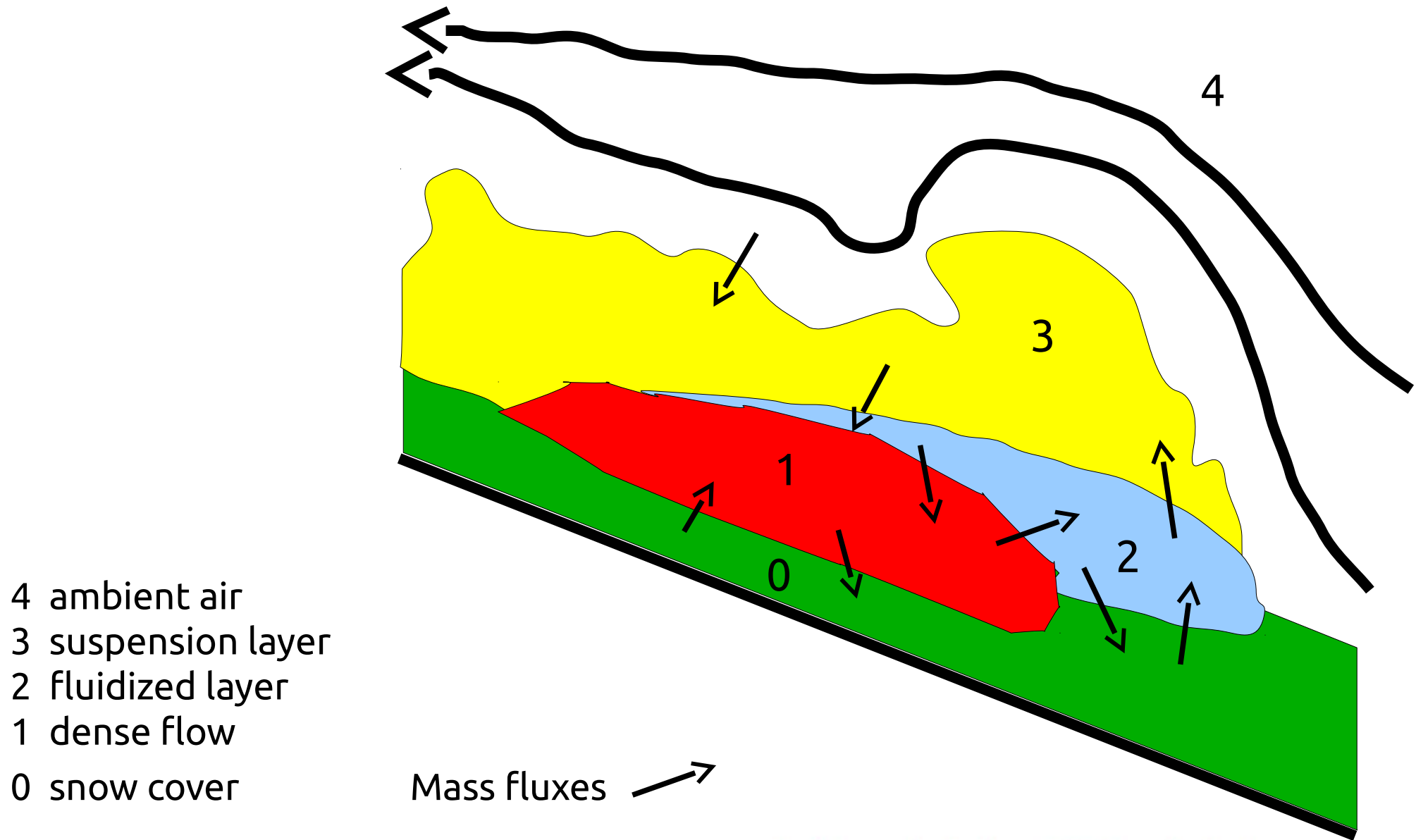
- The echo strength is in agreement with the schematic avalanche structure proposed below.  
Dense part moves much more slowly than fluidized layer.
- Approx. 2 m of snow cover are eroded during the first 10 s, i.e. during the passage of the fluidized head. Erosion rate up to  $250 \text{ kg}/(\text{m}^2\text{s})$ .

Snow entrainment is a very important, but poorly understood process in avalanche flow.



- *Sliding wet-snow avalanches:*  
Viscoplastic plug flow sliding on the bed (hard layer in snow pack or soil), possibly lubricated by water film. Slow.
- *Granular wet-snow avalanches:*  
High density. Coalescing particles, frictional flow regime, inverse grading. Slow.
- *Dense dry-snow avalanche:*  
High density, fracturing particles, frictional to collisional flow regime. Inverse grading may occur. Moderate velocities.
- *Fluidized dry-snow avalanches:*  
Medium density, various particle sizes, collisional to inertial flow regime. High velocities.
- *Powder snow avalanches:*  
Low density, small particles suspended by turbulence in the air. Particle collisions negligible. Boussinesq or non-Boussinesq.

## Present view of avalanche structure





## Order-of-magnitude estimates:

<i>Flow type</i>	<i>Density</i>	<i>Concentration</i>	<i>Mean free path</i>	<i>Granular flow regime</i>
	(kg/m <sup>3</sup> )	(—)	(Particle diam.)	
Dense	100–500	0.1–0.6	0–1	Frictional/ collisional
Fluidized	10–100	0.01–0.1	1–4	Collisional/ grain-inertial
Suspension	1–10	$< 10^{-2}$	$> 4$	Macro-viscous (turbulent)

Physical properties and transport processes differ substantially between flow types!



## Entrainment and deposition

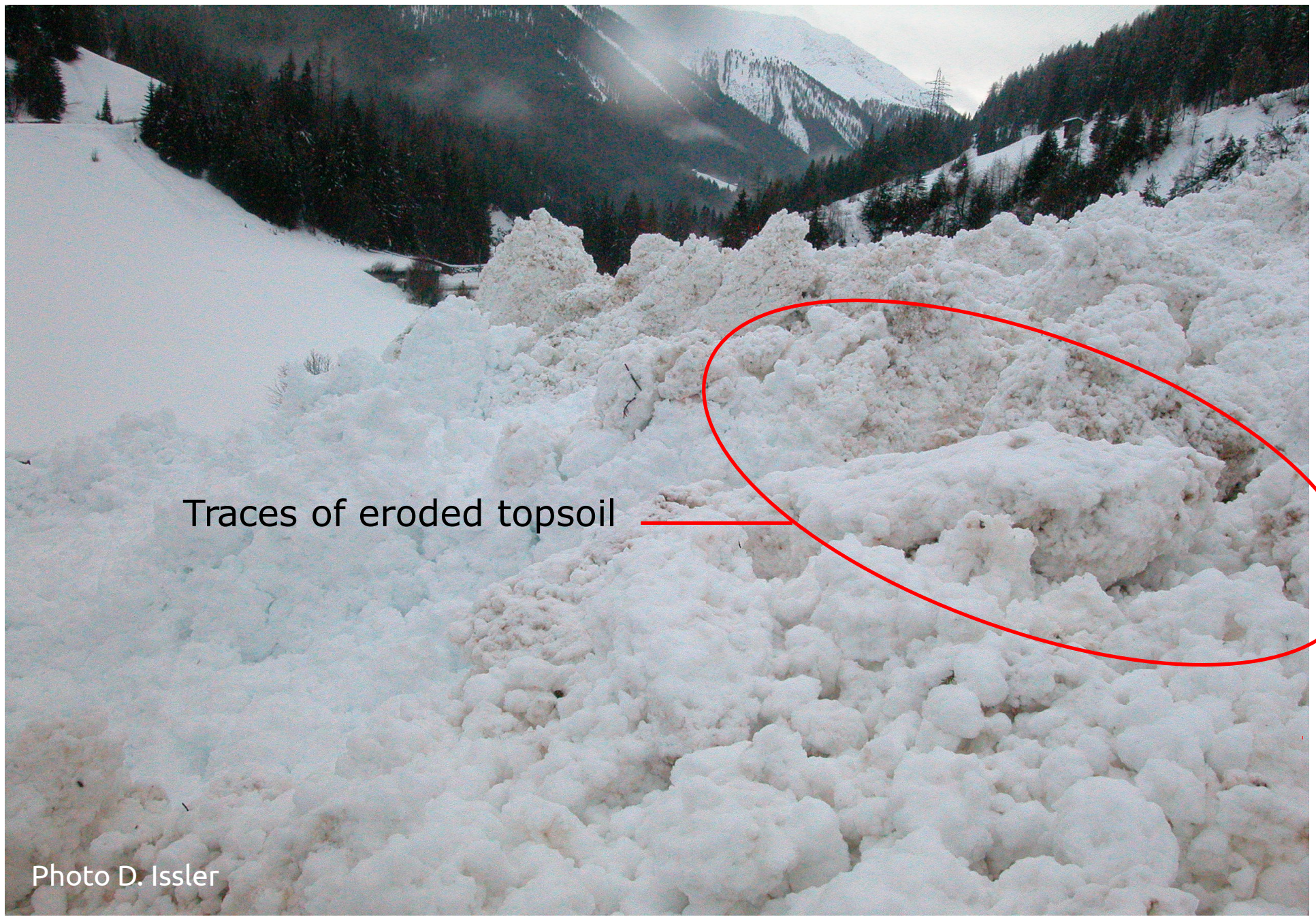
- Typical shear strength of fresh snow:  $\tau_s = 0.1\text{--}2 \text{ kPa}$ ,  
Typical grav. traction on avalanche:  $\rho g h \sin \theta = 0.5\text{--}3 \text{ kPa}$ .
- ⇒ Entrainment of snow cover is rule rather than exception!
- Typical starting zone is 5–30% of path length.
- ⇒ Avalanche mass may increase by large factor!
- Entrainment has a substantial effect on the flow dynamics (flow height, velocity, runout distance, impact pressure).
- Entrainment mechanisms are still poorly understood and crudely modeled (or neglected) in most models.





Mini slides of loose snow inside an avalanche path. Photo D. Issler, 2005.





Traces of eroded topsoil

Photo D. Issler

NGI



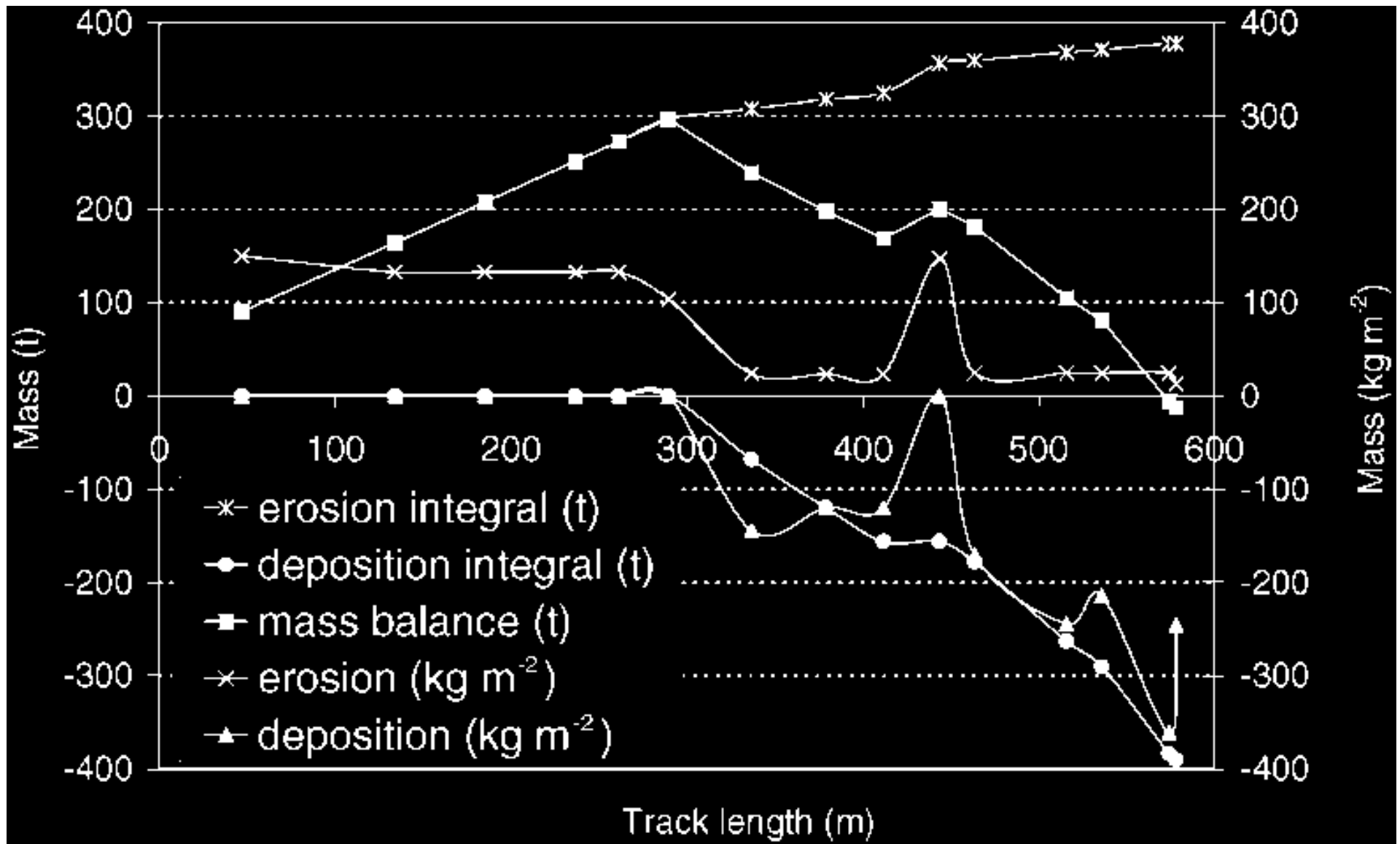


Dorfberg, Davos, Switzerland, 2005-03-20.

Photo Hansueli Gubler



## Spatial mass balance in a snow avalanche (Monte Pizzac test site, Italy, 1998)



From Sovilla et al., *Annals Glaciol.* **32** (2001), 230–236.

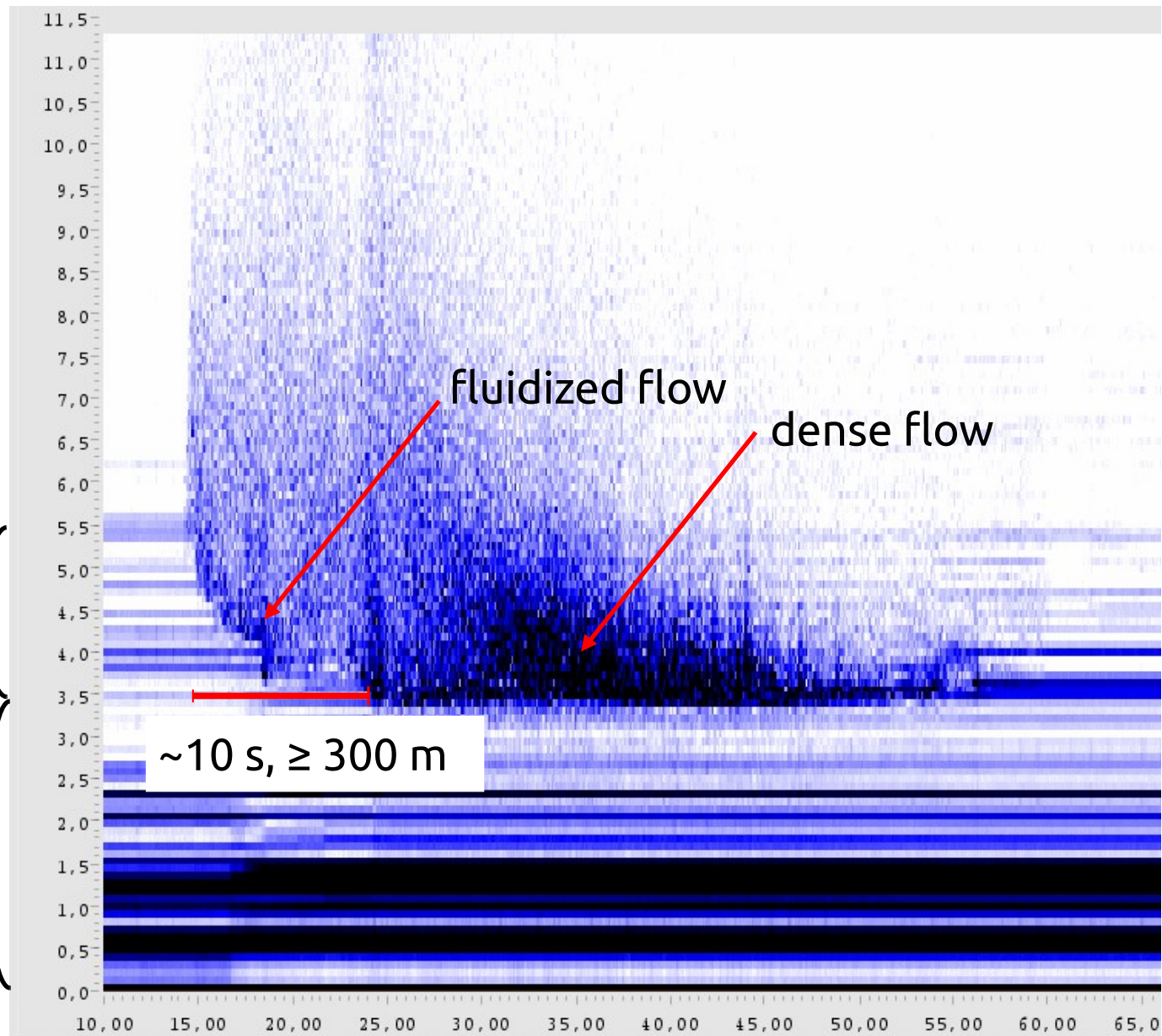
# FMCW radar plot of snow avalanche at Vallée de la Sionne

Observed entrainment rate:

**10–200 kg m<sup>-2</sup> s<sup>-1</sup>,**  
diminishing with time  
and erosion depth.

2 m of fresh snow eroded

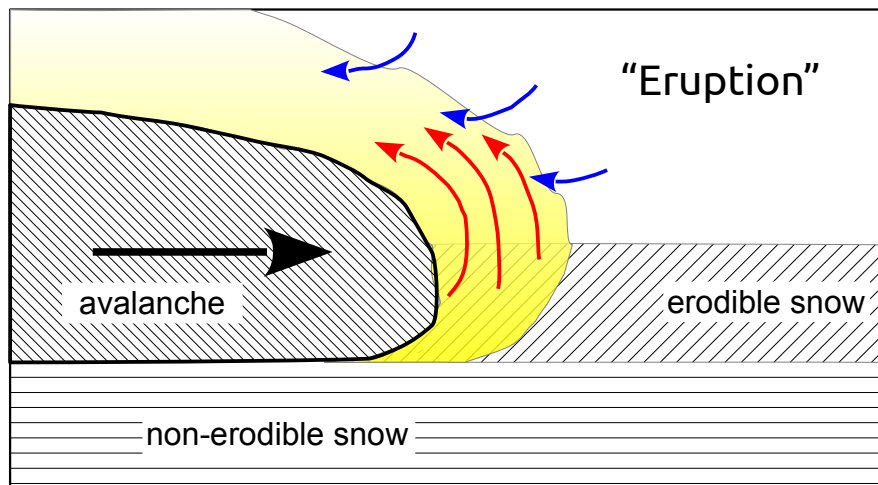
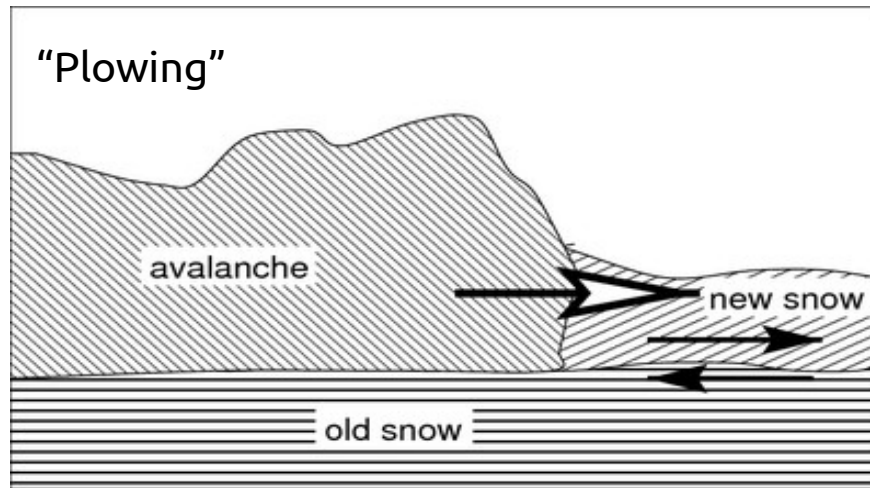
Hard old snow not eroded



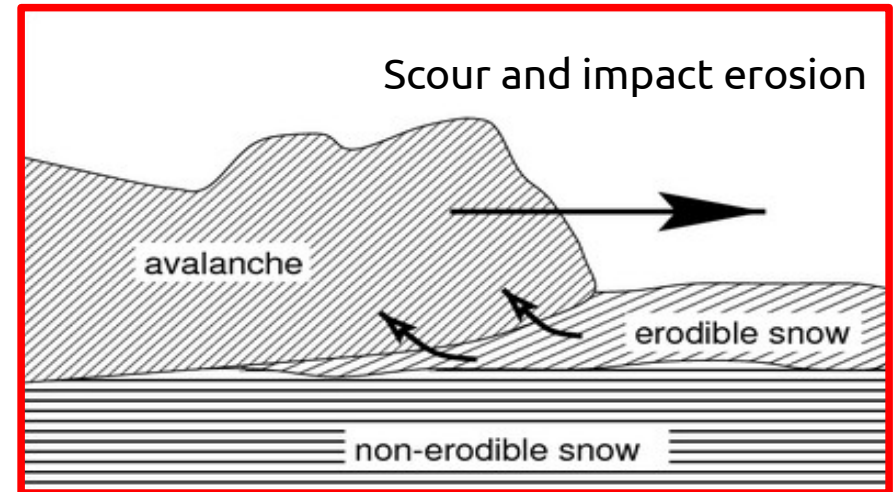
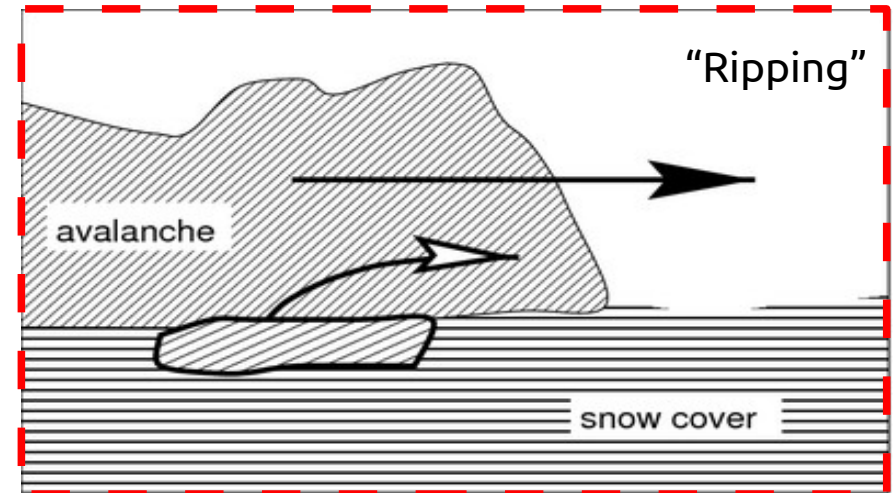


# Conjectured erosion mechanisms (Gauer & Issler, 2004)

## Frontal mechanisms



## Mechanisms acting along bottom



## The plowing mechanism:

- Clearly dominant in wet-snow avalanches.
- Possibly important in dry-snow avalanches as well, but clear experimental confirmation is still lacking.
- Open question for debris flows and pyroclastic flows.
- Likely condition for plowing to be possible: Flowing material must have higher strength than bed and sufficient weight.
- In laboratory granular flows, length of plowing zone =  $O(\text{flow height})$ .





## Observation of impact and abrasion traces



Ryggfonn 2003-04-6. Photo P. Gauer



Klosters 2006-03-12. Photo D. Issler

## Watch out for freak avalanches!

Some avalanches do things that even a seasoned expert may consider impossible (but the avalanche doesn't care what the expert thinks!!!).

Important in hazard mapping to consider these possibilities. Need both experience and physical insight.

“Freak behavior” in snow avalanches can be due to e.g.:

- Run-up height of fluidized and suspension layer
- Particular snow conditions
- Discontinuous behavior due to thresholds
- Funnel effects (?)







Brenva avalanche, Courmayeur, Italy, 1997-01-18. Image 1/4. Photographer unknown.

NGI

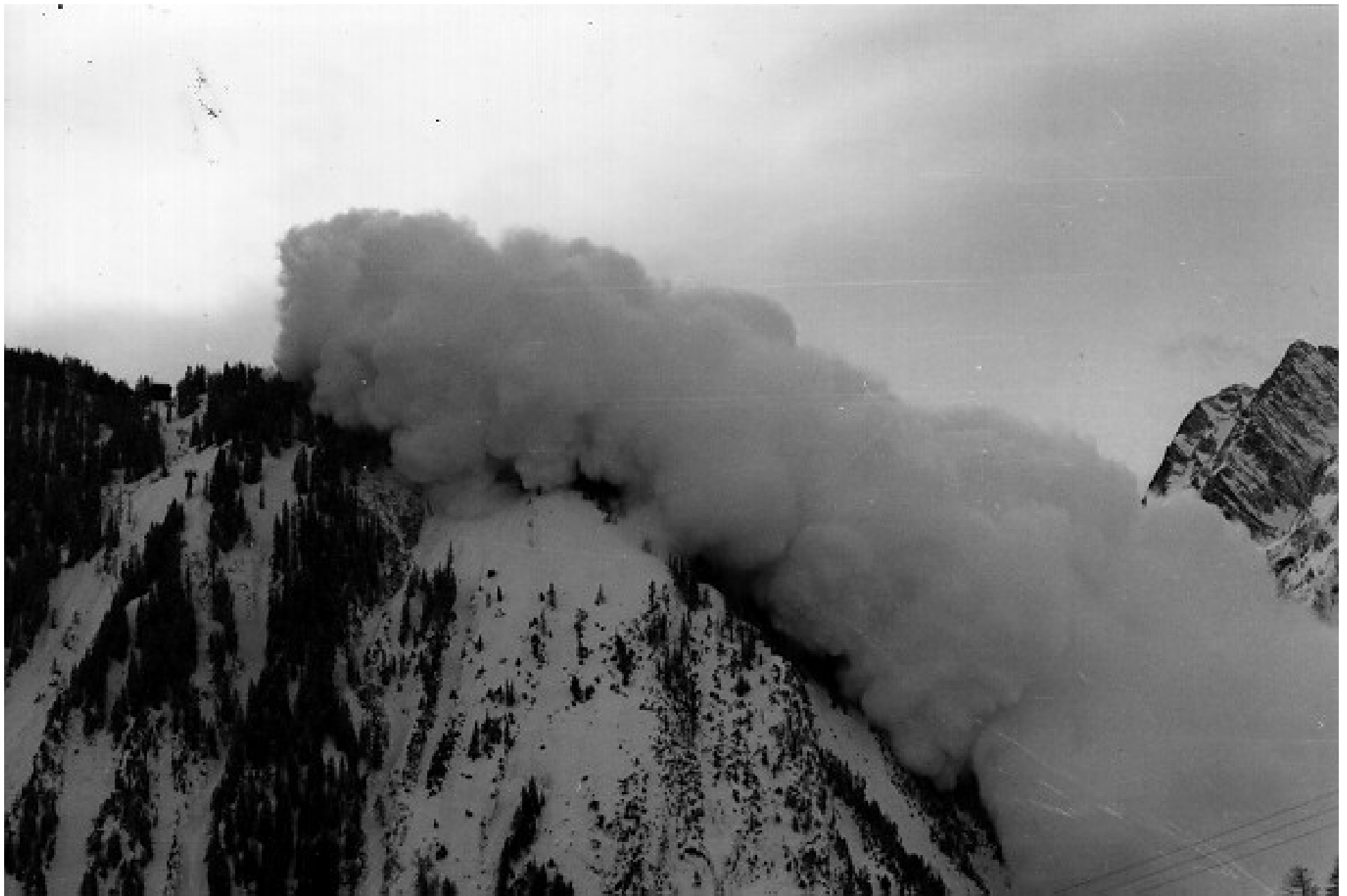


Brenva avalanche, Courmayeur, Italy, 1997-01-18. Image 2/4. Photographer unknown.





Brenva avalanche, Courmayeur, Italy, 1997-01-18. Image 3/4. Photographer unknown.



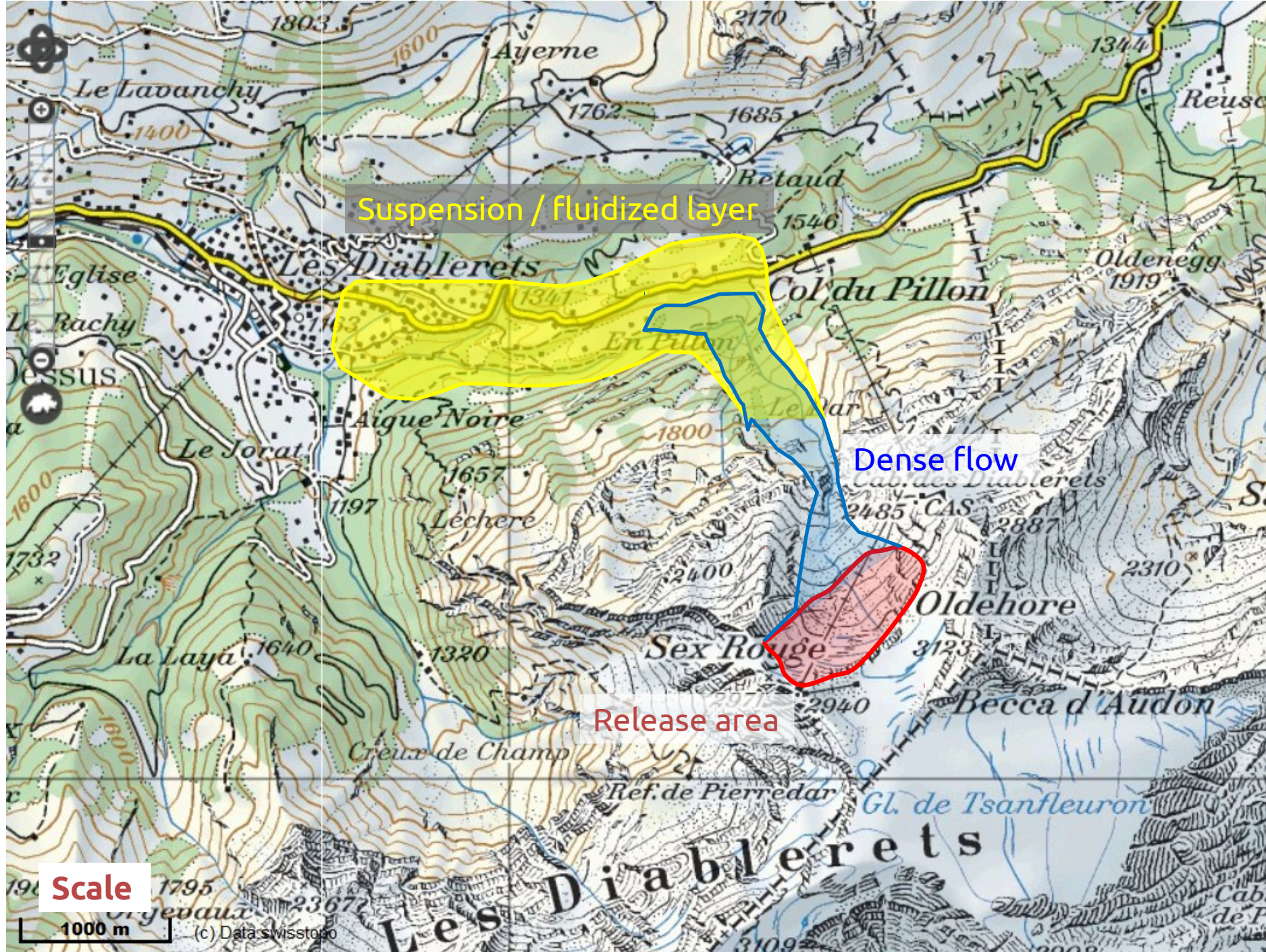
Brenva avalanche, Courmayeur, Italy, 1997-01-18. Image 4/4. Photographer unknown.

Some avalanches start with just a snowcat and become pretty large...

Example: *Col du Pillon*, western Switzerland, 1995-01-31

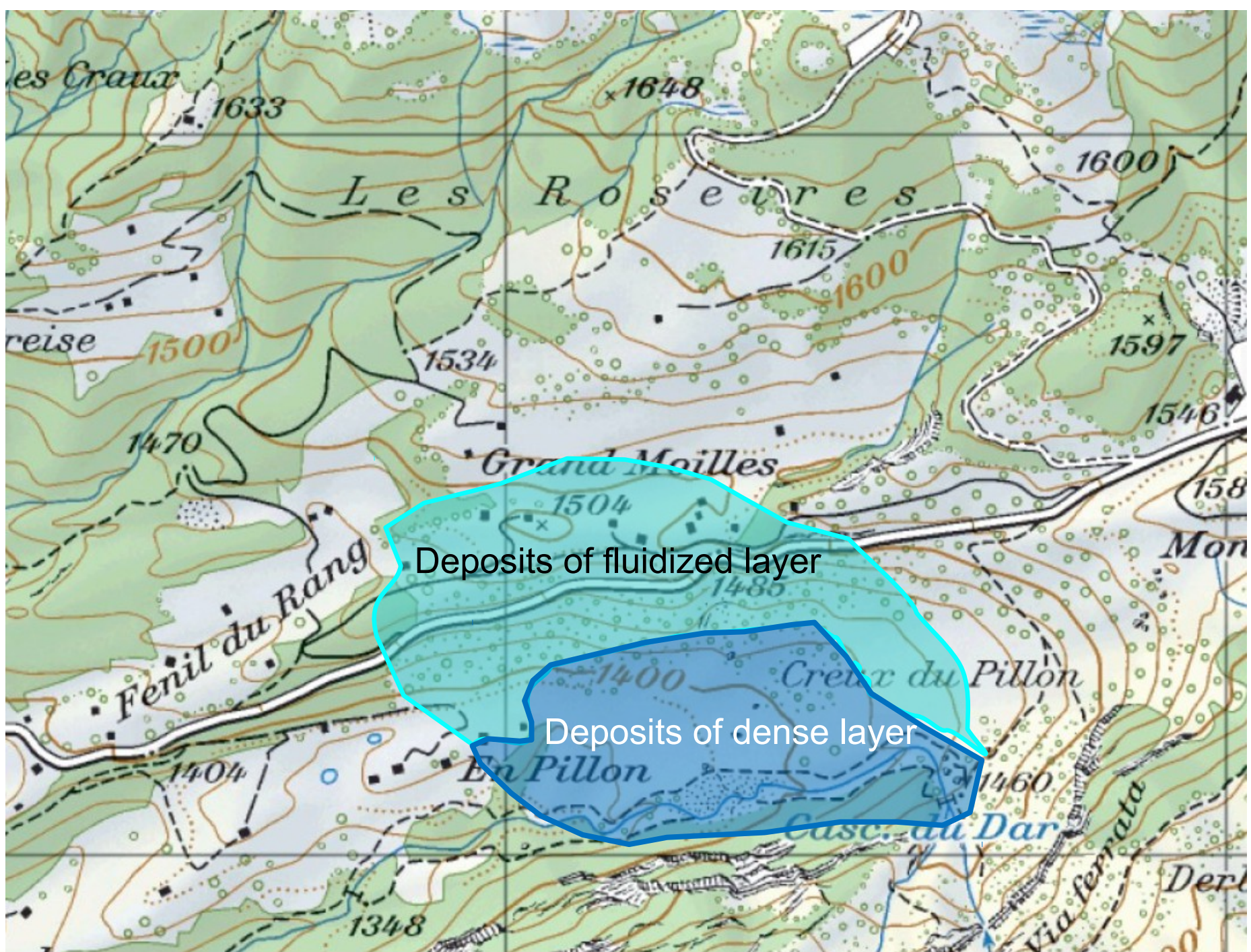
- Released when clearing snow from the entrance to the telepherique at ~ 2950 m a.s.l.
- Release mass approx. 2 mill. m<sup>3</sup>
- Dense flow deposit at ~1400 m a.s.l., depth up to 10 m
- Run-up of fluidized layer on opposite slope ~ 120 m, deposit depth on pass road up to 3 m over a length of 800 m, ~ 0.5 m on plateau
- Powder-snow cloud continued down the valley flank (without damage) for ~ 5 km





NGI







Wet-snow avalanches do not always follow straight lines...



Dorfberg, Davos, Switzerland. Photo SLF



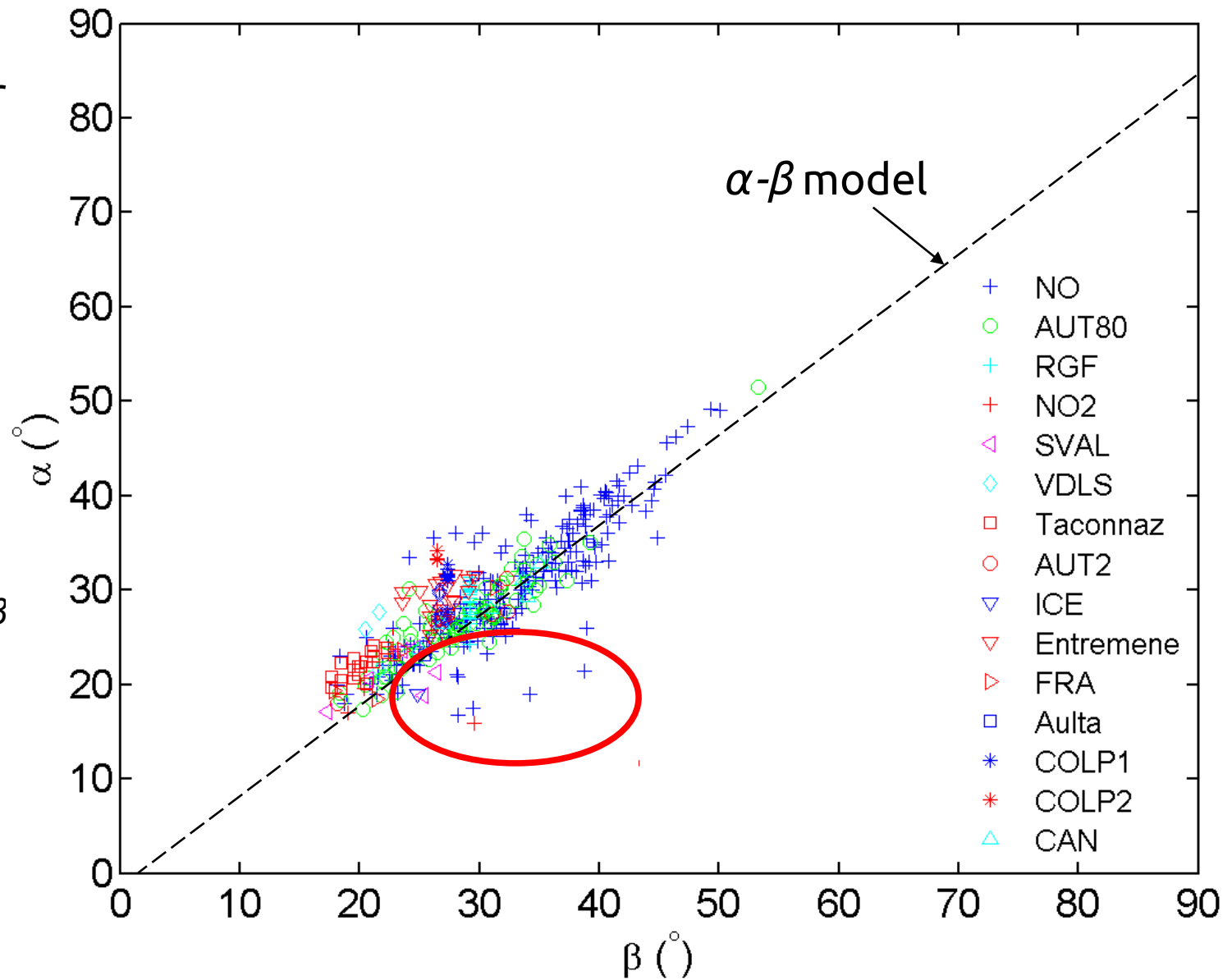
## Avalanches with very low values of run-out angle $\alpha$

Some avalanches have *much* longer runout than expected from topographic-statistical model.

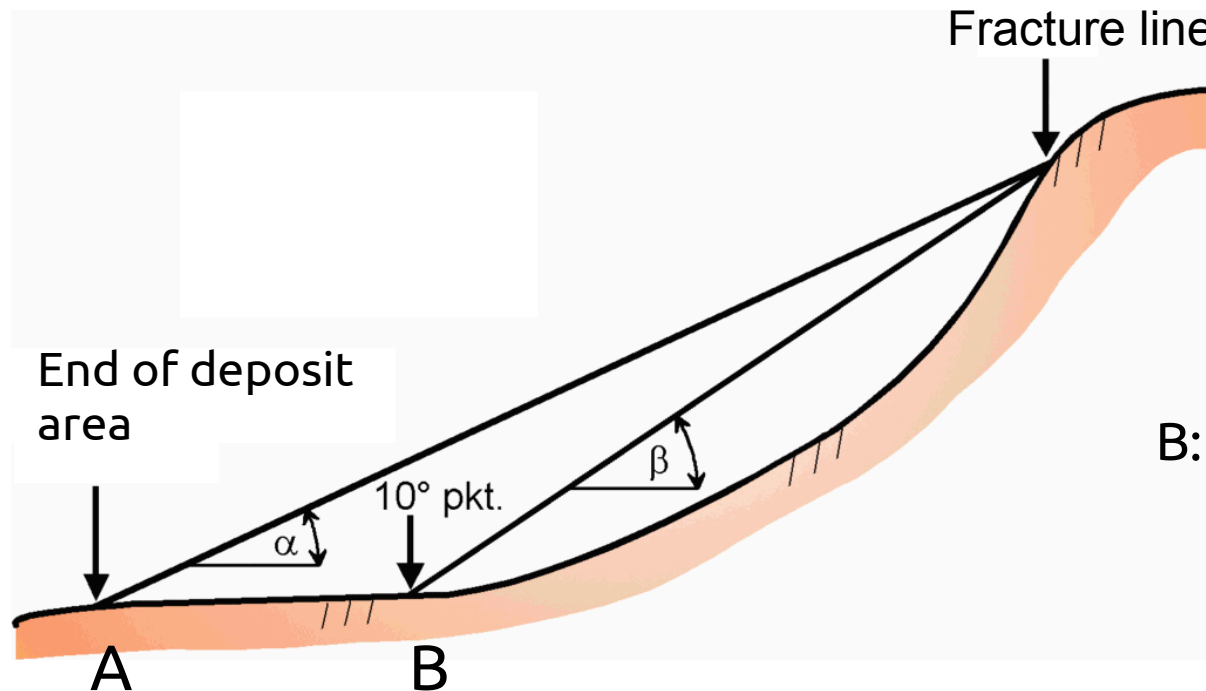
$\alpha = 14\text{--}16^\circ$  in extreme cases!

(See next slide for  $\alpha$ - $\beta$  model.)

Plot courtesy  
P. Gauer, NGI



# The statistical-topographical $\alpha$ - $\beta$ model (Lied and Bakkehøi, 1980)



B: Point where the slope angle falls below 10° (considered as beginning of run-out zone).

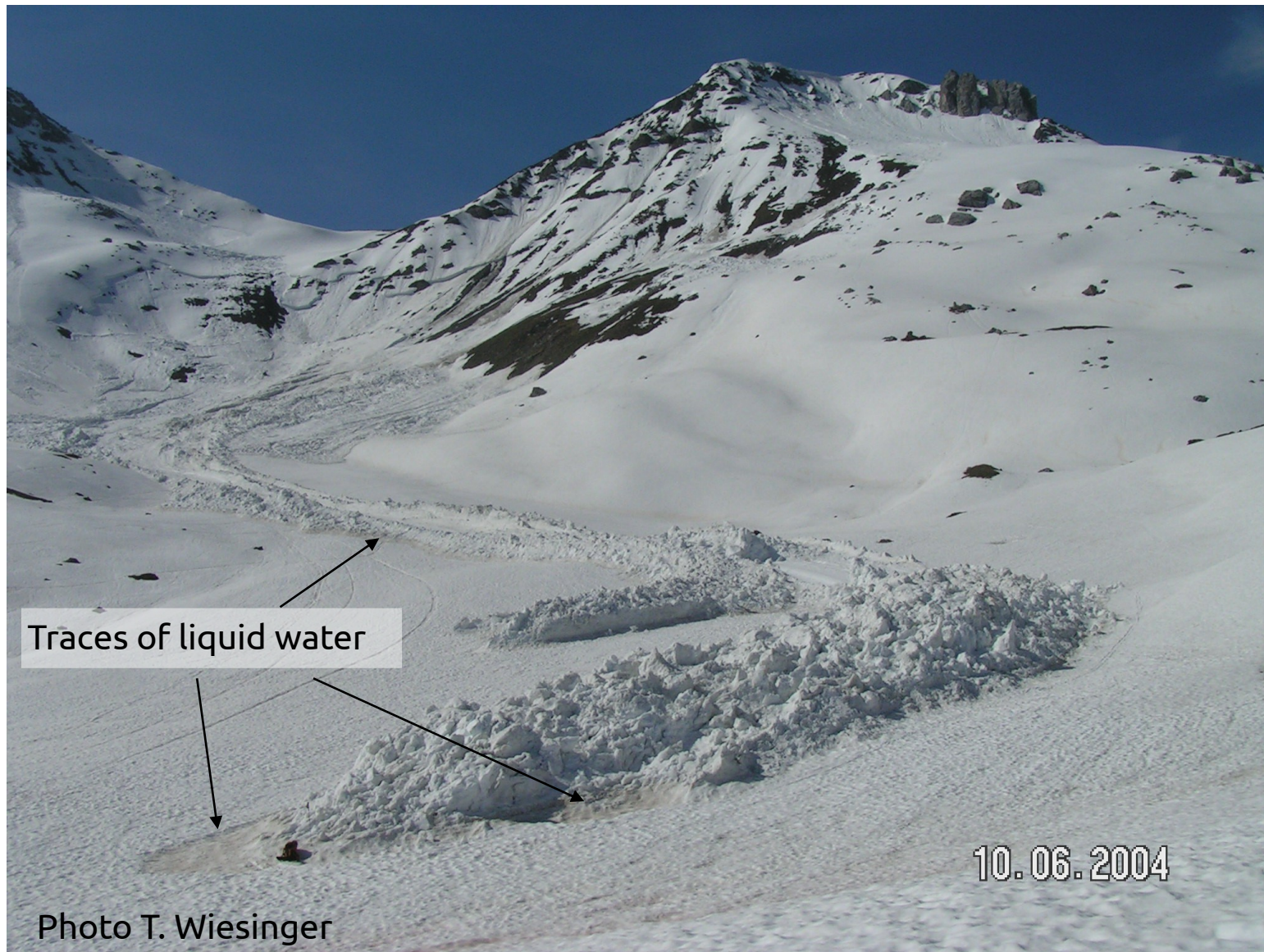
Norway:  $\alpha = 0.96 \beta - 1.4^\circ$ ,  $SD = 2.3^\circ$ ,  $R = 0.92$  (~ 200 avalanches)

Austria:  $\alpha = 0.95 \beta - 0.8^\circ$ ,  $SD = 1.5^\circ$ ,  $R = 0.96$  (~ 70 avalanches)

(Databases contain supposedly «extreme» avalanches for each path.)



Wet-snow avalanche near Davos, probably gliding on water film,  $\alpha = 16^\circ$

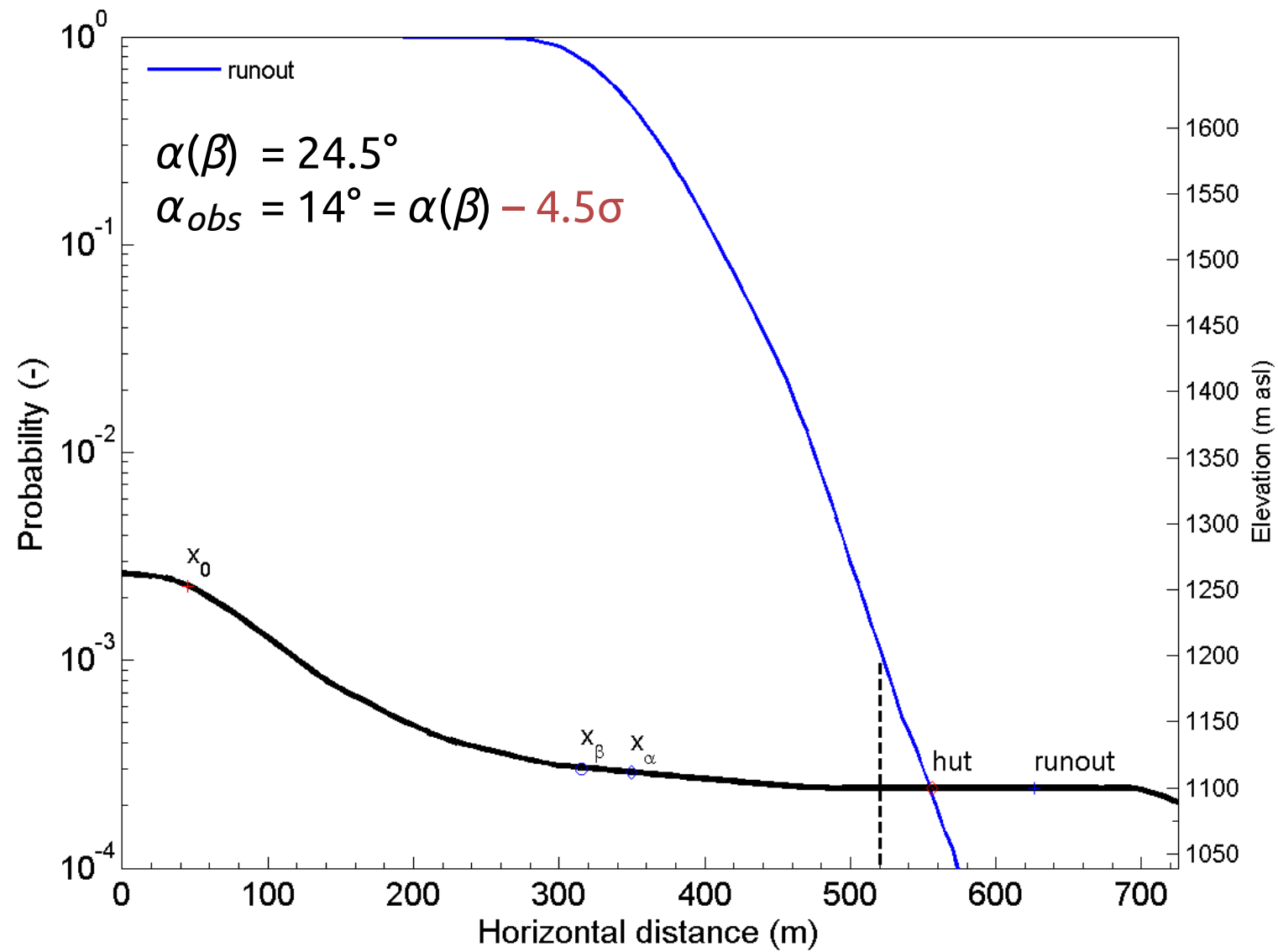




Dry-snow avalanche at Tyin, central Norway:  
Strongly fluidized and gliding on depth-hoar layer,  $\alpha = 14^\circ$  (!)



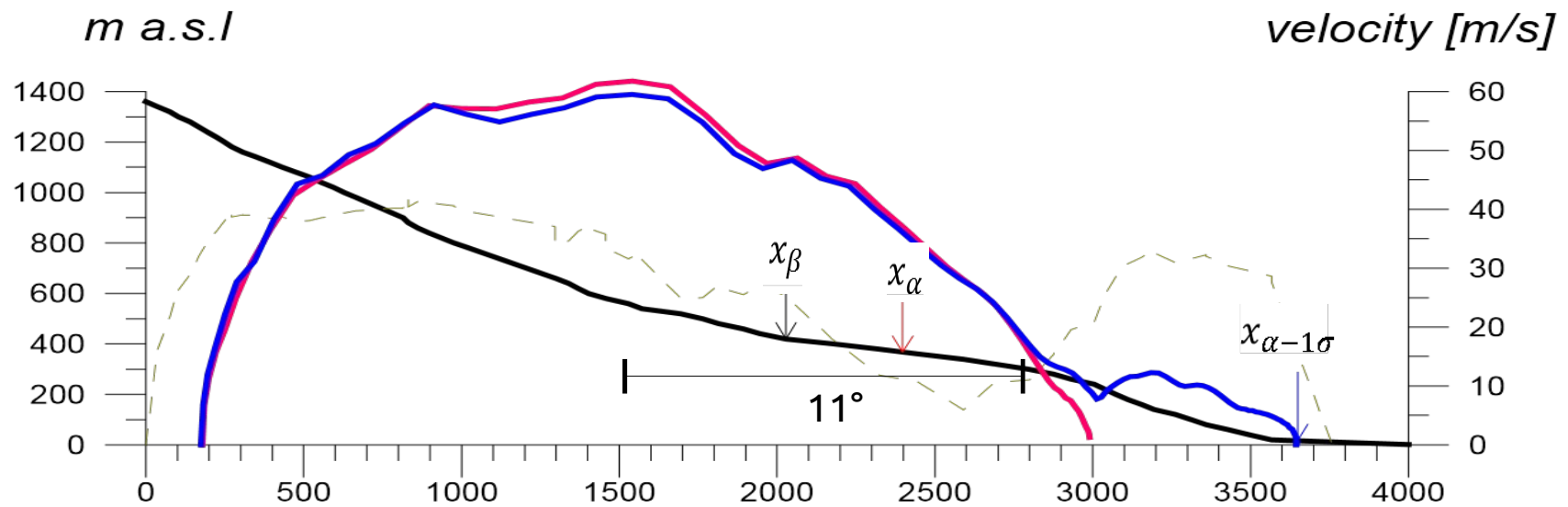
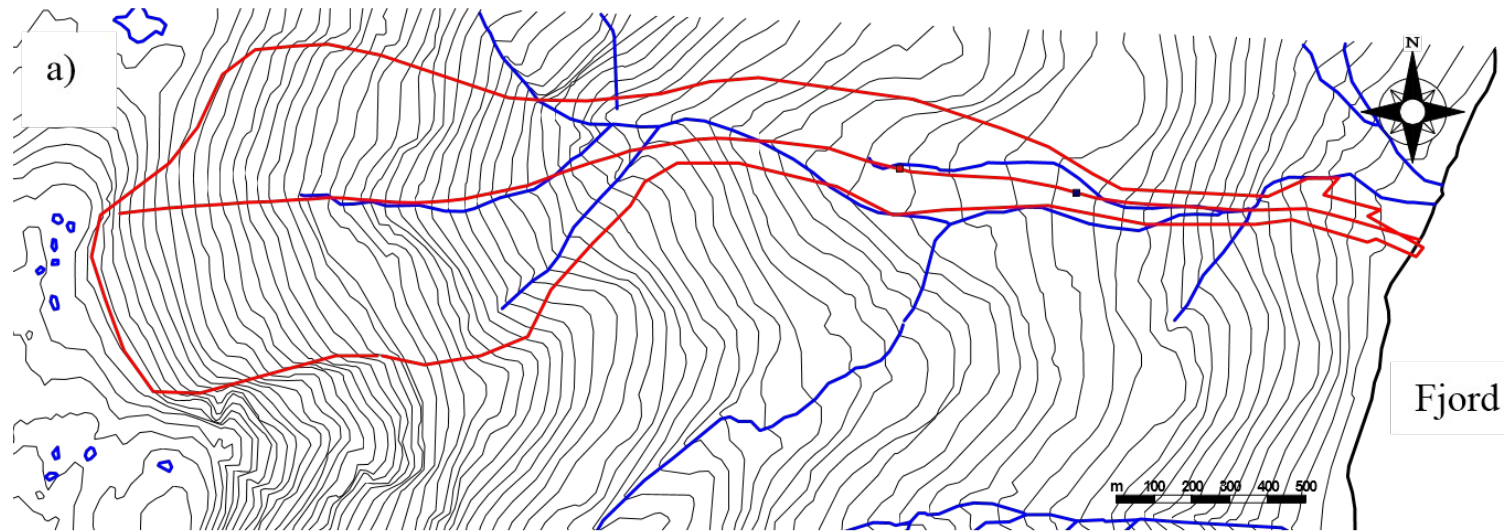




Plot courtesy P. Gauer, NGI



## Threshold behavior: The 1994 avalanche at Bleie (western Norway)





Conditions conducive to unusually long runout:

- Often on small to medium-sized gentle slopes
- Inclination of runout area  $\sim 10^\circ$
- Dry, cold, fine-grained snow
- Large supply of low-strength erodible snow
- Special conditions at the bed, e.g. cold depth-hoar layer with low cohesion
- High degree of fluidization
- Alternative: lubrication by water film (wet-snow avalanches)

These are avalanches with presumed return periods  $\geq 100$  years.





Destroyed house in Davos, Switzerland, 1968. Photo SLF.





Cars after the passage of a large avalanche at Arinsal, Andorra (Pyrenees), 1996



Snow avalanches may damage large forest areas (up to 1 km<sup>2</sup>)

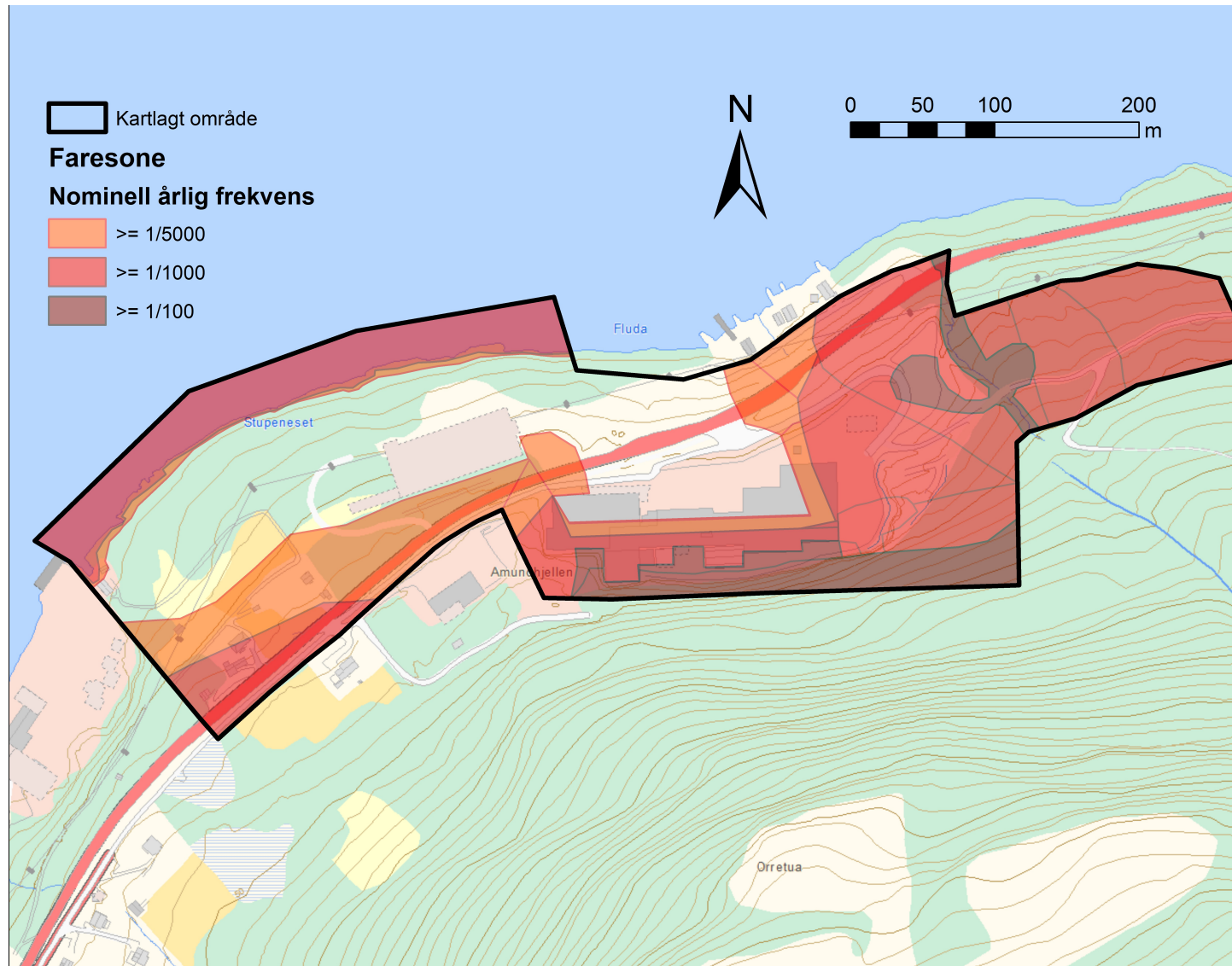




Even small avalanches can be a serious problem!

NGI





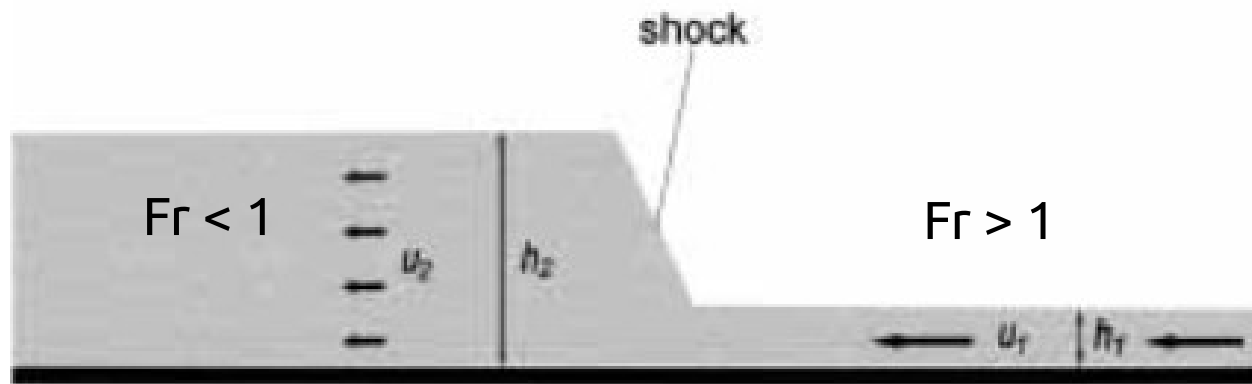
Example of a Norwegian GMF hazard map for return periods 100, 1000 and 5000 y

# Effects at avalanche impact on dams

## Supercritical overflow



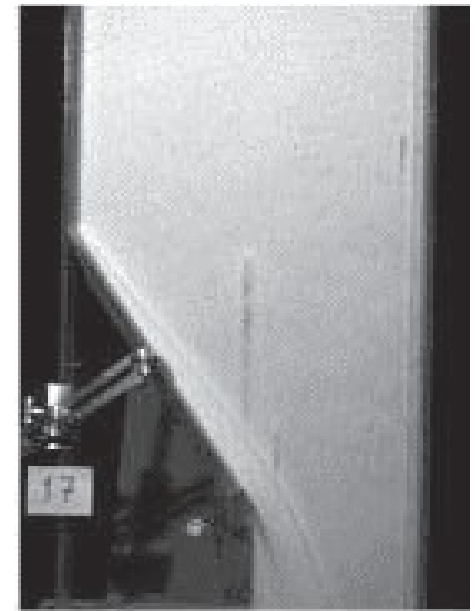
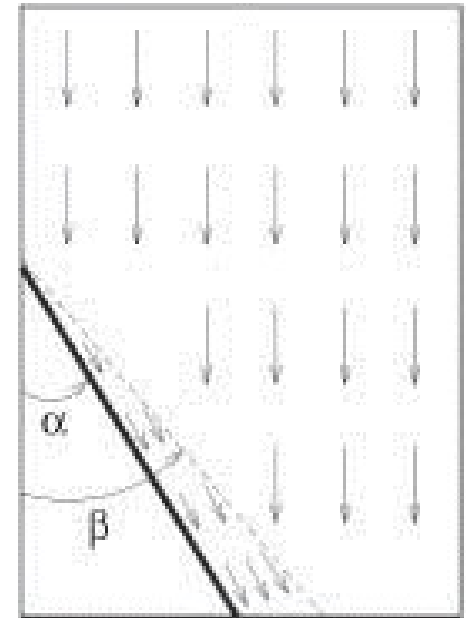
Shock formation at catching dam:  $u_2 = 0$ , shock travels upstream



(From T. Jóhannesson et al. (2009), The Design of Avalanche Protection Dams, EUR 23339)

## Why should shock theory be applicable to avalanche run-up on dams?

- Hydraulic jumps and supercritical overflow are natural consequences of the shallow water equations and do occur in Nature.
- Granular media behave like a fluid in many respects, and shock formation has been observed in chute flows against obstacles.
- Fast dry-snow avalanches can be characterized as granular flows.
- Some observations of avalanche deposits near deflection dams suggest that shock may have formed.



From Tai et al. (2001), *Annals Glaciol.* **32**, 281–284.



## How can numerical models help in the design of dams?

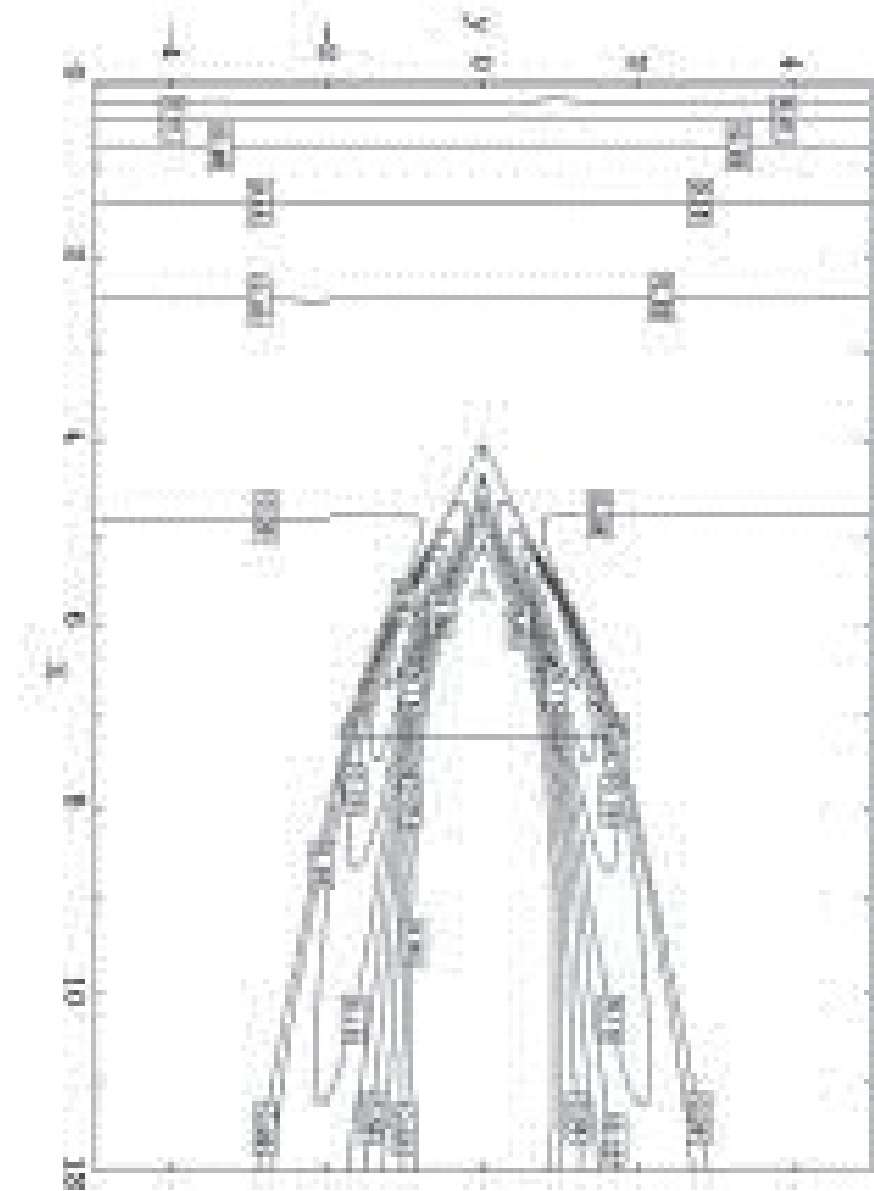
1. Determine approach velocity and flow depth of the design avalanche at the dam location.  
(Keep in mind that Voellmy or PCM-type models tend to underestimate velocity!)
2. Directly simulate flow of the avalanche against the dam with a quasi-3D model:
  - Need a numerically stable, shock-capturing code!
  - Need a correct, high-resolution terrain model (resolution  $\sim 1$  m)!!  
(May need different calibration of friction parameters at high resolution.)
  - Basic assumptions behind depth-averaged models violated, yet results are usable if slope breaks are not too extreme.
  - Energy loss in sharp bends is poorly modeled  
 $\Rightarrow$  obtain conservative results
  - Opens for optimization of dam location, shape and dimensions!





Chute experiment

From Tai et al. (2001), *Annals Glaciol.* **32**, 281–284.



Numerical simulation

## Summary of practical needs wrt. dynamical avalanche models:

- Numerical models are but one of several tools and methods used by the expert!!! (Gut feeling is also important...)
- Model must be easy to use (intuitive, integrated in GIS environment).
- Quasi-3D or 3D, but must be fast ( $\leq 300$  s /simulation on PC)!
- Must be robust.
- Must be well calibrated and validated.
- Detailed reproduction of minor flow details is not required because numerical modeling entails
  - Major conceptual uncertainties (flow rheology, erosion,...),
  - Extrapolation of initial conditions to return periods up to 5000 y,
  - Only minor numerical issues in comparison with the above errors.



### 3. A lesson to be learnt from statistical analysis

Typical dynamical avalanche models in practical use in 2013:

- Assume dense flow with constant density 200—300 kg/m<sup>3</sup>, neglect other flow regimes.
- Depth-averaged, assume uniform velocity profile.
- Erosion model: none or empirical.
- Assume bed friction to consist of dry (Coulomb) friction and «turbulent» drag (Voellmy, 1955; Perla et al., 1980):

$$\sigma_{xz} = \mu g h \cos \theta + k \bar{u}^2$$

$\mu = 0.15 \dots 0.4$ ,  $k = 0.0025 \dots 0.025$  from calibration against observed run-out distances.

Recommended parameters depend strongly on avalanche size and return period.

- A few more advanced approaches exist (Norem-Irgens-Schieldrop, Jop-Forterre-Pouliquen).



*Parameter variability* in a typical model like RAMMS, SAMOS-AT:

- Physically justified variability (measurable variability):
  - Variable snow temperature and humidity
  - Terrain roughness, forest, etc.
  - Variable particle size due to slab break-up and comminution
- Variability due to model shortcomings:
  - Flow-regime transitions and density change neglected
  - Snow entrainment effects neglected
  - Voellmy fluid is poor approximation to rheology of dense flow.

Attempts to calibrate simple models wrt. many criteria (e.g. RAMMS):

- Climate zone, altitude, return period, forest (physically justified)
- Avalanche size, terrain curvature (due to model deficiencies)



## A word of caution for users of Voellmy or PCM-type models:

«Turbulent» drag term is a built-in limiter for flow velocity:

$$\bar{u}_{\infty} = \sqrt{(1/k) g h (\sin \theta - \mu \cos \theta)}$$

- With  $\theta = 30^\circ$ ,  $h = 1.5$  m,  $\mu = 0.2$ ,  $k = 0.006$  or  $\xi = 2500$  m/s<sup>2</sup>:

$$\bar{u}_{\text{inf}} < 30 \text{ m/s}$$

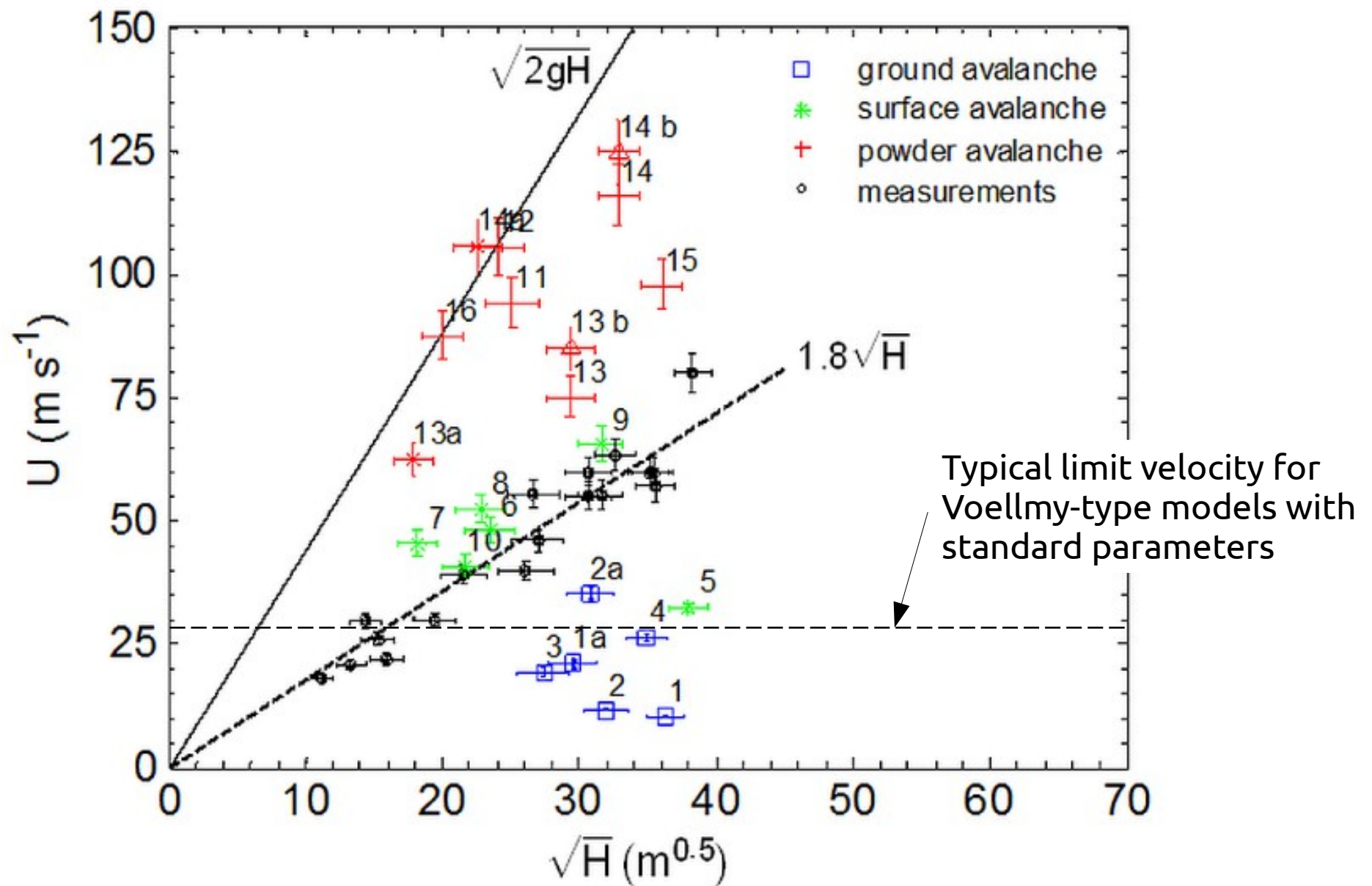
in contradiction with velocity measurements – should be ~ 60 m/s!

- Compilation of velocity measurements from a large variety of paths indicates trend

$$\bar{u}_{\text{max}} = (0.5 \dots 0.7) \sqrt{g H_{\text{drop}}}$$

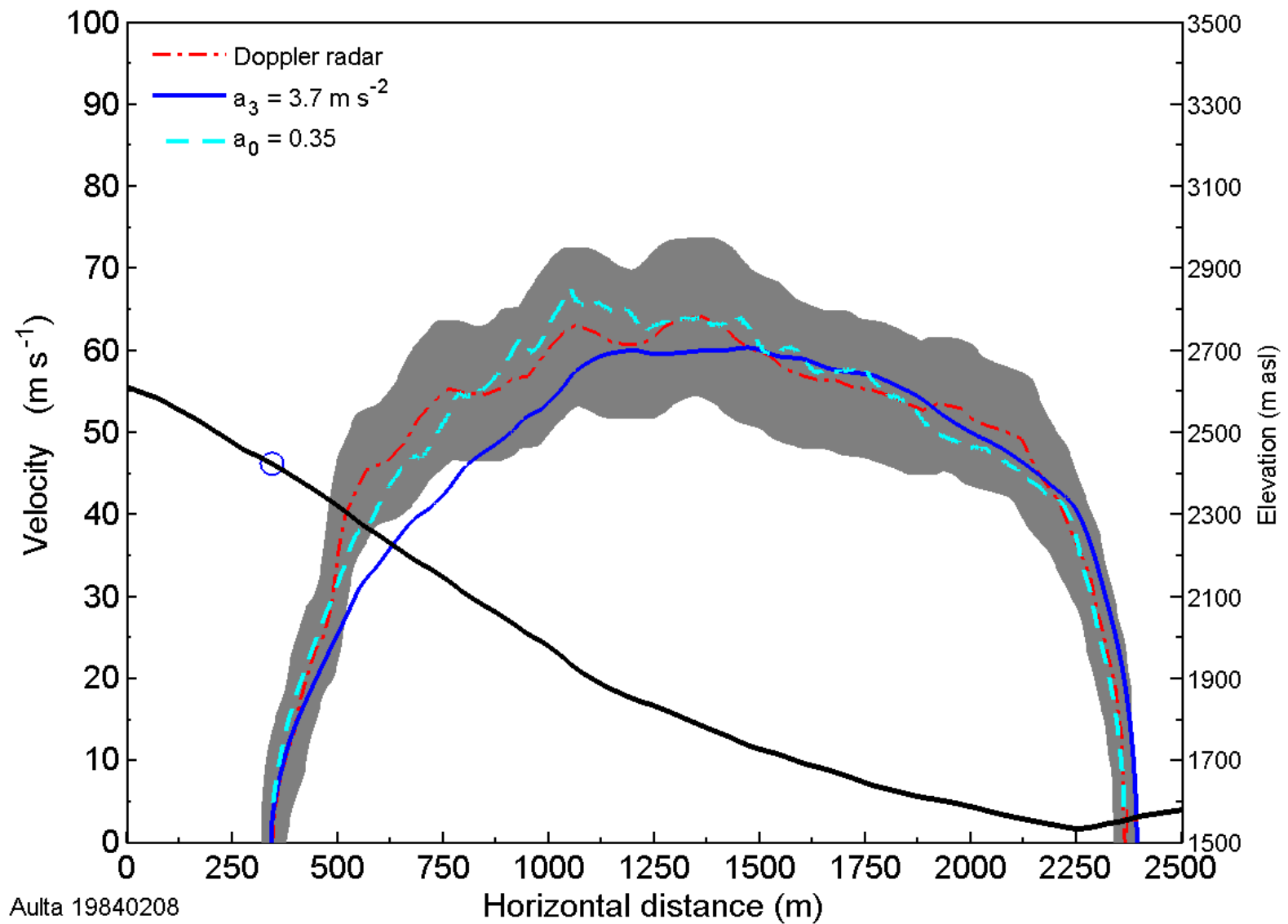
- Especially relevant for design of mitigative measures!





From (P. Gauer, *Cold Regions Sci. Technol.*, 2013)

Simulation of velocity data with Coulomb model (from (Gauer et al., 2010)):



Velocity measurements were often neglected in model calibrations (scarcity of data).

Coulomb-type model with constant friction coefficient  $\mu$  does much better job in reproducing run-out distance *and* maximum velocity than Voellmy-type models.

**BUT**

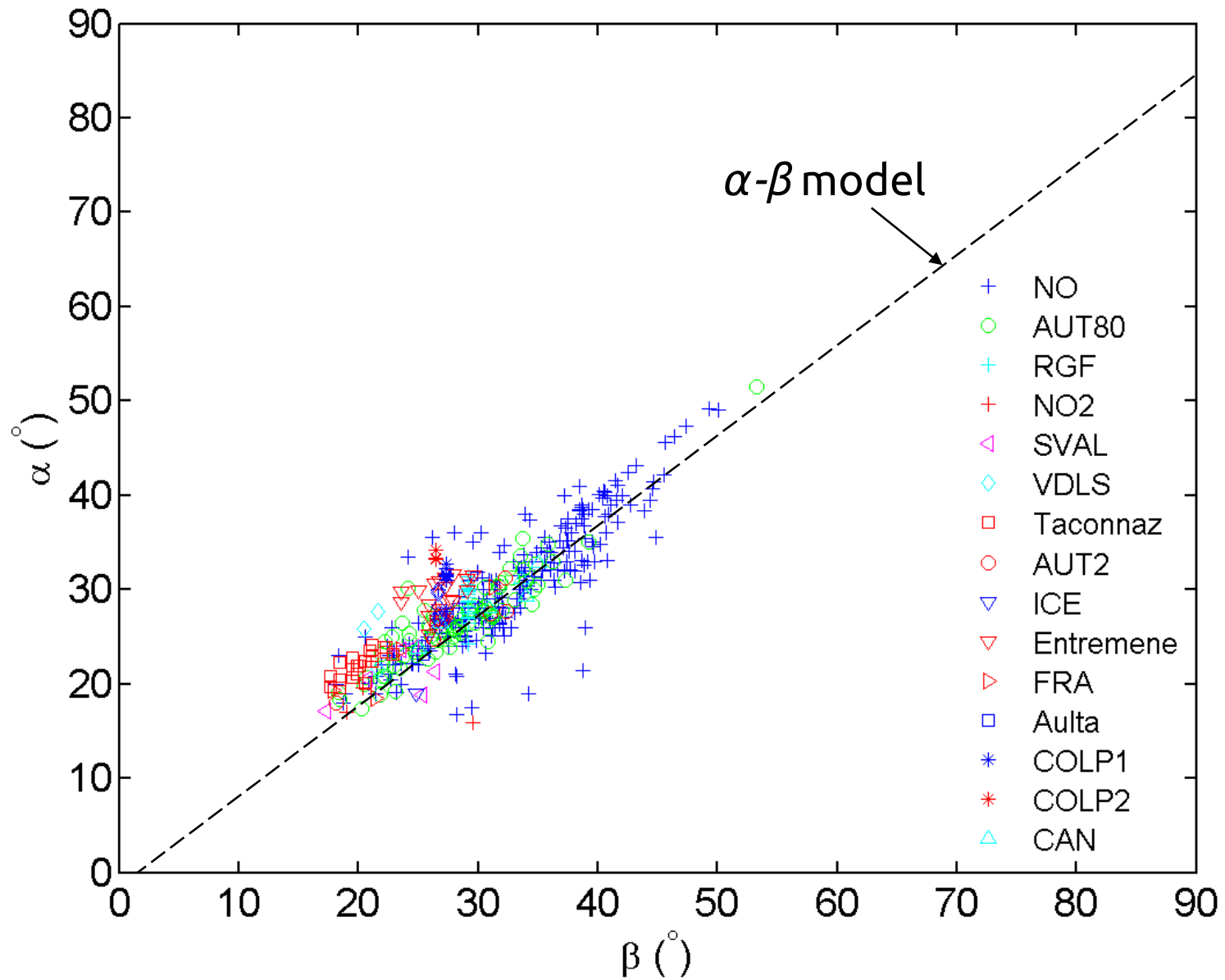
Run-out angle  $\alpha = \arctan(\mu)$  varies with average slope angle from fracture line to beginning of run-out zone:

$$\alpha = 0.96 \beta - 1.4^\circ \quad (\text{calibration for Norway})$$

- ☞ What does that mean in terms of avalanche dynamics?
- ☞ Which *physical* model is able to reproduce this?



## Compilation of data from 300—400 observed «extreme» avalanches



Plot courtesy  
P. Gauer, NGI



## 4. How to model flow-regime transitions in snow avalanches?

### B2FR – a block model switching between two flow regimes

- Norem–Irgens–Schieldrop (NIS) rheology incorporates dry friction from persistent particle contacts and particle collision effects (dispersive stresses).
- At sufficiently high shear rates, effective stress and Coulomb friction vanish. Material expands, but NIS model does not modify the density.
- With constant flow depth, NIS block model is equivalent to PCM model.
- Potential for richer dynamics if fluidization modifies the rheological parameters!

(Norem et al., 1989, *Annals Glaciol.* **13**, 218–225.  
Issler and Gauer, 2008. *Annals Glaciol.* **49**, 193–198.)



## The granular view:

- At macroscopic scale, *frictional* and *collisional* regimes can coexist at same location.
- *Frictional regime*:  
Mean free path  $\rightarrow 0$ , continuous contact between particles,  
Coulombian friction
- *Collisional regime*:  
Short-duration collisional contacts,  
dispersive pressure  $\sim (\text{shear rate})^2$ , but also  
dispersive shear stress  $\sim (\text{shear rate})^2$
- *Fluidization* occurs when and where the dispersive pressure supports the avalanche weight.  
Seems to require slopes with  $\tan \theta \sim 1$ , however!





Two possible causes for fluidization to consider:

*A) Purely granular mechanism:*

*Dispersive pressure* from collisions between particles overcomes normal load.

Conditions:      high shear rates,  
                         sufficiently elastic collisions  
                         dispersive shear stresses small

*B) Pneumatic mechanism:*

Air flow over avalanche creates stagnation pressure at snout, underpressure on the head.

Conditions:      high velocity  
                         ? small cohesion in avalanche



## Amended formulation of NIS rheology:

For simplicity, consider plane shear flow in x-z plane here.

$$\sigma_{xx} = -p_e - p_u - \rho(v_3 + v_2 - v_1)\dot{\gamma}^2$$

$$\sigma_{yy} = -p_e - p_u - \rho v_3 \dot{\gamma}^2$$

$$\sigma_{zz} = -p_e - p_u - \rho(v_3 + v_2)\dot{\gamma}^2$$

$$\tau_{xz} = c + \mu p_e + \rho m \dot{\gamma}^2$$

$p_e$  effective pressure (through long-lasting grain-grain contacts)

$c$  cohesion [Pa]

$v_{1-3}$  viscometric coeff. [m<sup>2</sup>]

$p_u$  pore pressure

$\mu$  dry friction [–]

$m$  shear viscosity [m<sup>2</sup>]



Salient features of this rheology:

- Overburden weight is carried by pore pressure ( $p_u$ ), persistent grain–grain contacts ( $p_e$ ), and grain–grain collisions. Relative importance depends on shear rate.
- Coulomb friction dominates at low shear rates, granular collisions at high shear rates.
- Normal stresses are *not* isotropic.
- Velocity profile is typical of granular flows.
- Effective pressure  $p_e$  may vanish at high shear rate  
⇒ *fluidization*





Solution for steady gravity-driven shear flow:

Neglect cohesion and pore pressure. Then

$$\rho g h \cos \theta = p_e + \rho (v_2 + v_3) \dot{\gamma}^2$$

$$\rho g h \sin \theta = \mu p_e + \rho m \dot{\gamma}^2$$

Obtain

$$p_e = \rho g (h - z) \cos \theta \frac{m / (v_2 + v_3) - \tan \theta}{m / (v_2 + v_3) - \mu}$$

$$\dot{\gamma}^2(z) = \frac{g (h - z) \cos \theta (\tan \theta - \mu)}{m - \mu (v_2 + v_3)}$$

⇒ Steady-state flow only for  $\mu < \tan \theta < m / (v_2 + v_3)$   
Implies the condition  $m > \mu (v_2 + v_3)$



- Bed-normal and shear components of dispersive stress:

$$\begin{pmatrix} \sigma_n^{(d)}(z=0) \\ \sigma_s^{(d)}(z=0) \end{pmatrix} = \rho_p \begin{pmatrix} v_n(c) \\ v_s(c) \end{pmatrix} \dot{\gamma}^2(z=0) \approx \frac{25}{4} \rho_p \begin{pmatrix} v_n(c) \\ v_s(c) \end{pmatrix} \frac{\bar{u}^2}{h^2}$$

- Effective stress:

$$\sigma_{n,\text{eff.}}(z=0) = \rho(g h \sin \theta - \kappa \bar{u}^2) - \frac{25}{4} \rho_p v_n(c) \frac{\bar{u}^2}{h^2}$$

- Resulting expression for bed shear stress:

$$\sigma_s^{(b)} = \underbrace{\max \left( \rho(g h \cos \theta - \kappa \bar{u}^2) - \frac{25}{4} \rho_p v_n(c) \frac{\bar{u}^2}{h^2}, 0 \right)}_{\text{fluidization criterion}} + \frac{25}{4} \rho_p v_s(c) \frac{\bar{u}^2}{h^2}$$

## What happens at fluidization (according to NIS)?

- If  $\tan \theta > m/(v_2 + v_3)$ , dispersive pressure supports entire overburden, and  $p_e = 0 \Rightarrow$  **expansion**.
- Where  $p_e = 0$ , fluidization takes place throughout entire depth simultaneously.
- NIS model **parameters must depend on density** and particle properties, but model does not specify how.
- Assume flow-regime transitions to be rapid  
 $\Rightarrow$  Use algebraic instead of differential equation to determine local depth-averaged density.



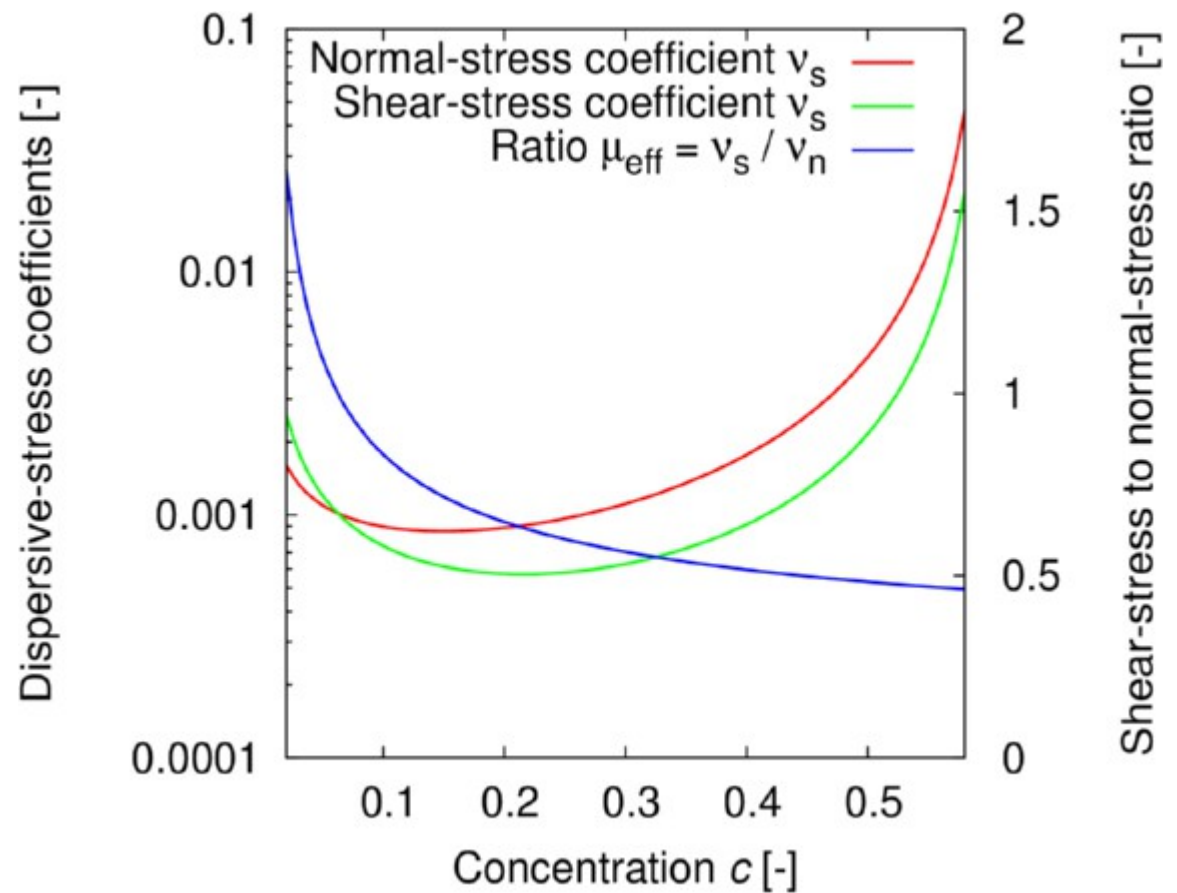


Extension to variable density:

Theoretical calculations (Pasquarell et al., 1988) and numerical simulations (Campbell and Gong, 1986) of 2D stress tensor as a function of particle concentration may be approximated by

$$v_n(c) = Q c^{-q} (c_{\max} - c)^{-r}$$
$$v_s(c) = R \cdot (1 + S c^{-s}) v_n(c)$$

with  $q, s \approx 0.5$ ,  $r \approx 1.5$ ,  
 $Q \approx 10^{-4}$ ,  $R \approx 0.2$ ,  
 $S \approx 1$ ,  $c_{\max} \approx 0.6$ .



If (*normal dispersive pressure*) > (*overburden*):

Shear rate at the bed, flow depth and particle concentration are adjusted such that

Mass conservation

$$h' \cdot c' = h \cdot c$$

Momentum conservation

$$\frac{2}{5} \dot{\gamma}' h' = \bar{u} = \frac{2}{5} \dot{\gamma} h$$

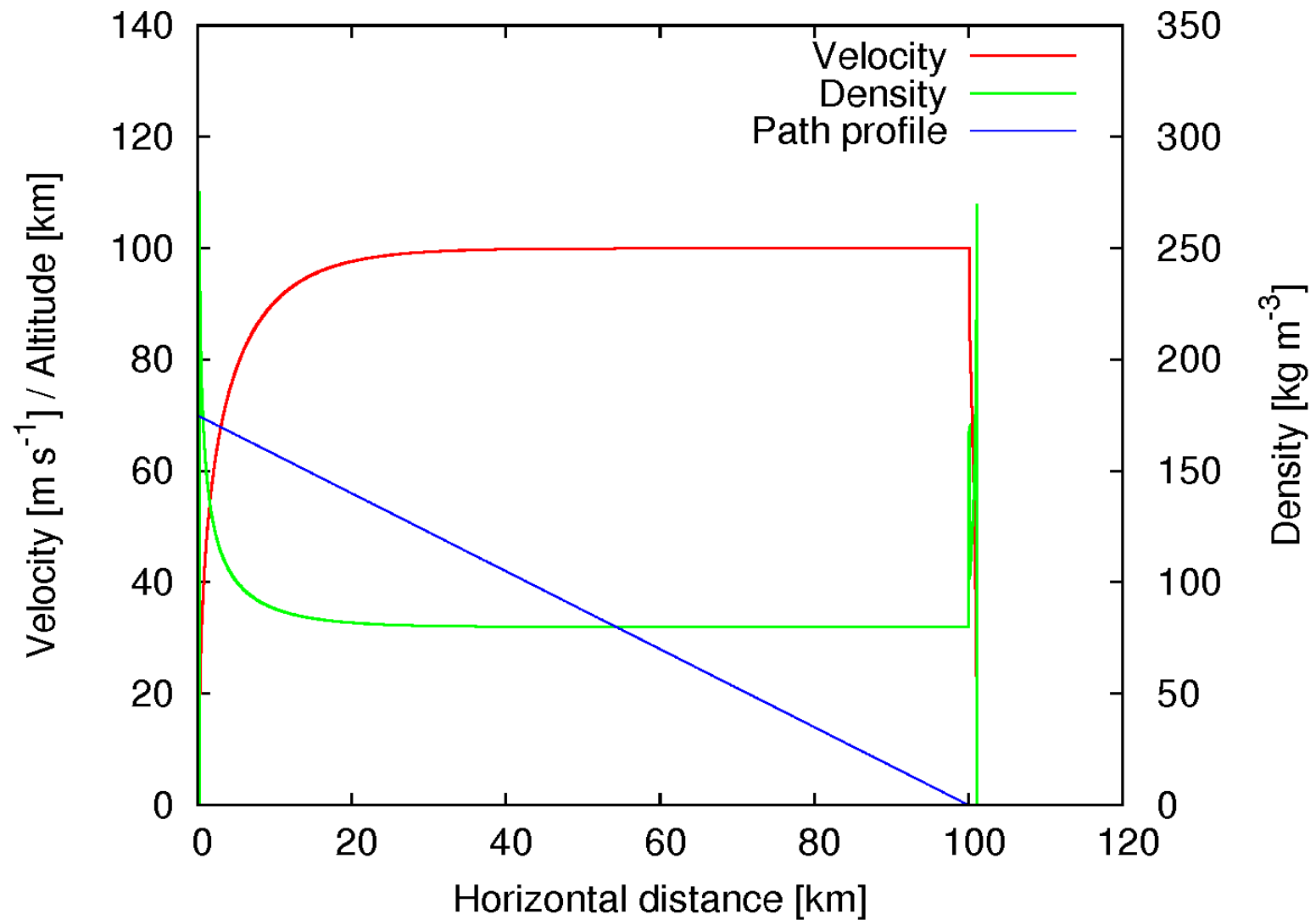
Normal-force balance

$$\rho_p v_n(c') \dot{\gamma}'^2 = \rho' (g h' \cos \theta + \kappa \bar{u}^2)$$

(Actually, the model is a little more complicated due to aerodynamic lift and air entrainment.)

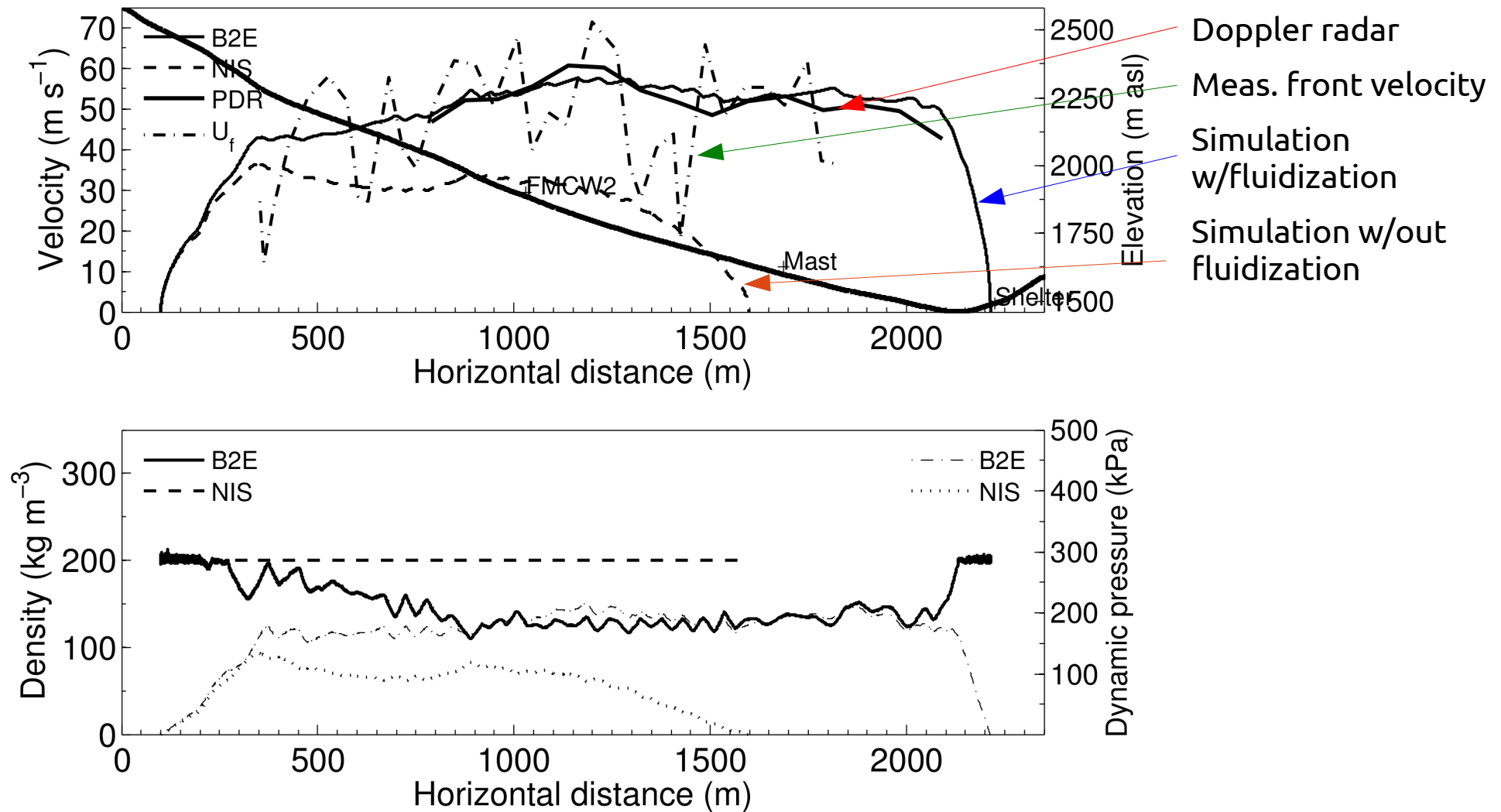


Test run on 35° slope, with  $h_0 = 1.0$  m,  $\mu = 0.5$ , no entrainment  
(Note scales – not meant to be a realistic case!)

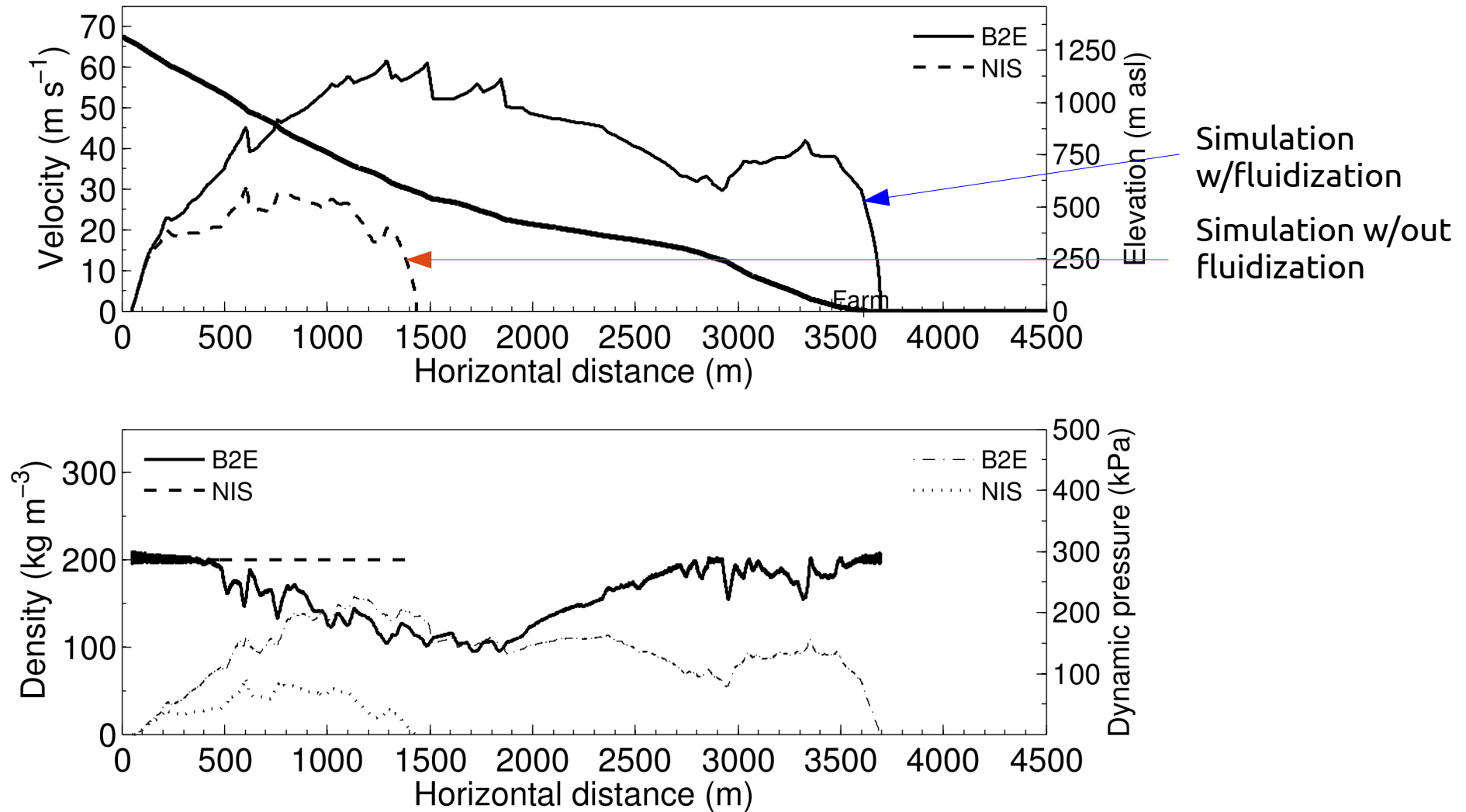




Comparison with measured avalanche at Vallée de la Sionne, 1999-02-10:  
 Dry friction  $\mu = 0.50$ , aerodynamic lift coeff.  $C_L = 1.7$



Comparison with observed avalanche at Bleie, Norway, 1994-01-27:  
Dry friction  $\mu = 0.50$ , aerodynamic lift coeff.  $C_L = 2.0$



# Testing the behavior of B2FR in regard to $\alpha$ - $\beta$ relation

Simulations on synthetic profiles:

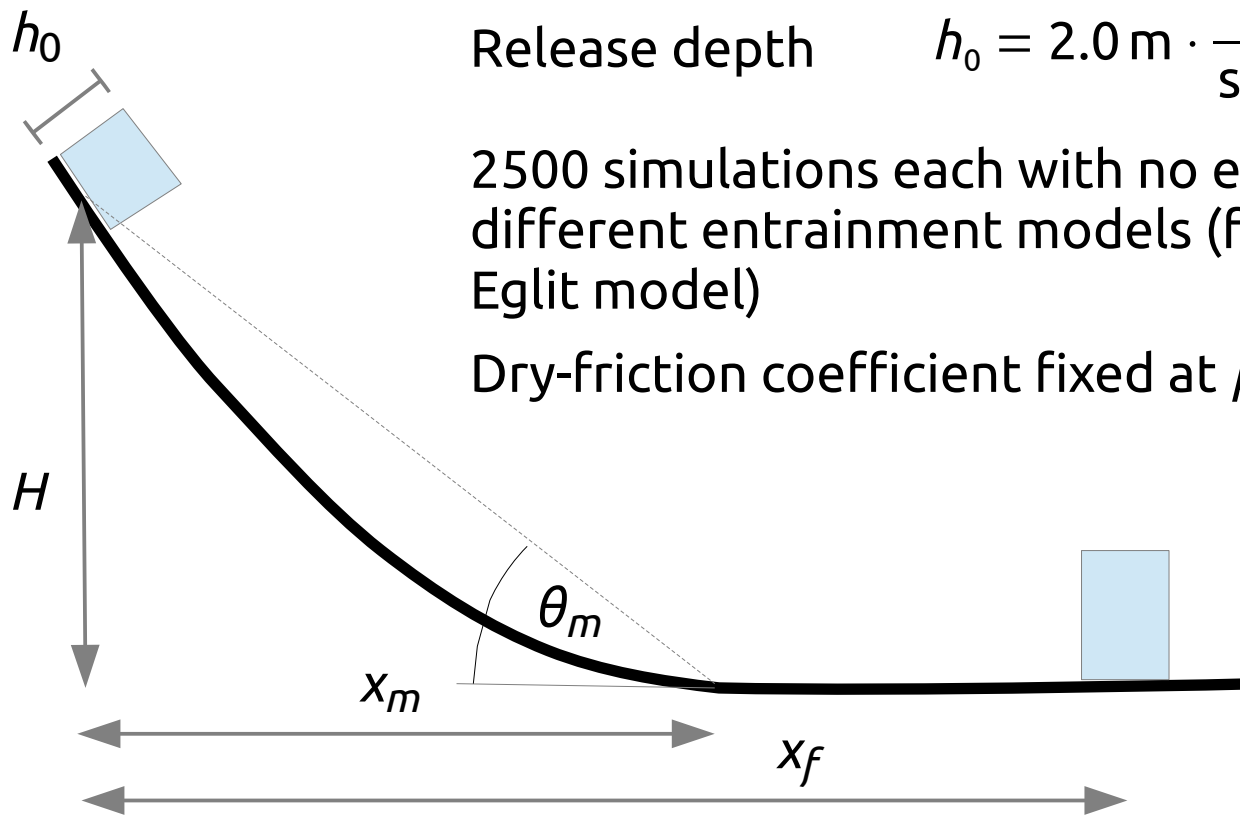
Parabolas with horizontal runout

$300 \text{ m} < x_m < 4000 \text{ m}$ ,  $10^\circ < \theta_m < 70^\circ$  randomly selected with uniform distribution

Release depth  $h_0 = 2.0 \text{ m} \cdot \frac{0.291}{\sin \theta_r - 0.202 \cos \theta_r}$

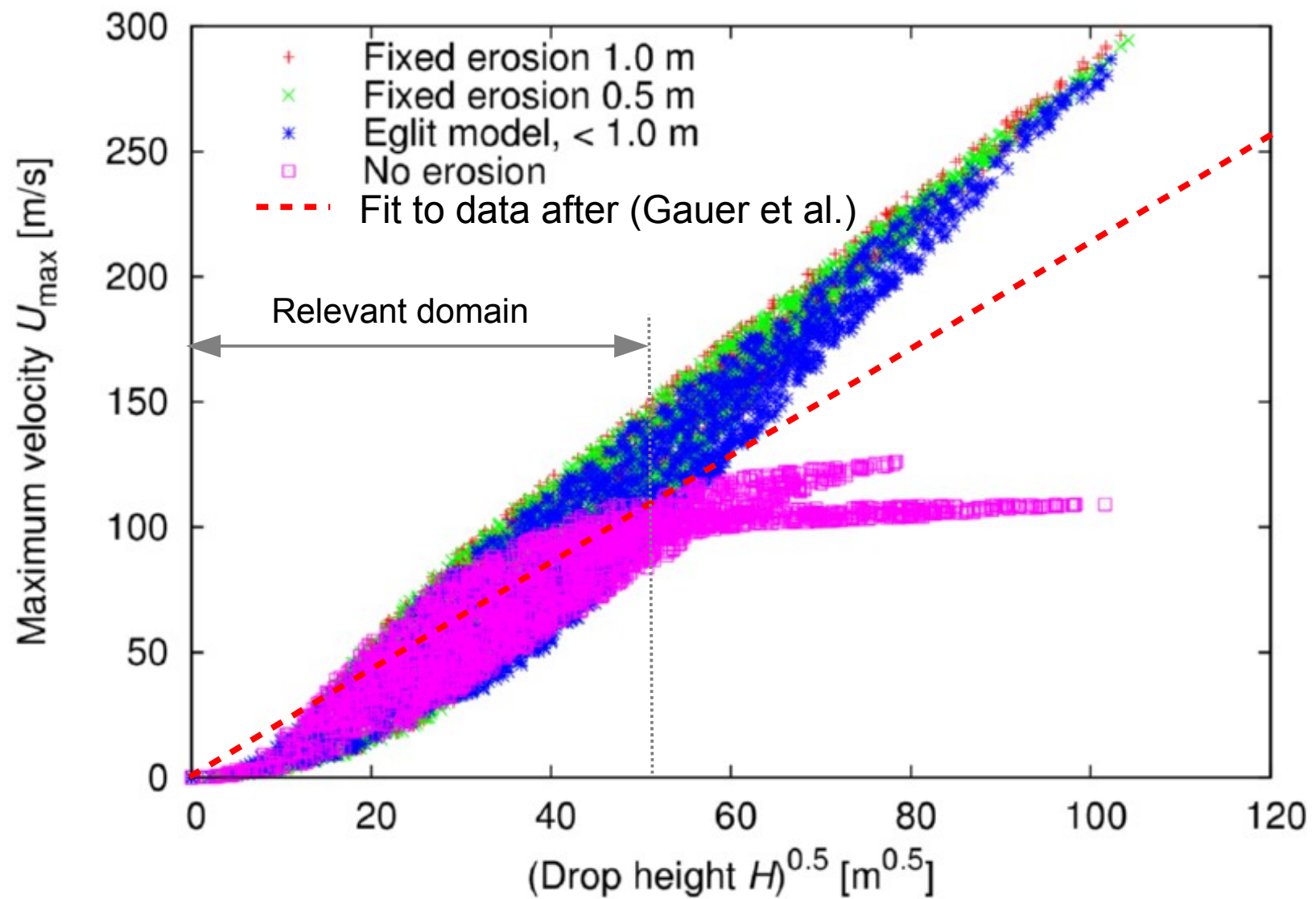
2500 simulations each with no entrainment and 2 different entrainment models (fixed 0.5 m, fixed 1.0 m, Eglit model)

Dry-friction coefficient fixed at  $\mu = 0.5$



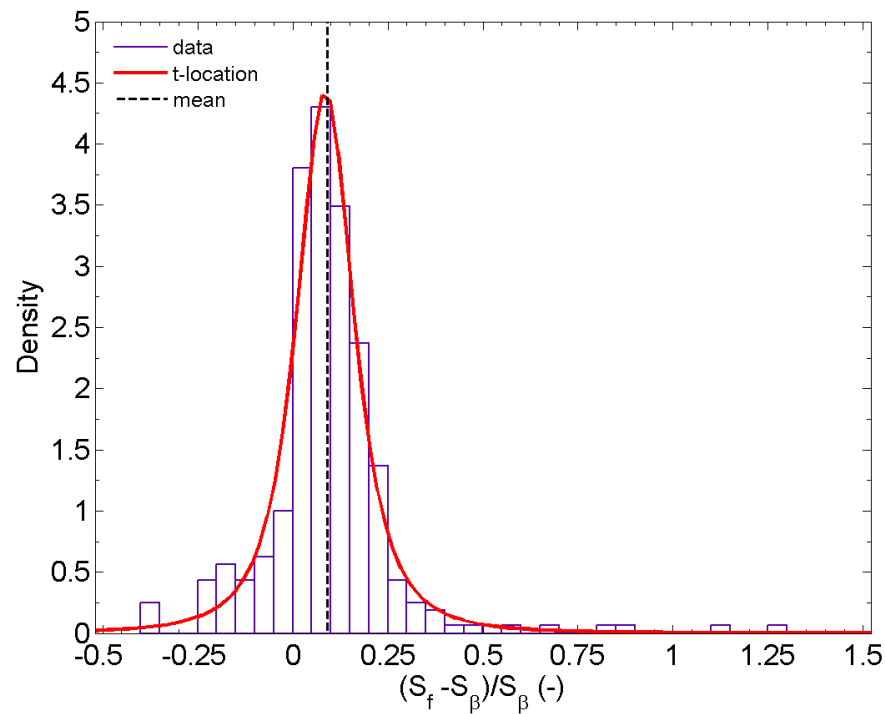


## Simulation of maximum velocities:

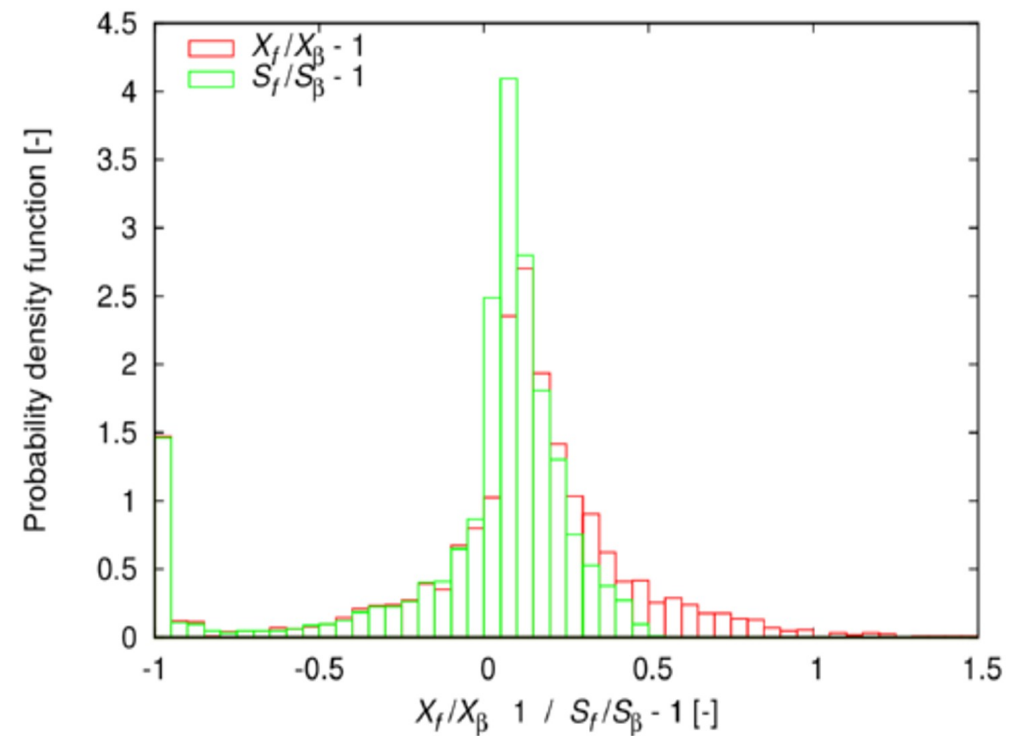


## Simulation of distribution function of runout ratio:

Data of ~320 real avalanches  
(from (Gauer et al., 2010))

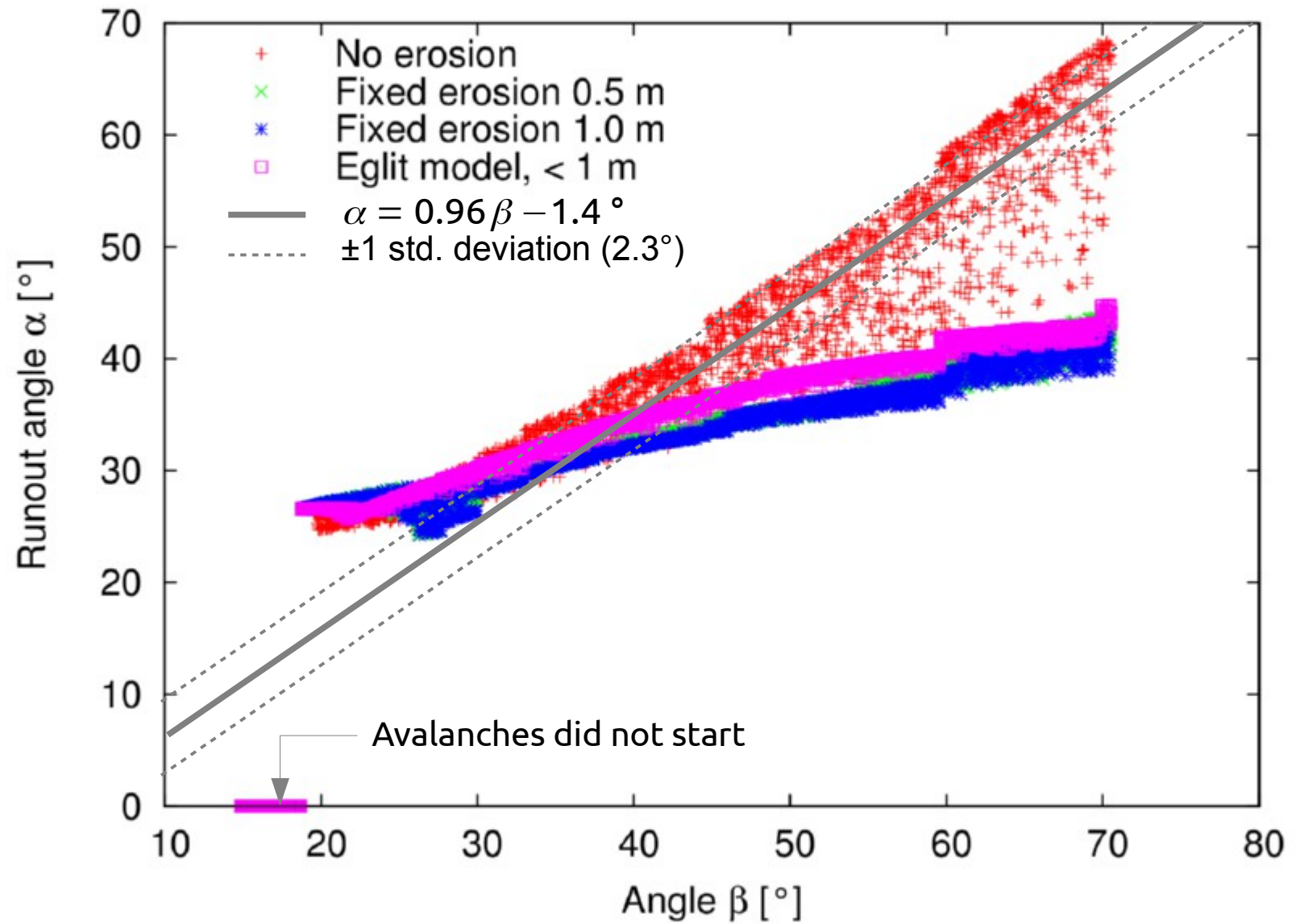


Simulations with B2FR  
on synthetic profiles



**N.B.** The two data sets have different ranges/distributions of  $H$  and  $\beta$ !

## Simulation of $\alpha$ - $\beta$ relationship:





## Assessment of first attempt at modeling fluidization

- Block-model approach is too simplistic, but front behavior is reproduced.
- Fluidization does not progress to the assumed densities of the fluidized layer (30–100 kg/m<sup>3</sup>), but stops at 100–150 kg/m<sup>3</sup>.
- Very diverse avalanches can be reproduced well with small (and explainable) variations of  $\mu$  ( $\pm 10\%$ ) and aerodyn. lift coeff.  $C_L$  ( $\pm 20\%$ ).
- However, entrainment plays an important role!
- General trend  $U_{\max} \propto \sqrt{g H_{\text{drop}}}$  is reproduced within observable range.
- Empirical correlation between  $\alpha$  and  $\beta$  angle is **not** reproduced.

## 5. Erosion, entrainment and all that

Modeling entrainment is a long-standing, unresolved problem!

- First (depth-averaged) avalanche flow models with entrainment published around 1965 (Eglit, Grigorian and coworkers, Lomonossov MSU).
- Models used in practice in 2013 mostly disregard erosion/deposition.
- Models with erosion typically have a freely adjustable parameter.

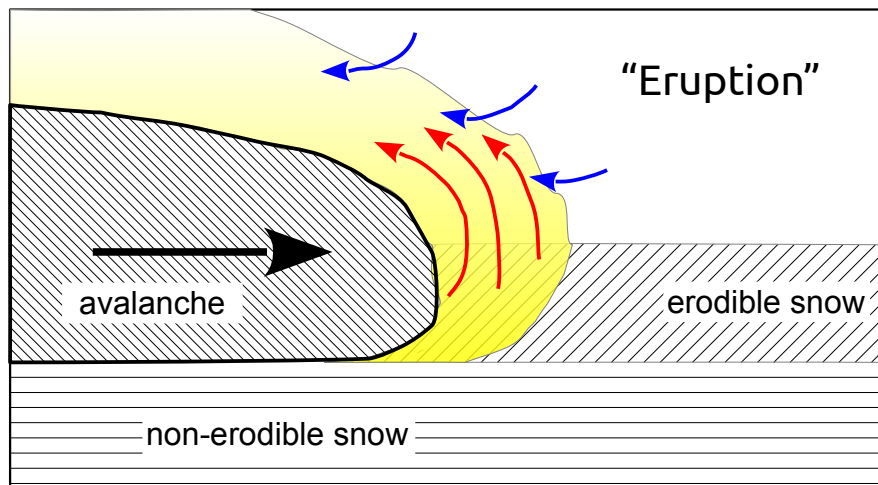
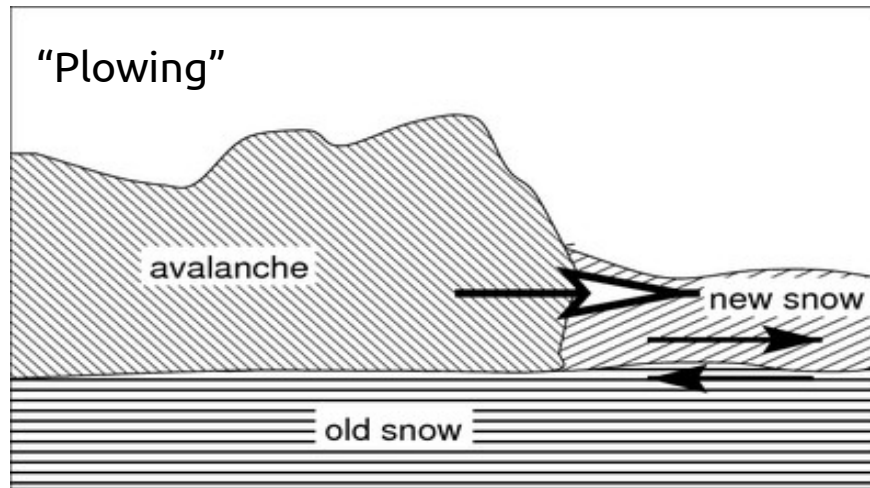
Major difficulties:

- Experimental data still scarce (but improving)
- Several relevant mechanisms
- Wide range of conditions (snow and flow properties)

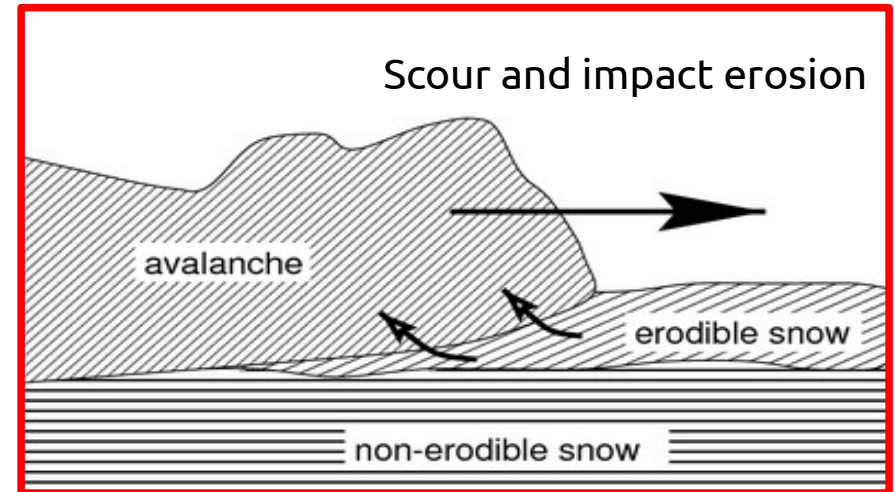
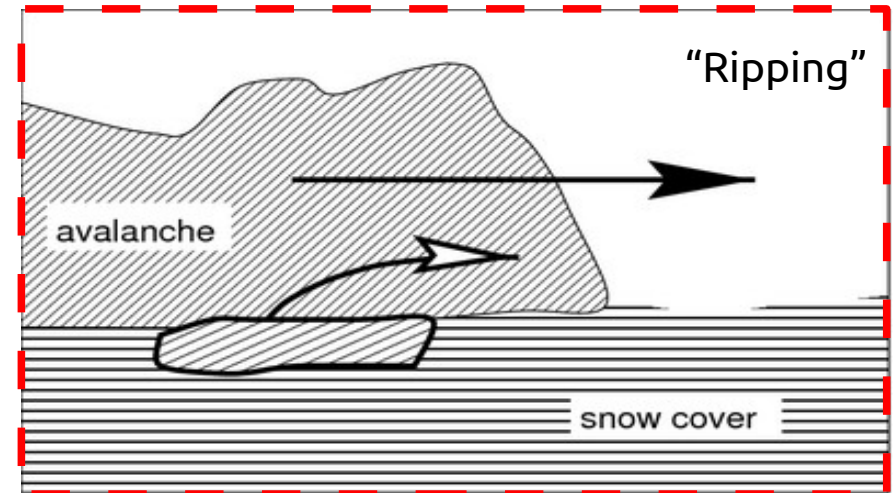


# Conjectured erosion mechanisms (Gauer & Issler, 2004)

## Frontal mechanisms



## Mechanisms acting along bottom





## Application to «consulting-grade» models:

Pursue three different lines of attack:

*A) Take the block-model more seriously than it deserves:*

- Assume uniform velocity profile
- Assume friction law w/out erosion remains valid with erosion

*B) Uniform, quasi-stationary flow and simple rheology:*

- Solve model analytically
- Study interaction between erosion and rheology

*C) Uniform, non-stationary flow and range of rheologies:*

- Solve model numerically (1D in bed-normal direction)
- Study how driving force is partitioned between erosion and acceleration



*Assumptions in the present attempts:*

- Consider only entrainment along flow bottom.
- Perfectly brittle behavior of **bed material – breaks at stress  $\tau_c$** .  
No energy required to break the snow cover.  
 $\tau_c \sim 0.1 \dots 10$  kPa.
- Bed material regarded as a continuum.
- Bed does not fail catastrophically if shear strength  $\tau_c$  is exceeded.  
(Implies essentially that  $\tau_c$  grows with depth.)

*Physical consideration:*

Entrainment rate must be determined by rheology of GMF and shear strength  $\tau_c$  of bed material. ***No free parameters!***

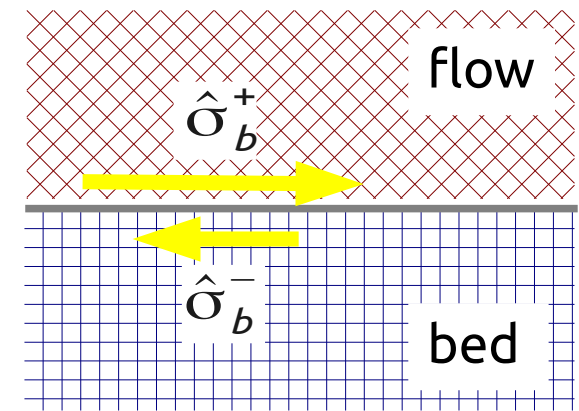


## A) Analytic solution for sliding blocks

- Assume a bed ( $b$ ) friction law of the form

$$\hat{\sigma}_b^+ \equiv \frac{\sigma_{xz}(z=b^+)}{\rho} = \hat{f}(\bar{u}, h, \dots)$$

Shear stress at top of bed:  $\hat{\sigma}_b^- = \hat{\tau}_c$ .



- Jump condition for x-momentum across bed–flow interface:

$$w_e \cdot (u(b^+) - u(b^-)) = w_e \bar{u} = \hat{\sigma}_b^+ - \hat{\sigma}_b^- = \hat{f}(\bar{u}, h, \dots) - \hat{\tau}_c$$

Now immediately find the entrainment rate:

$$q_e = \rho w_e = \begin{cases} 0 & \text{if } f(\bar{u}, h, \dots) \leq \tau_c, \\ \frac{f(\bar{u}, h, \dots) - \tau_c}{\bar{u}} & \text{else.} \end{cases}$$



For the Voellmy bed friction law:

$$\hat{\sigma}_b^+ = \text{sgn}(\bar{u}) \left( \hat{\sigma}_n \tan \delta + k \bar{u}^2 \right)$$

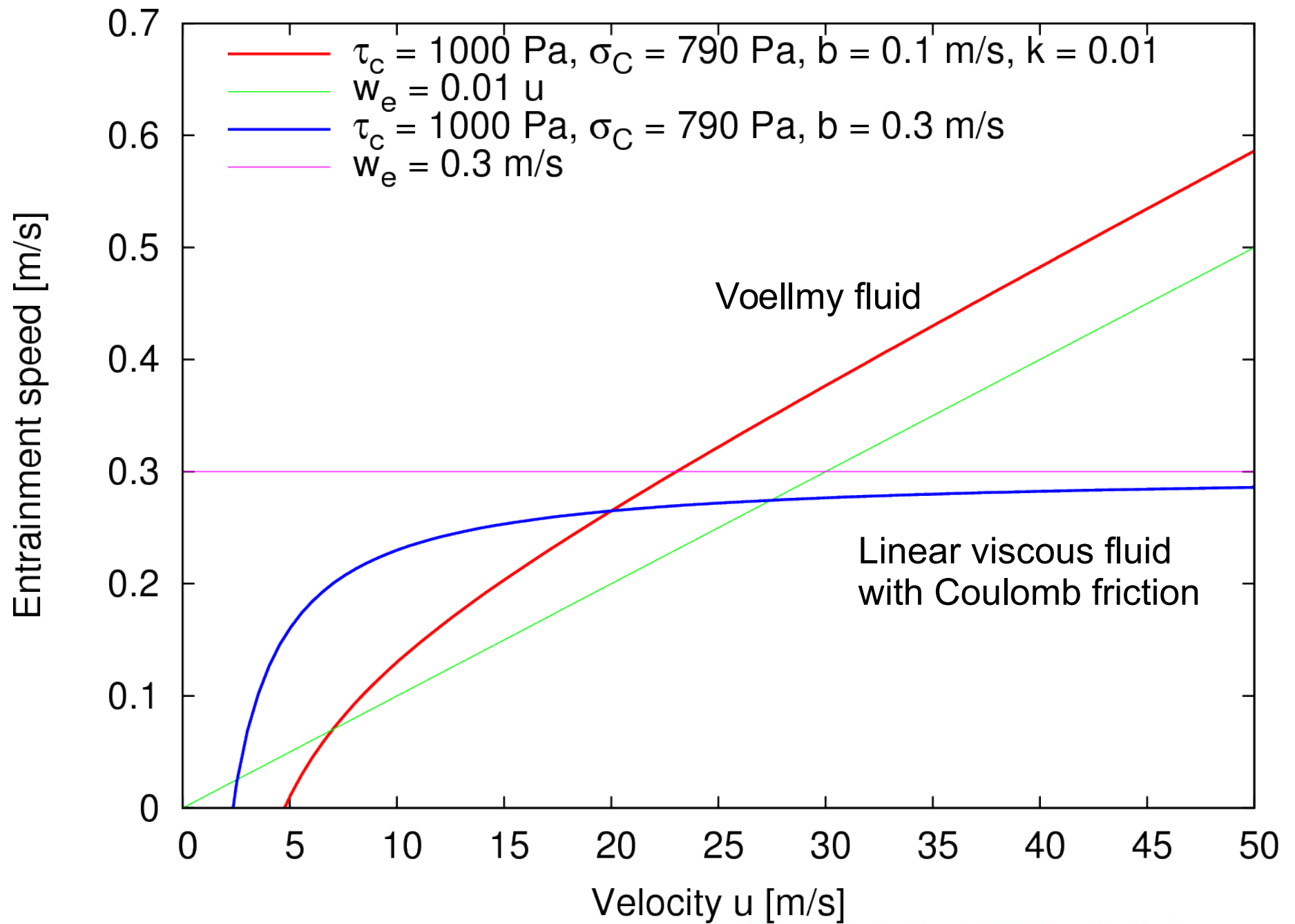
with  $\sigma_n$  = normal stress on bed,  
 $\delta$  = bed friction angle (assume  $\delta < \theta$ )

$$w_e = \begin{cases} 0 & \text{if } |\bar{u}| \leq \sqrt{\frac{\hat{\tau}_c - \hat{\sigma}_n \tan \delta}{k}}, \\ k \bar{u} - \frac{\hat{\tau}_c - \hat{\sigma}_n \tan \delta}{\bar{u}} & \text{else.} \end{cases}$$

Compare this with the popular entrainment assumption (e.g. RAMMS):

$$w_e = c \bar{u} \quad \text{with } c > 0 \text{ arbitrary}$$





## Entrainment relation derived from block-model considerations:

- Easy to implement in Voellmy and Coulomb-type models that assume sliding at the bed and no shearing in the flow body.
- Shear strength of the snow cover is decisive, need not be uniform in the entire path. Typical values are 0.5–2 kPa.

Differences compared to the “traditional” model implemented e.g. in RAMMS:

- Erosion threshold: bed shear stress > snow cover strength,  $\sigma_b = \tau_c$ .
- Velocity dependence of erosion determined by velocity dependence of friction law.
- In case of Voellmy fluid: erosion coefficient fixed at  $c = k$ .

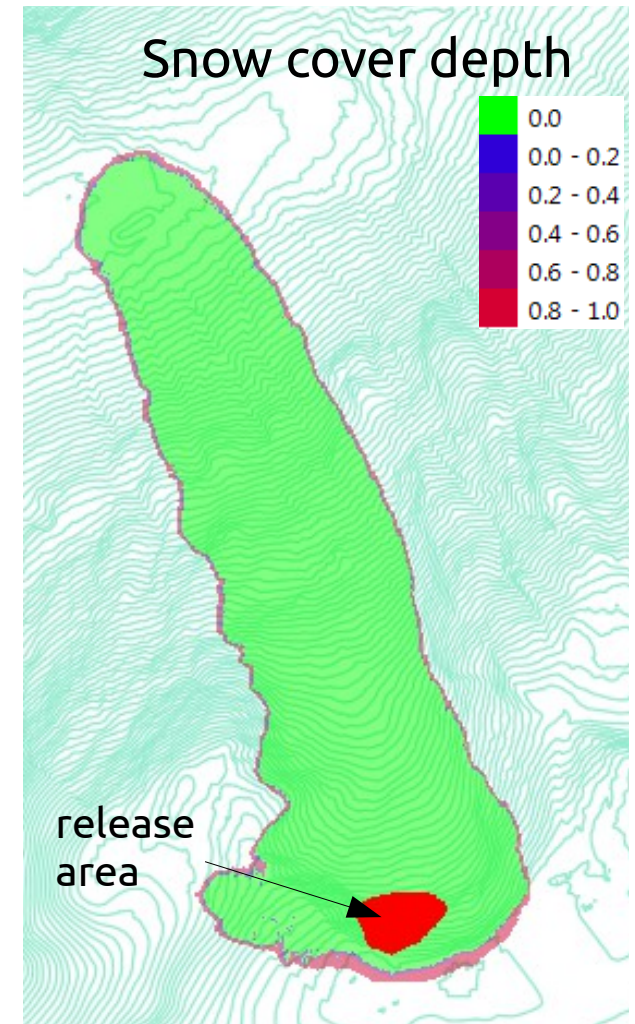
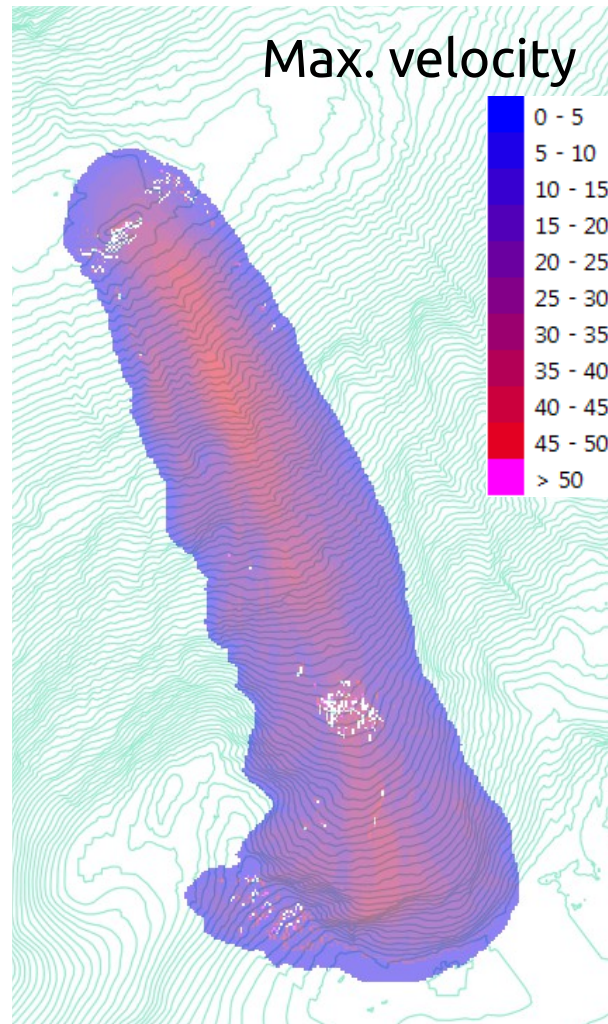
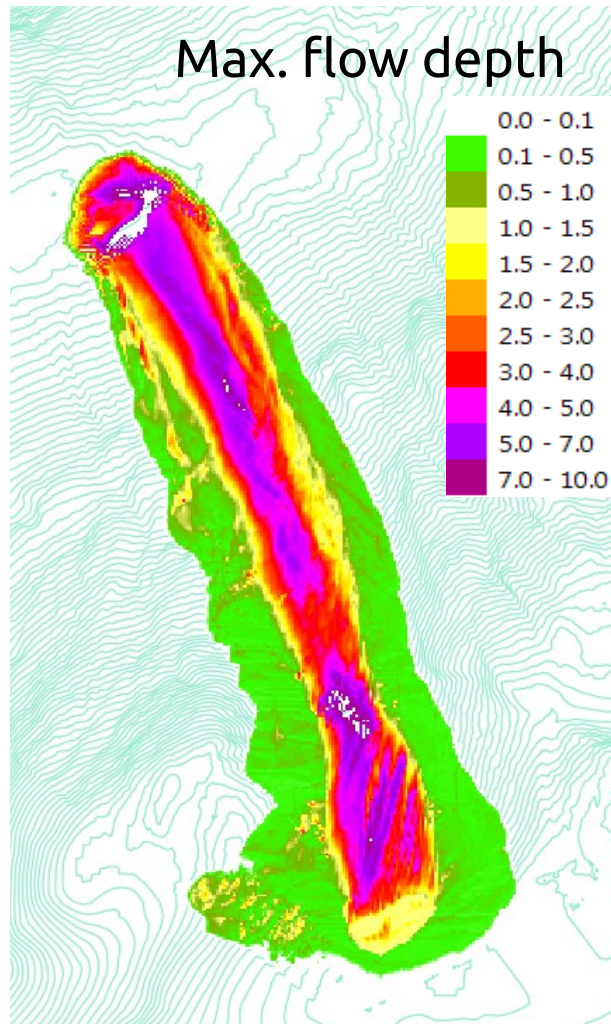




Ryggfonn avalanche 1993-03-27

Simulation with "traditional" entrainment relation  $w_e = 0.2 u$ ,

$\mu = 0.4$ ,  $k = 0.001$

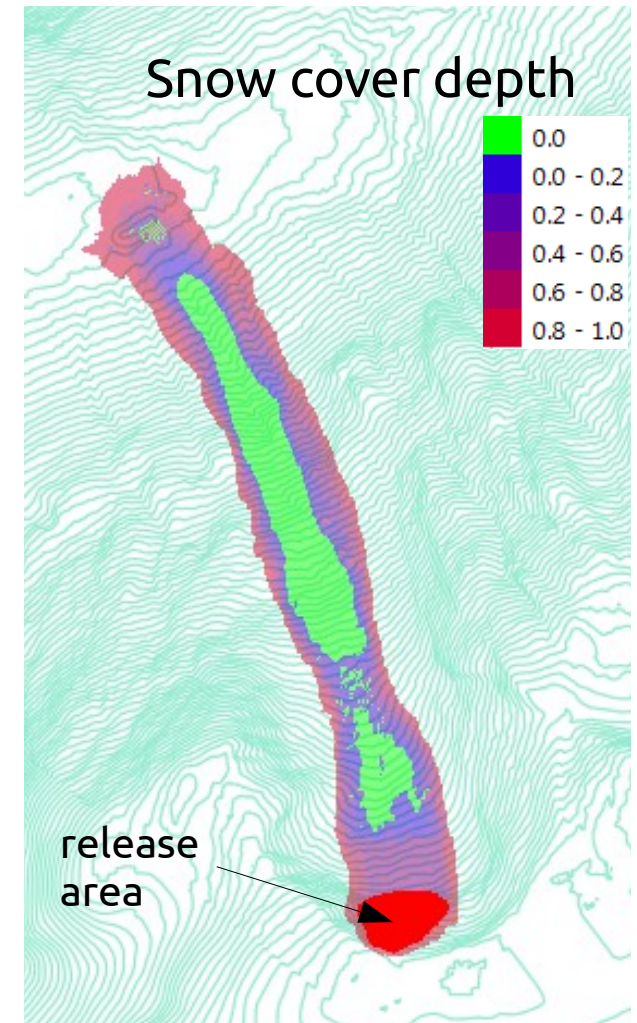
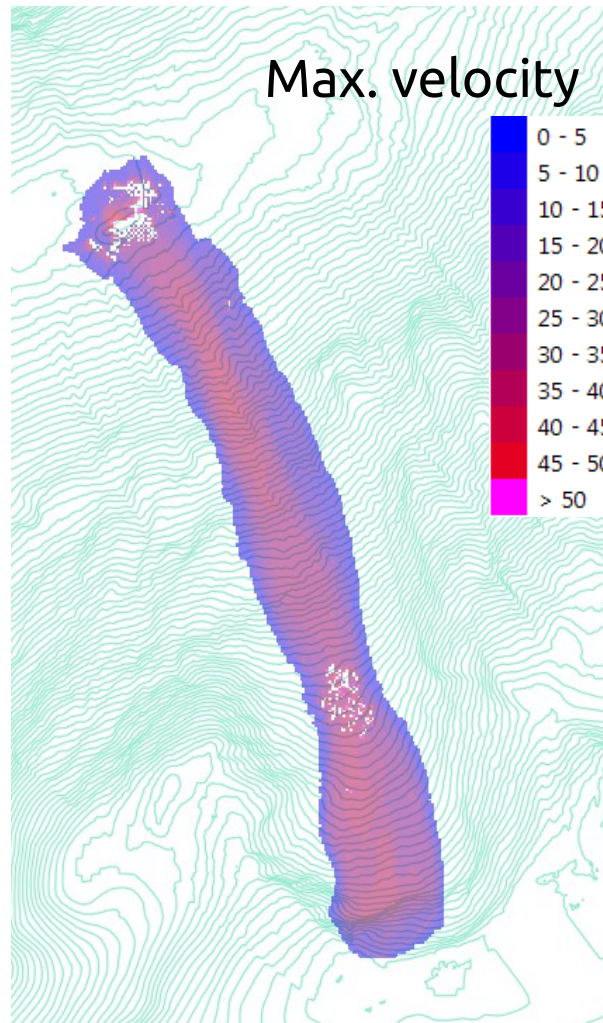
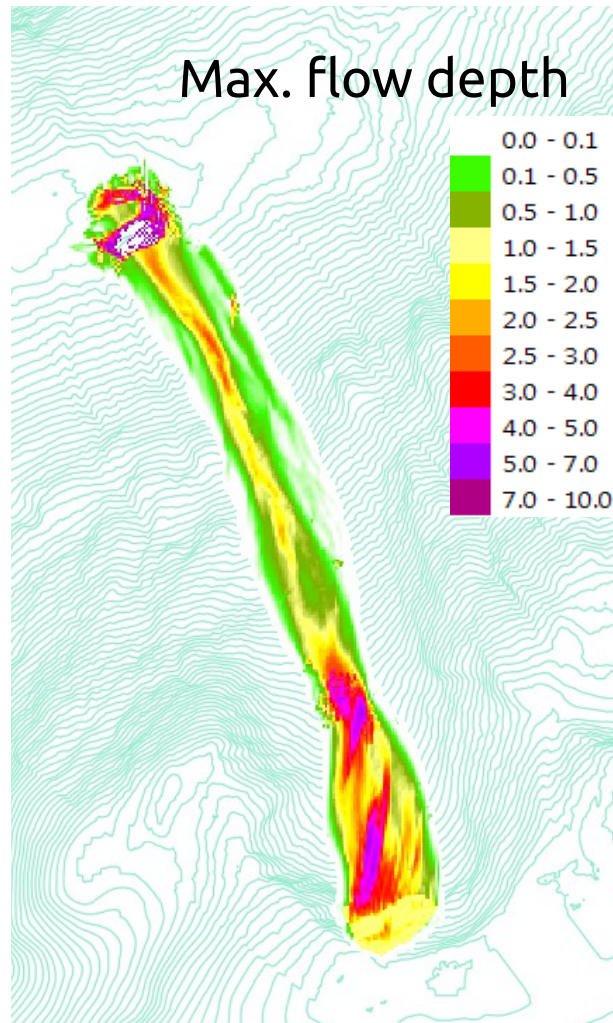




Ryggfonn avalanche 1993-03-27

Simulation with “traditional” entrainment relation  $w_e = \frac{0.001}{u}$ ,

$\mu = 0.4$ ,  $k = 0.001$  ←

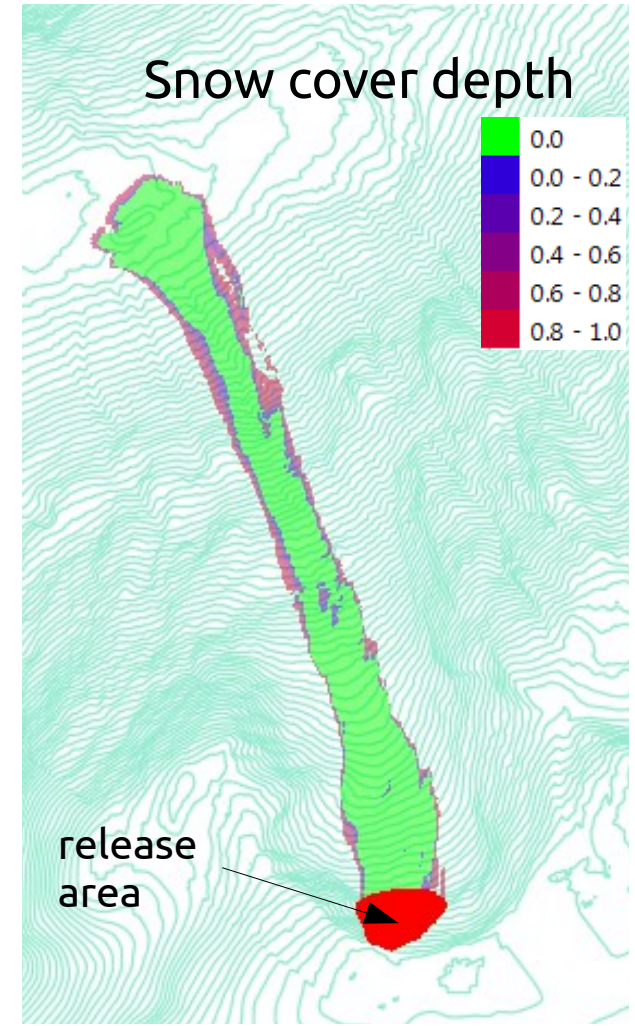
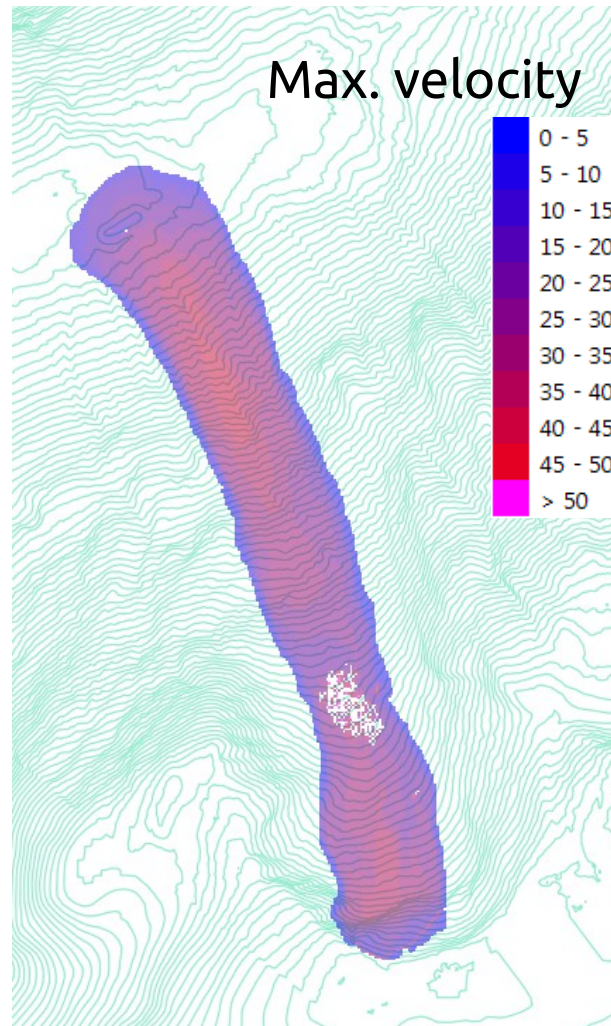
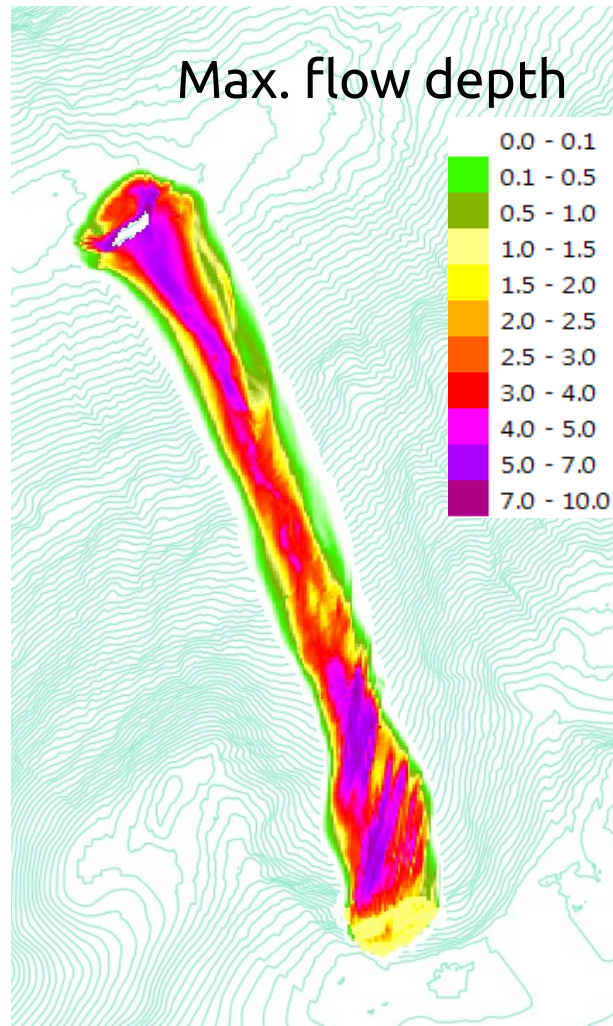




Ryggfonn avalanche 1993-03-27

Simulation with proposed entrainment relation,  $\mu = 0.4$ ,  $k = 0.001$

Snow shear strength varies with altitude from 1 to 1.2 kPa.





## Preliminary assessment:

- Shear strength of the snow cover is decisive, need not be uniform in the entire path. Typical values are 0.5–2 kPa.
- Results are markedly different from the “traditional” assumption  $w_e = c u$  with  $0.2 \leq c \leq 1$ .
- Difference less pronounced if  $c = k$  chosen in the “traditional” model.
- Further tests (and snow-strength measurements!) are needed before the proposed model can be used *prognostically*.
- Open question whether  $w_e \sim 1/u$  in a Coulomb model gives plausible results.
- Consider implementing depth-dependent shear strength.

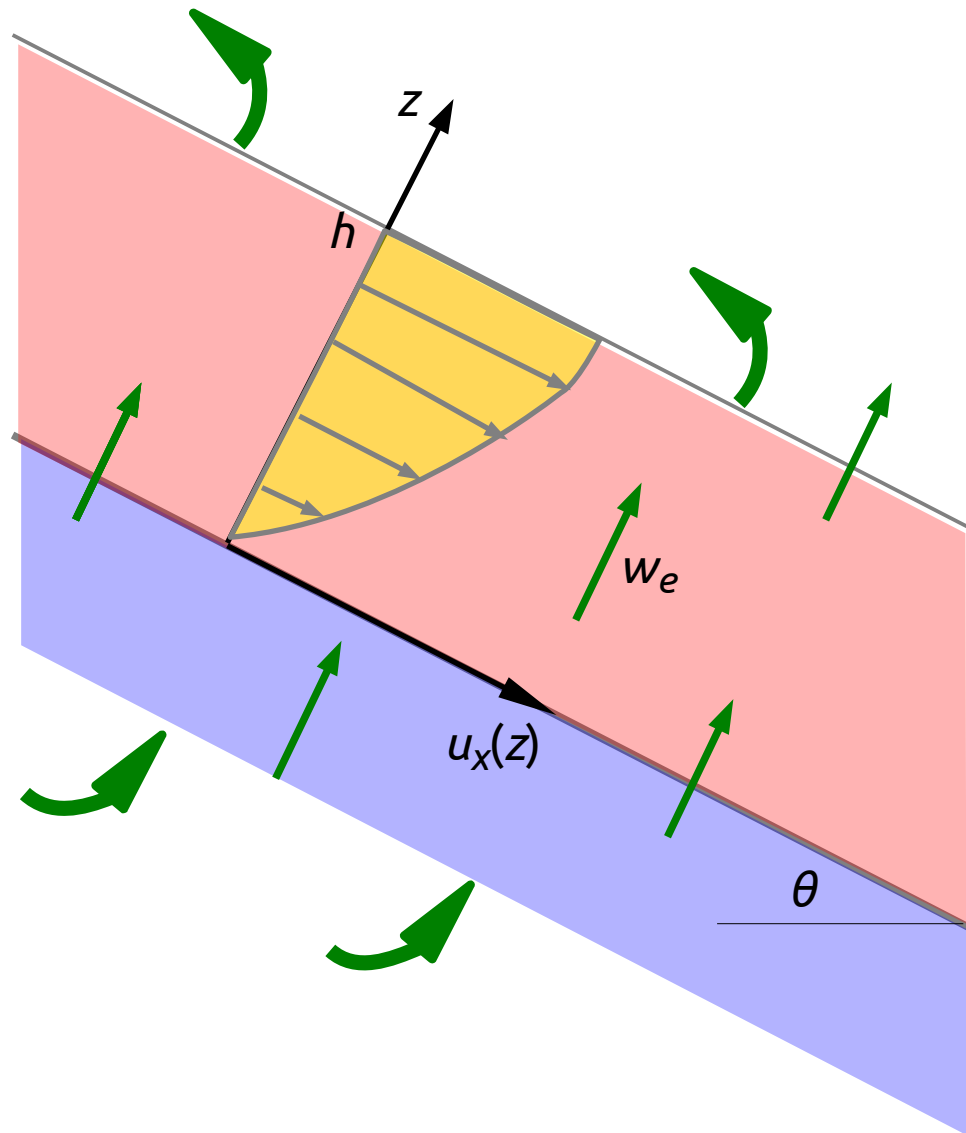


## B) An analytic toy model

- Models with uniform velocity profile are unrealistic and will eventually be superseded by (somewhat) more physical rheologies.
- Depth-averaged models typically assume velocity profile corresponding to equilibrium solution for simple-shear flow. Entrainment will modify the velocity profile, but how?
- How can the erosion rate be determined from the flow variables and the bed properties?

Start by studying the problem in the simplest setting (at the expense of realism...).





Infinitely long inclined plane

Steady flow, flow height  $h$

Laminar Newtonian fluid, viscosity  $\nu$

Perfectly brittle bed material with shear strength  $\tau_c < \tau_0 \equiv \rho g h \sin \theta$

Flow height held constant by replenishing bed at the entrainment rate and skimming flow at same rate.

Momentum balance simplifies to

$$\begin{aligned} w_e \dot{\gamma} &= g \sin \theta + \frac{1}{\rho} \frac{d\sigma_{xz}}{dz} \\ &= g \sin \theta + \nu \frac{d\dot{\gamma}}{dz} \end{aligned}$$

$$(\dot{\gamma} \equiv du/dz)$$



## Procedure:

1. Assume entrainment velocity  $w_e$  to be given, solve ODE

$$\frac{d\dot{\gamma}}{dz} - \frac{w_e}{\nu} \dot{\gamma} = -\frac{g \sin \theta}{\nu}.$$

2. Find appropriate boundary condition, determine physically consistent entrainment rate.

First-order ODE easy to solve for Newtonian (or Bingham) fluid, other rheologies lead to non-linear equations:

$$u(z) = \frac{g \sin \theta}{w_e} \left[ z - \frac{\nu}{w_e} \left( 1 - e^{-w_e z / \nu} \right) \right]$$
$$\tau(z) = \frac{\rho \nu g \sin \theta}{w_e} \left( 1 - e^{-(h-z) w_e / \nu} \right)$$



## Boundary condition for bottom shear stress $\tau_b$ :

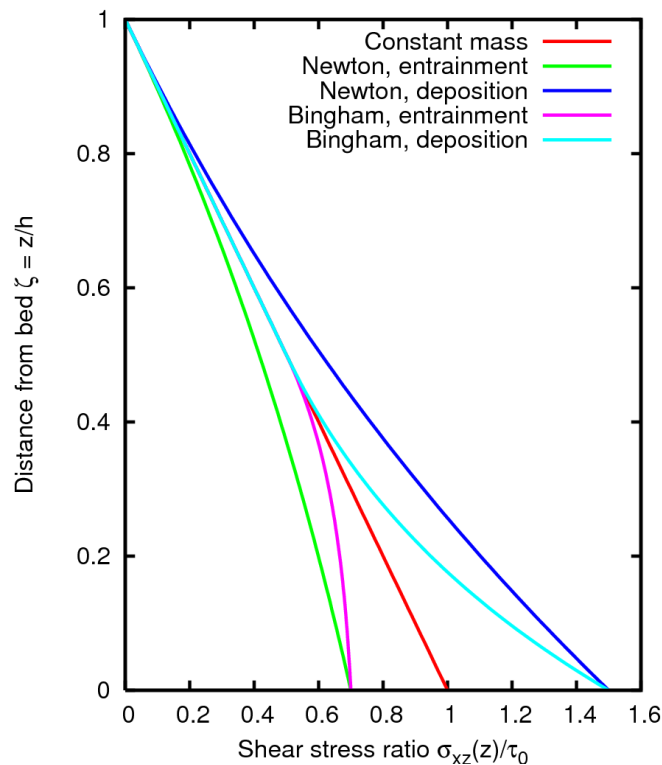
- $\tau_b \geq \tau_c$  for erosion and entrainment to be possible.
- If  $\tau_b < \tau_c$ , erosion stops,  $\tau_b$  rapidly increases to  $\tau_0 = r g h \sin \theta > \tau_c$ , erosion resumes.
- If  $\tau_b > \tau_c$ , more mass is eroded but less excess shear stress available to entrain the eroded mass, so  $\tau_b$  must decrease again.

⇒ Equilibrium value for the bottom shear stress is  $\sigma_b = \tau_c$ .

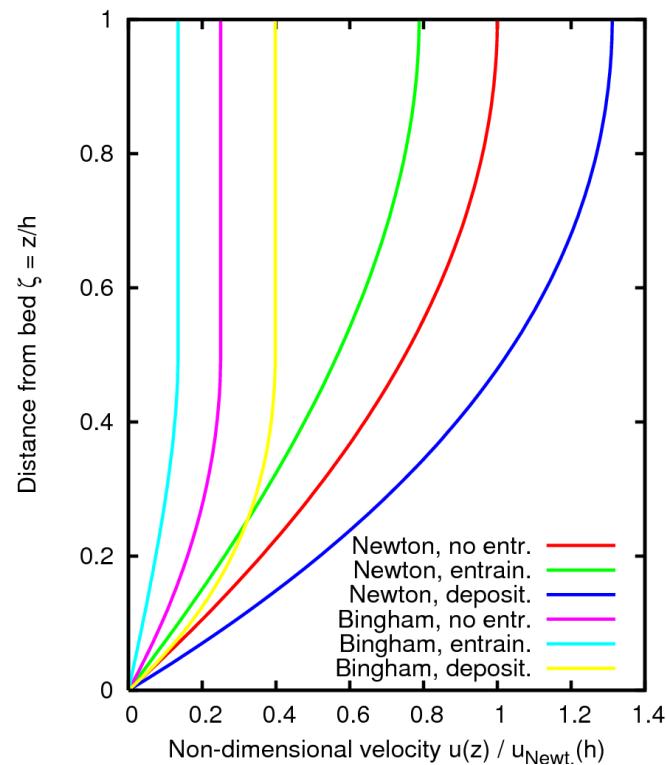
⇒ Entrainment speed  $w_e$  can be determined (numerically) from

$$\tau_c = \frac{\rho v g \sin \theta}{w_e} \left( 1 - e^{-h w_e / v} \right)$$

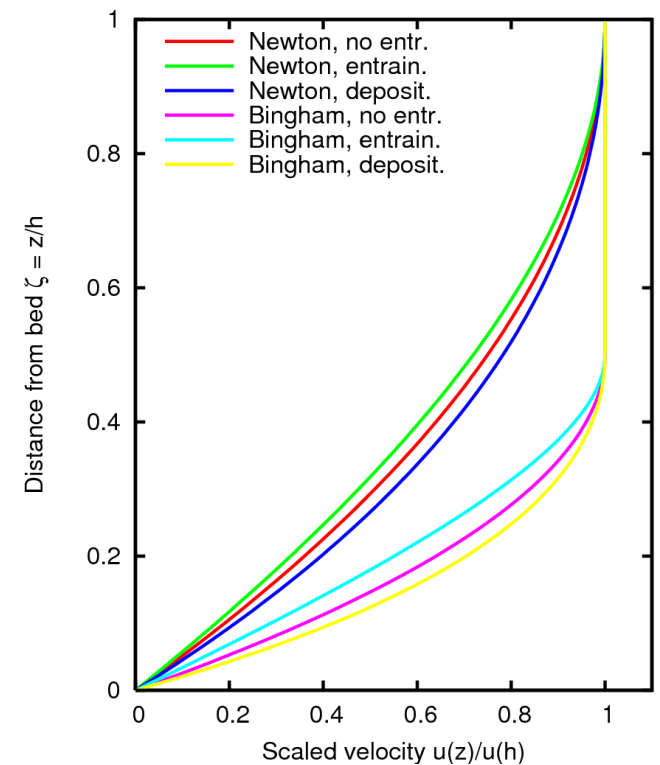
N.B. Similar b.c. proposed for aeolian transport by Owen (1964).



Excess shear stress is used for entraining the eroded material.



Entrainment reduces the equilibrium flow velocity, deposition increases it.



*Shape* of the velocity profiles is moderately modified by entrainment or deposition.



## *Does the model give realistic entrainment rates?*

- Assume      slope angle       $\theta = 30^\circ$   
                 flow height       $h = 1 \text{ m}$   
                 density       $\rho = 200 \text{ kg m}^{-3}$   
                 viscosity       $\nu = 0.0556 \text{ m}^2 \text{ s}^{-1}$
- This gives    “gravitational traction”       $\tau_0 = 1000 \text{ Pa}$   
                 surface velocity       $u_h = 45.0 \text{ m s}^{-1}$  without entrainment
- Then the entrainment rates and velocities are

$\tau_c \text{ [Pa]}$	$u_h \text{ [m s}^{-1}\text{]}$	$w_e \text{ [m s}^{-1}\text{]}$	$q_e \text{ [kg m}^{-2} \text{ s}^{-1}\text{]}$
500	28.2	0.089	17.8
700	35.5	0.042	8.4
900	41.9	0.012	2.4
1000	45.0	0.0	0.0

## *What can we learn from this model?*

- Entrainment modifies the velocity profile.
- Entrainment and rheology are intimately coupled.
- The boundary condition at the bed interface plays a decisive role.
- The erosion rate is determined by physical parameters only.

## *What are the shortcomings of this model?*

- Flow height artificially held constant.
- Applies only to (quasi-)stationary situations
- No analytic solutions found for non-linear rheologies.
- Need to solve non-linear equation at each step and node.



## Extension of the toy model to real-world situations

Extension to non-stationary situations based on the following approximation:

- Try to estimate entrainment rate for flow depth  $h$  and non-equilibrium speed  $u$  on slope with inclination  $\theta$ .
- Consider a fictitious equilibrium flow with same  $h$  and  $u$  on a slope inclined at  $\theta'$ .
- Choose  $\theta'$  such that equilibrium speed  $u'$  on  $\theta'$  matches  $u$ .
- Fictitious equilibrium flow has same physical conditions at erosion front as real non-equilibrium flow.
- Use equilibrium erosion speed  $w_e'(\theta')$  for non-equilibrium  $w_e(\theta)$ .





Use scaling:

Bed shear strength  $\tau_c = \psi_c \cdot \rho g h \sin \theta$

Flow yield strength  $\tau_y = \psi_y \cdot \rho g h \sin \theta$

Velocity  $u(z) = v(z/h) \cdot \frac{g h^2 \sin \theta}{2 \nu}$

Erosion speed  $w_e = \chi \cdot \frac{\nu}{h}$

After some non-trivial manipulations one gets the non-linear equation

$$\left( \frac{v(1)}{2} + \frac{\psi_c}{\chi} \right) \cdot \left( 1 - e^{-\chi} + \frac{\psi_y}{v(1)/2 + \psi_c/\chi} \right) = \psi_c - \psi_y$$

(Issler and Jóhannesson, NGI Technical Note 20110112-00-1-TN)



Also obtain an expression for the flow acceleration:

$$\frac{d\bar{u}}{dt} = g \cdot \sin \theta \cdot (1 - \psi_c) - \frac{v(1)}{2} \chi$$

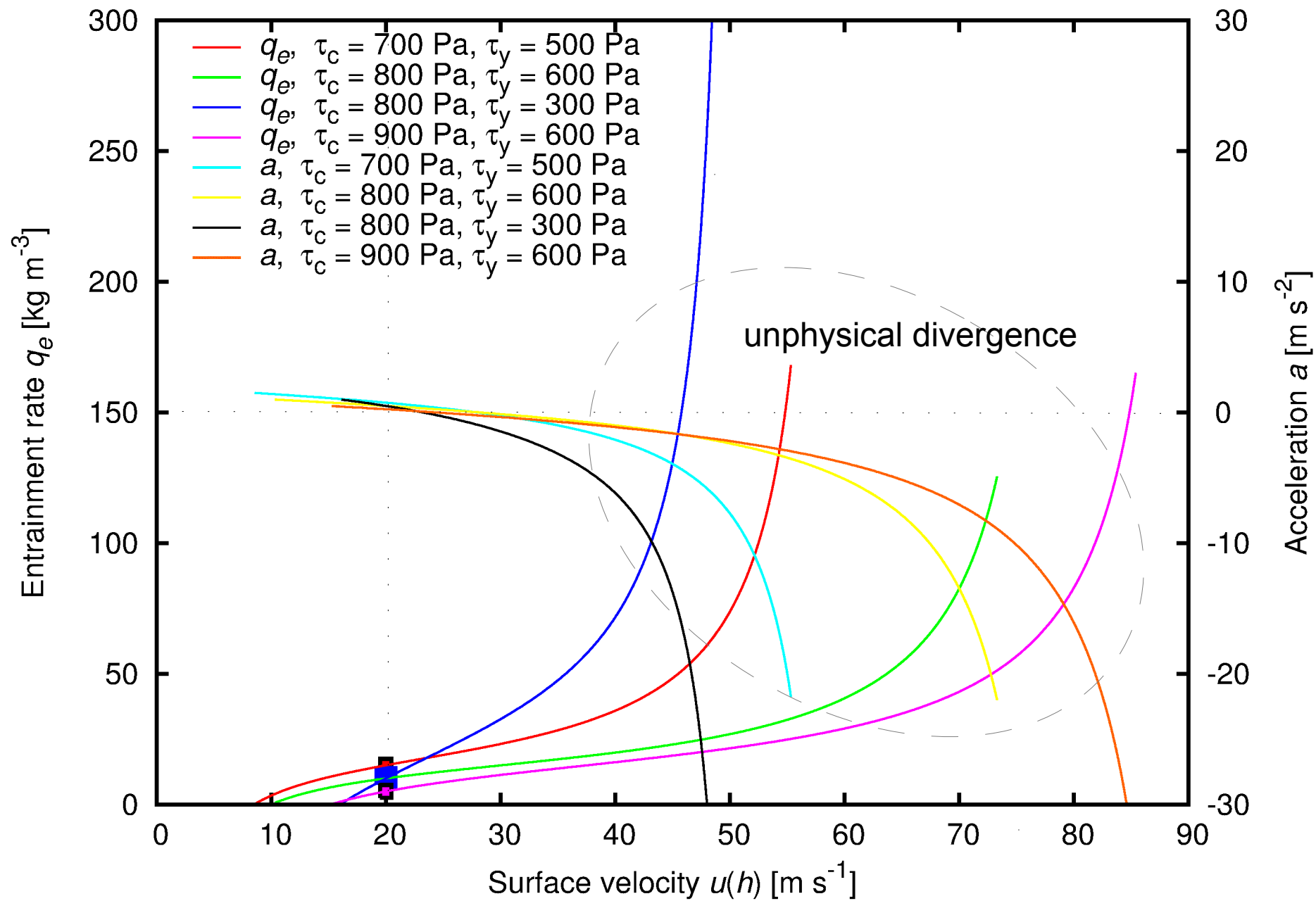
Fictitious slope angle  $\theta'$  must be less than  $90^\circ$ . This implies

$$\frac{v(1)}{2} \chi - \psi_c < \frac{1}{\sin \theta}$$

Next slide: Dependence of  $w_e$  on  $u(h)$  for different values of  $\tau_y$  and  $\tau_c$ .  
Slope angle  $30^\circ$ ,  $h = 1$  m.

Viscosity  $\nu$  is chosen such that equilibrium value of  $u(h) = 20$  m/s.





## Practical considerations:

- Need to solve non-linear transcendental equation for every node and every timestep
  - ☞ Computationally too costly.
- Possible solution:  
Tabulate solutions in three-dimensional look-up table (in terms of dimensionless parameter values).
- Extendability to realistic rheologies is questionable (no analytic solution found yet for differential equation for shear rate).



## C) Uniform non-stationary numerical model

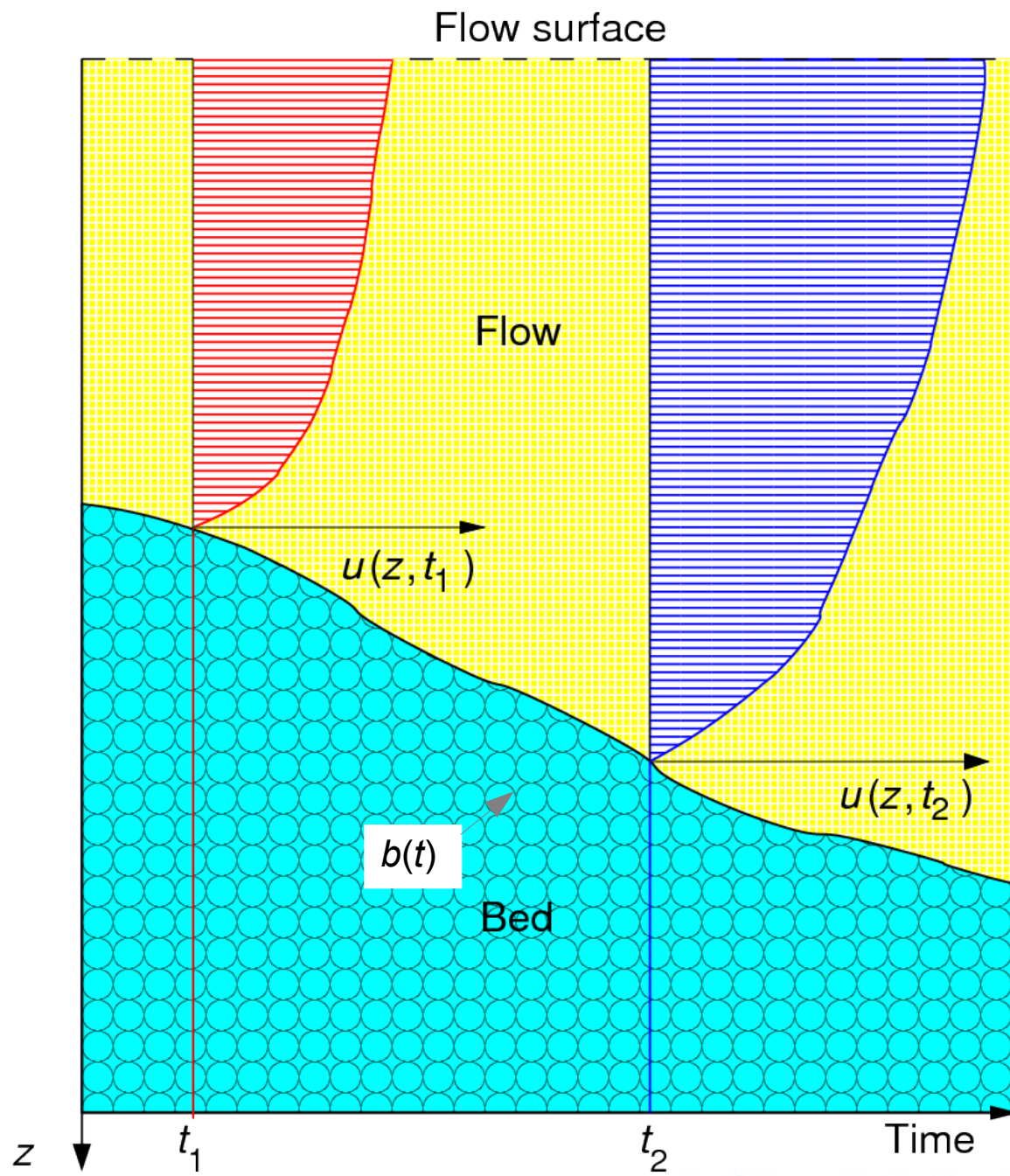
- Infinite-slope approximation
- 1D model to compute evolution of velocity profile and erosion front.
- Momentum balance equation in variable domain  $0 \leq z \leq b(t)$ .

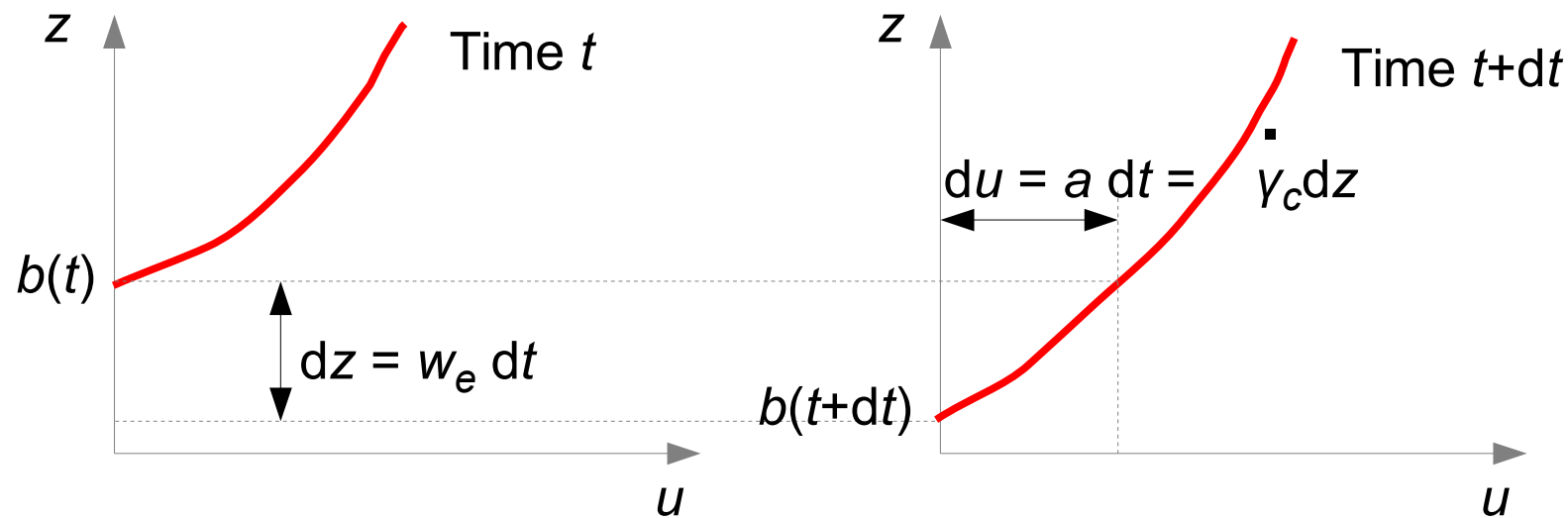
$$\partial_t u = g \sin \theta + \partial_z \hat{\sigma}$$

- Initial condition:  $b(t_0) = b_0$ ,  $u(z, t_0) = u_0(z)$ .
- Boundary conditions:  $u(b(t), t) = 0$ ,  $\sigma(0, t) = 0$ ,  $\sigma(b(t), t) = \tau_c$ .
- Entrainment speed  $w_e = -db/dt$  must be determined by *local* conditions at interface, i.e., by shear stress gradient.
- Rheology connects shear stress to shear rate gradient.

(Issler & Pastor, 2013. *Annals Glaciol.* **52**(58), 143–147)







- Velocity at time  $t + dt$  of particles eroded at time  $t$ :

$$u(b(t), t+dt) = 0 + (g \sin \theta + \partial_z \hat{\sigma}) dt .$$

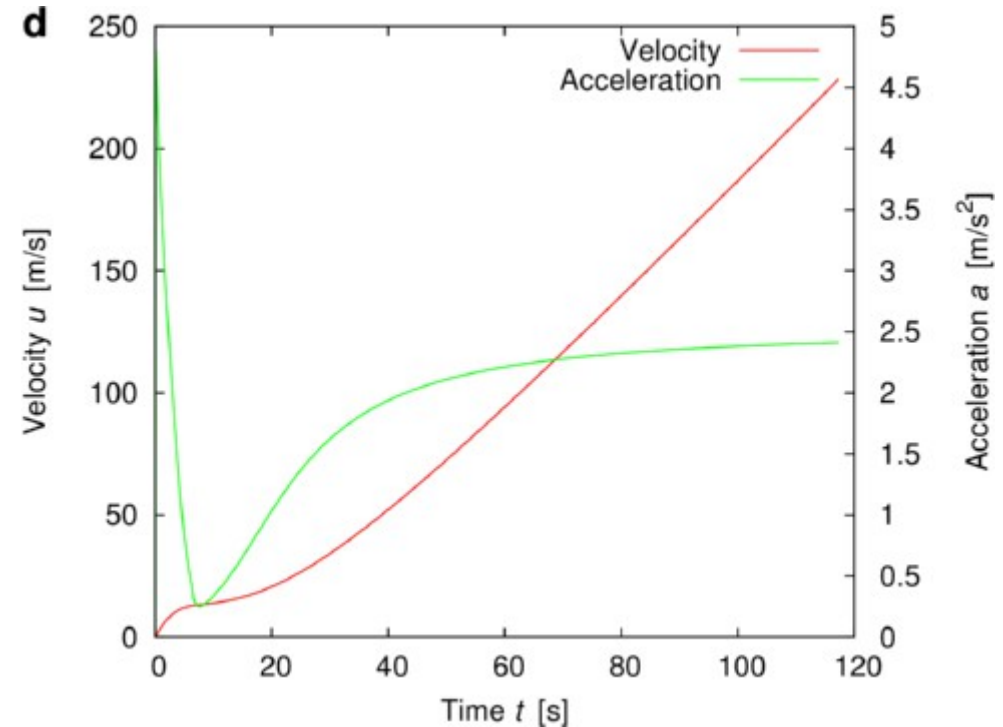
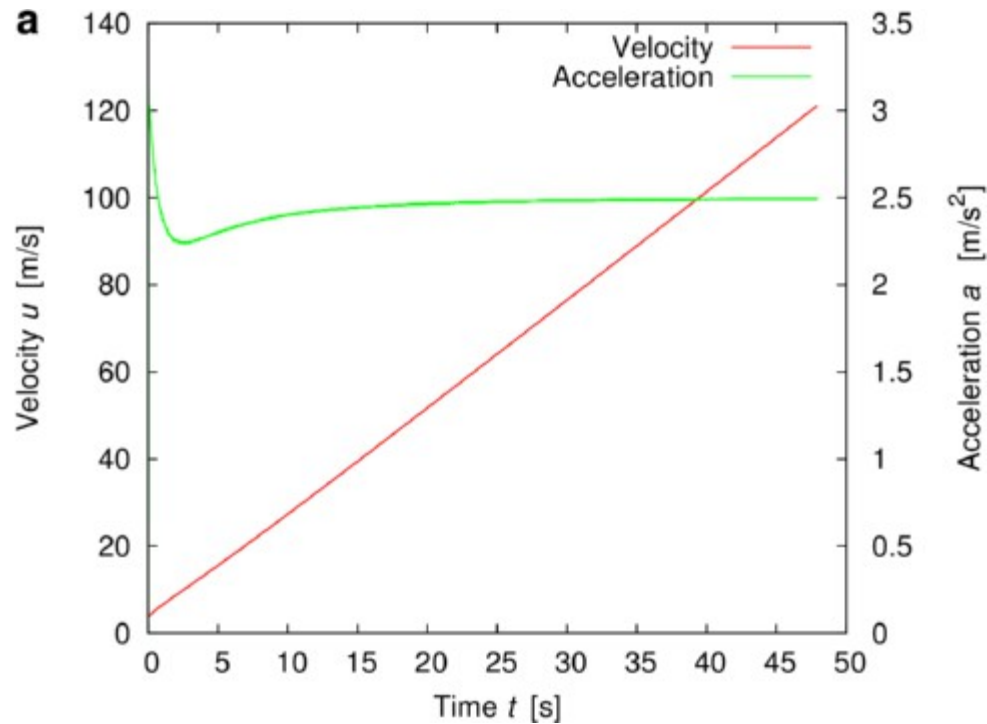
- Shear rate at erosion front must be critical shear rate:

$$\dot{\gamma}(b, t) = \frac{u(b, t+dt) - 0}{dz} = \frac{(g \sin \theta + \partial_z \hat{\sigma}(b, t)) dt}{w_e(t) dt} \stackrel{!}{=} \dot{\gamma}_c \quad \text{where } f(\dot{\gamma}_c, b) = \tau_c$$



$$w_e(t) = \frac{g \sin \theta + \partial_z \hat{\sigma}(\dot{\gamma}_c, b, \dots)}{\dot{\gamma}_c}$$

## Newtonian vs. Bagnoldian fluid: Time evolution of depth-averaged velocity and acceleration



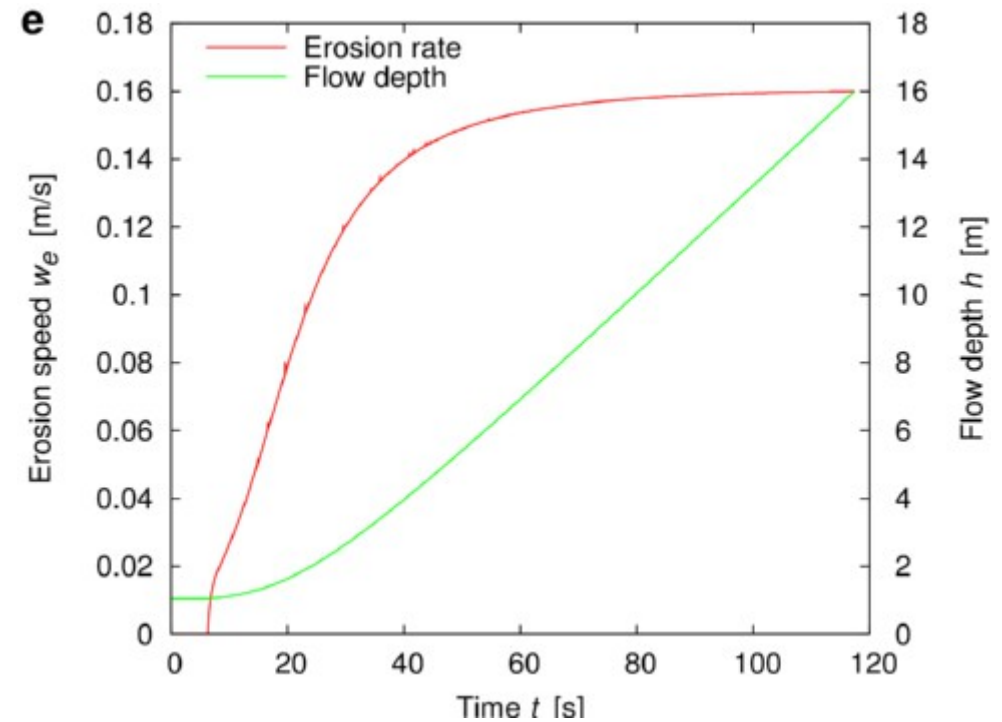
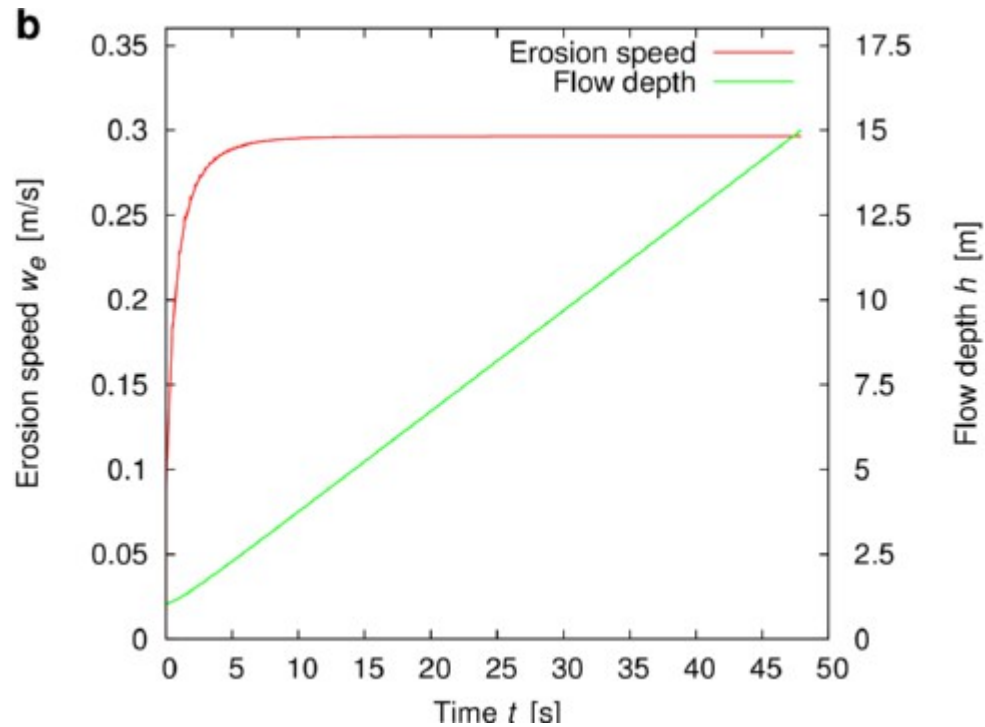
In both cases slope angle 30°, same initial flow height.  
Different initial velocities and bed shear strengths.

Result: *Same asymptotic acceleration  $a = 2.5 \text{ m/s}^2$  !*

NGS

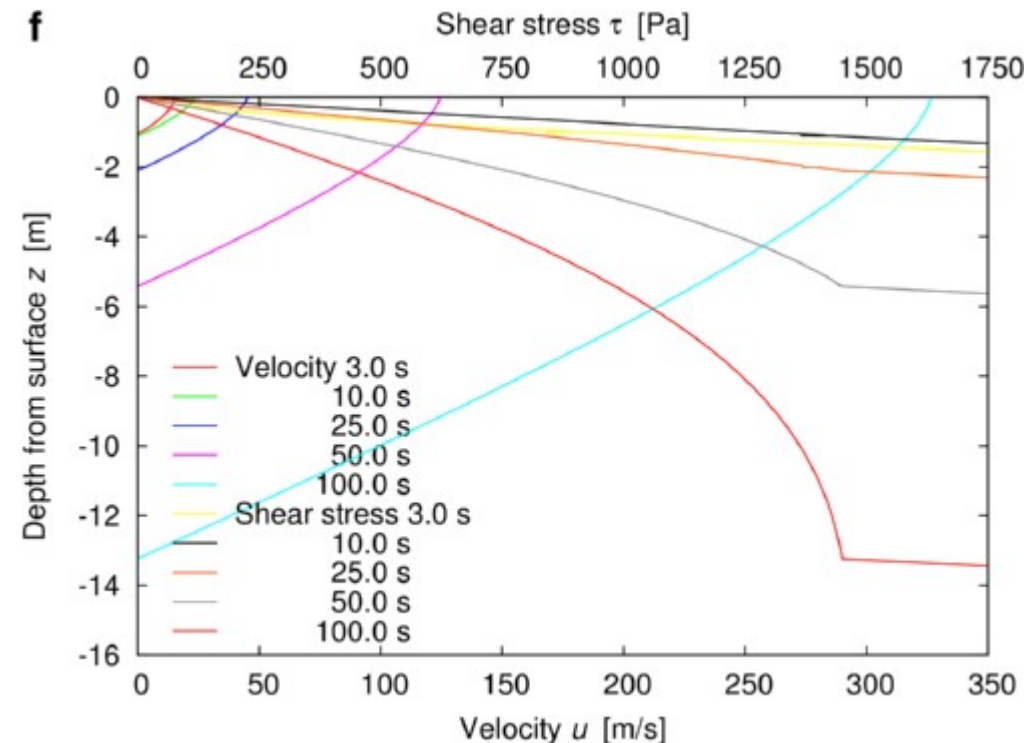
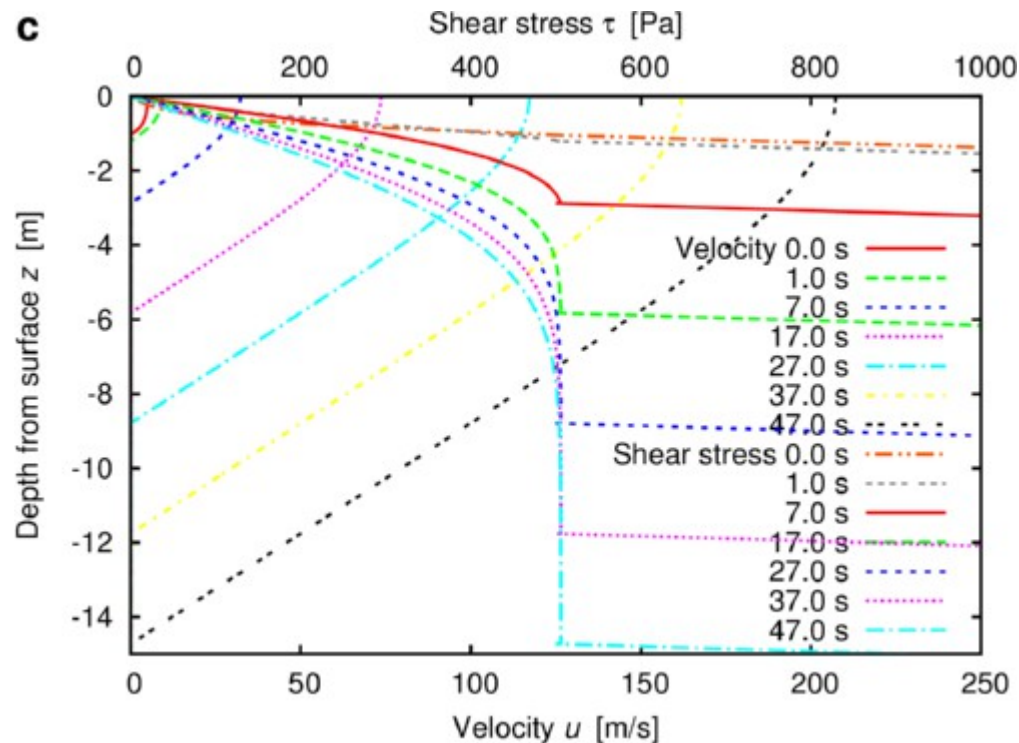


## Newtonian vs. Bagnoldian fluid: Time evolution of flow depth and erosion rate



In both cases: Erosion rate tends towards asymptotic value (at flow depths hardly occurring in nature).

## Newtonian vs. Bagnoldian fluid: Time evolution of shear stress and velocity profiles



In both cases: Linear velocity profile except near surface.  
Shear stress profile nearly linear near surface.

Different: Near-surface velocity profile depends on rheology.

NGI

# Can we understand the numerical results?

## Preliminary inferences from the numerical simulations:

After initial phase, *independent of rheology*,

- the flow accelerates uniformly at  $\approx \frac{1}{2} g \sin \theta$ ,
- the erosion rate is constant, the flow depth grows linearly,
- the velocity profiles are quite flat near the bed.

👉 *This looks almost like a granular flow with Coulomb friction!*

Recent statistical reanalysis of  $\sim 300$  extreme dry-snow avalanches (Gauer et al., 2010; Gauer, 2013) indicates

- Coulomb model with strongly *slope-dependent* friction coefficient gives best fit for both runout distance and front velocity,
- maximum velocity grows as  $\sim (\text{drop height})^{1/2}$ .



Seek asymptotic solution to point-mass equations with the following properties:

$$h(t) = h_0 + w_e t, \quad \bar{u}(t) = \bar{u}_0 + \bar{a} t, \quad w_e, \bar{a} = \text{cst.}$$

Then, equation of motion  $\frac{d(h\bar{u})}{dt} = h g \sin \theta - \hat{\tau}_c$  transforms into

$$\dot{\bar{u}}(t) = g \sin \theta - \frac{\hat{\tau}_c}{h(t)} - \bar{u}(t) \frac{\dot{h}(t)}{h(t)} = g \sin \theta - \underbrace{\frac{(\hat{\tau}_c + w_e \bar{u}_0) + w_e \bar{a} t}{h_0 + w_e t}}_{\text{must be indep. of } t} \stackrel{!}{=} \bar{a}$$

Simple algebra yields

$$\bar{a} = \frac{g \sin \theta}{2}, \quad w_e = \frac{1}{\bar{u}_0} \left( \frac{1}{2} g h_0 \sin \theta - \hat{\tau}_c \right)$$



Perhaps somewhat surprising...

*... but in nearly perfect agreement with the simulations!*

(Less than 1% discrepancy – due to setting entrainment rate to 99% of theoretical value to avoid oscillations.)

**N.B.** Both relations are independent of rheology! However, rheology determines relation between  $h_0$  and  $\bar{u}_0$  as well as velocity profile.

Open question: Need better understanding of stability and domain of attraction of this solution. (It appears to be rather stable!)



## Use of the 1D depth-resolved erosion model with depth-averaged flow models

Key point: Non-dimensionalize equations of the 1D model and tabulate the corresponding erosion rates in look-up tables for the depth-averaged model

Relevant dimensionless parameters for NIS-type models:

$$\omega = w_e / u$$

$$Fr = u / (g h \sin \theta)^{1/2} \text{ (Froude number)}$$

$$Cb = \tan \theta / \mu$$

$$Ba = k / h^2$$

$$\psi = \tau_c / (g h \sin \theta)$$

Need a 4D look-up table with  $O(10^6)$  elements!

Populating this table is in progress, but is not trivial.



## Conclusions concerning erosion modeling:

1. Erosion function depends crucially on flow rheology. This makes validation of erosion models difficult.
2. Consistent erosion functions have no adjustable parameters.
3. Stress boundary condition at bed–flow interface is central. Perfectly brittle behavior is an interesting candidate for snow avalanches.
4. Bottom erosion by scour should be complemented by frontal erosion by plowing or eruption.
5. May need to obtain data on shear-strength profile of new-snow layers and to implement this in numerical flow models.



## 6. Transformation of the flowing material



Photo A. Errera, 2010.



## Progressive break-up of the flow material may be decisive in certain situations:

### Snow avalanches:

- General wisdom: Break-up of original slab usually is fast and need not be modeled explicitly.
- In small avalanches, break-up sometimes does not progress sufficiently and sliding stops on steep slopes.
- However, even in big avalanches, small particles may still be ground down to grain size.
- In granular materials in the collisional flow regime:

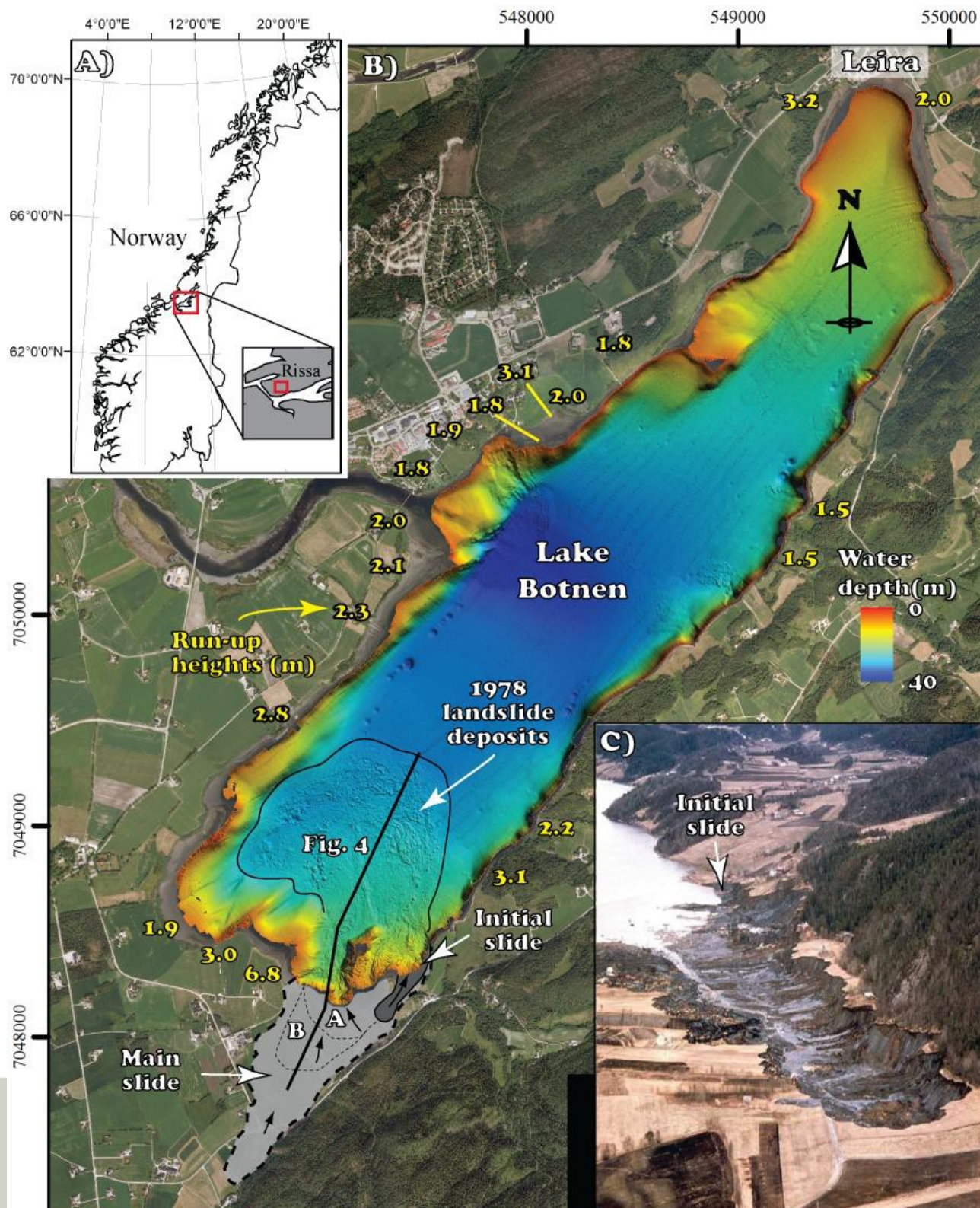
$$\sigma_{xz} \propto \dot{\gamma}^2 d^2$$

i.e., at constant shear stress, shear rate and velocity increase strongly with progressive comminution!



## Quick-clay slides:

- Sensitive marine clays, frequent in Scandinavia, eastern Canada, Alaska and northern Siberia near the coast.
- Salt that holds them stable (flocculated), may be leached out after isostatic rebound and exposure to rain, etc.
- When shear strength is exceeded, *remolding* sets in and shear strength, viscosity drop by several orders of magnitude.
- Potential for disastrous slides without visible precursor signs.
- Release area may be a gentle slope, run-out angle can be extremely low, slide volume often several million cubic meters.
- ***Progression of remolding in the initial phase is decisive for extent of slide.***



Quick-clay slide at Rissa (Norway), 1978.

From (L'Heureux et al., 2012).

For a commented amateur video of the event, see <http://www.ngi.no/en/Areas-of-research-and-development/Soil-and-rock-slides/The-Quick-Clay-Landslide-at-Rissa---1978/>.